GFP tagged Hsp60 used to investigate the translocation of Hsp60 in response to mitochondrial stress in HeLa cells

A thesis

submitted in partial fulfilment

of the requirements for the degree

of

Master of Science in Biological Sciences

at

The University of Waikato

by

Matthew Edward Short

THE UNIVERSITY OF
WAIKATO
Te Whare Wānanga o Waikato

2013

Abstract

Heat shock protein 60 (Hsp60) is a mitochondrial stress protein that is elevated in response to mitochondrial impairment. It is involved in protein folding and, more recently, it has been identified as a signalling molecule. It has been found elevated in patients suffering from diabetes, atherosclerosis and cardiomyopathy. In order to investigate the translocation of Hsp60 from mitochondria we employed RG224428, a plasmid housing genes for a human Hsp60 connected to a green fluorescent protein (GFP) bound at the C-terminus. The plasmid was cloned inside DH5α *E. coli* (DH5α) and purified using an endotoxin-free plasmid extraction kit. Using endotoxin-free DNA we transfected the human cervical cancer cell line HeLa with the Hsp60-GFP DNA. It has been found that endotoxin (or otherwise known as lipopolysaccharide) can affect Hsp60 expression in mammalian cells, so by using endotoxin-free plasmid DNA we could induce controlled stress treatments without the unwanted effects the DH5α endotoxin would exhibit. Propidium iodide staining found the plasmid posed very low-to-no toxicity on HeLa cells. Mitochondrial staining using Mitotracker CMX Ros showed that the Hsp60-GFP was being taken up by mitochondria almost exclusively. High-glucose and sodium azide were used to stress the transfected HeLa cells and the translocation of the Hsp60-GFP signal was recorded using an Olympus FV1000 laser scanning confocal microscope.

We found that the Hsp60-GFP colocalises with mitochondria to a high degree. We also found that high-glucose can be linked to the translocation of Hsp60-GFP out of mitochondria. The results here support published data that suggest higher glucose concentrations may play a role in the translocation of Hsp60 out of mitochondria and into extracellular fluids. We have also found that the use of

fluorescent-confocal microscopy may provide a useful way to detect the movement of the biomarker Hsp60 under stress and therapeutic treatments.

Acknowledgements

Firstly, I would like to thank my supervisor, Dr Ryan Martinus, for all his efforts to keep me on the path towards success these past two years. His knowledge and expertise have been a strong foundation for my work. I am also grateful for the effort you spent helping me improve my thesis.

Thank you to Luke Hall and Richard Hales for your friendship and support during our time in the Cellular and Molecular Biology Laboratory. Thanks also to Kerry Allen for keeping our lab organised and helping me learn to use various apparatus.

Thanks also to the staff and students in the Molecular Genetics and the Microbes and Proteins laboratories for giving me advice and letting me use all of your stuff. And also a special thanks to Olivia Patty for giving me the encouragement and support I needed to get my project going.

I am also grateful to Dr Barry O'Brien for helping and teaching me to use the confocal microscope. Your wisdom and expertise are much appreciated. Also, thank you to Cheryl Ward for helping me develop the template for this thesis.

I am last, but not least, grateful to my family for their support and encouragement which have helped keep me focused on my degree. Jaimee, a special thank you to you for everything you do to make life a happier place.

Table of Contents

List of Figures

Chapter 3

Chapter 4

List of Equations

List of Abbreviations

6-APA, 6-amino penicillanic acid

ADP, adenosine diphosphate

AdvHsp, adenoviral vector incorporated with heat shock protein

AGE, advanced glycation end-product

ANP, atrial natriuretic peptide

Apaf1, apoptotic protease activating factor 1

ApoE-null, apolipoprotein E-null

arsR, arsenate resistance

Arx, aristaless related homeobox

ATP, adenosine triphosphate

Bax, Bcl-2-associated X protein

Bcl-2, B-cell lymphoma 2

Bcl-XL, B-cell lymphoma-extra large

BiPSCs, β-cells pluripotency-induced pancreatic stem cells

BMI, body mass index

BNP, brain natriuretic peptide

Brdu, Bromodeoxyuridine

CMV, cytomegalovirus

DAG, diacylglycerol

db/db, diabetic mutant strain

DCCT, Diabetes Control and Complications Trial

DCM, dilated cardialmyopathy

DH5α, *Escherichia coli* DH5α

DISC, death inducing-signalling complex

DMEM, Dulbecco's modified Eagle's medium

DMSO, dimethyl sulphoxide

DNA, deoxyribonucleic acid

ECM, extra cellular matrix

EDIC, Epidemiology and Diabetes Complications

EDTA, ethylenediaminetetraacetic acid

ELISA, enzyme-linked immunosorbent assay

Endo-free, endotoxin-free

EPR, electron paramagnetic resonance

ETC, electron transport chain

FADD, FAS-associated protein with death domain

FasR, FAS receptor

FBS, foetal bovine serum

FCA, Freund's complete adjuvant

Foxo1, forkhead box protein O1

GAPDH, glyceraldehydes 3-dehydrogenase

GC, good control, good glycaemia control

GFAT, glutamine:fructose-6-phosphate amidotransferase

GFP, green fluorescent protein

GHb, glycated haemoglobin

GlcNAc, N-acetylglucosamine

GLUT, glucose transporter

GSH, glutathione

GTE, glucose tris EDTA

HAT, histone acetyltransferase

Hb, haemoglobin

HDAC, histone deacetylase

HIP, human proislet peptide

HOMA, homeostatic model assessment

Hsp, heat shock protein

HSPD1, human Hsp60 protein gene

HUVEC, human umbilical vein endothelial cells

IAP, inhibitor of apoptosis

ICAM-1, intercellular adhesion molecule 1

ICT, internal charge transfer

IFG, impaired fasting glucose

IFN, interferon

IGT, impaired glucose tolerance

IL, interleukin

INGAP, islet neogenesis associated protein

iPSCs, pluripotency-induced pancreatic stem cells

KK-Ay, Kuo Kondo-yellow spontaneous mutation

LAD, left anterior descending artery

LB, lysogeny broth

LLC-PK1, porcine renal tubular epithelial cells

LPS, lipopolysaccharide

LSCM, laser scanning confocal microscope

LVDD, left ventricular diastolic dimension

Mafa, mast cell function-associated antigen

MGO, methlglyoxal

Mif4, macrophage migration inhibitory factor 4

Mitotracker, Mitotracker CMX Ros

mRNA, messenger RNA

MSA, mouse serum albumin

MyD88, myeloid differentiation primary response gene

NAD+, nicotinamide adenine dinucleotide

NADPH, reduced nicotinamide adenine dinucleotide phosphate

NEAA, non-essential amino acids

NF-κB, nuclear factor-κB

Ngn3, neurogenin 3

NK, natural killer

NOD, non-obese diabetic

^{o}C, degree Celcius

Opti-MEM, optimised Eagle's minimum essential media

OTC, ornithine transcarbamylase

p53, protein 53

PARP, poly(ADP-ribose) polymerase

Pax4, paired-box-containing gene 4

PBS, phosphate buffered saline

PC, poor control, poor glycaemia control

PC12, rat pheochromocytoma 12 cells

PC-GC, poor control followed by good control

PDK1, 3-Phosphoinositide-dependent protein kinase 1

PDX1, pancreatic and duodenal homeobox 1

PEG, polyethylene glycol

PET, Photo induced electron transfer

PI, propidium iodide

PKC, protein kinase C

PP cells, pancreatic polypeptide cells

r, overlap coefficient

RAGE, receptor for advanced glycation end-product

Reg, regenerating, regulation

RFP, red fluorescent protein

RIP, receptor interacting protein

RNA, ribonucleic acid

RO, reverse-osmosis distilled

ROS, reactive oxygen species

RT, room temperature

S.E.M., standard error of the mean

SDS, sodium dodecyl sulphate

SET complex, protein complex involved in DNA cleavage

siRNA, small interfering RNA

Sp1, specificity protein 1

SPG, spastic paraplegia

Spi, serpin

sRAGE, truncated receptor for advanced glycation end-product

TBE, tris borate EDTA

TCA, citric acid cycle

TE, tris EDTA,

TENS, tris EDTA NaCl SDS

TGF-β, transforming growth factor-β

THP-1, human acute monocytic leukaemia cells

TLR4, toll-like receptor 4

TNFR1, tumor necrosis factor receptor 1

TNFα, tumour necrosis factor α

TRADD, tumour necrosis factor type 1-associated death domain

UKPDS, United Kingdom Prospective Diabetes Trial

UV, ultra-violet light

VEGF, vascular endothelial growth factor

WHO, World Health Organisation

1 Literature Review and Research Aims

This chapter discusses the complicated disease Diabetes mellitus in relation to its biology and biochemistry. Details are taken from current literature and provide insight into the degree of complexity that this disease employs. The eukaryotic Hsp60 protein, implicated with Diabetes, is then reviewed followed by its primary host organelle, mitochondria. Later, various experiments that have provided the basis for much of our own study are highlighted. At the conclusion of this chapter our aims and objectives will be explained.

1.1 Diabetes Mellitus

1.1.1 The Diabetic Condition

Diabetes mellitus affects more than 250 million people worldwide. It is a pandemic disease affecting people from all countries, cultures and economic classes. Diabetes, for most is an obstinate condition stunting the lives of those it inflicts and those who care for them. It has been estimated that in 2007 the U.S. alone spent $116 billion treating diabetes and paying for concurrent patient care (Fowler 2010). In New Zealand it was estimated that approximately 3.7% of individuals aged above 15 have diabetes. This figure equates to approximately 150,000 people. The prevalence of diabetes differs between ethnic groups but universally increases with age (as high as 14.9% in European elderly) (Moore & Lunt 2000). The figures increase every year as new cases are diagnosed. The medical bill for the treatment and analysis of diabetic patients within the Counties-Manakau District was $66 million higher for diabetics than for non-diabetics. As the population increases, the incidence of diabetes may also

increase leading to more suffering and a larger bill for public health (Jackson *et al.* 2009).

Patients generally fall into one of two categories, those with type 1 diabetes and those with type 2 diabetes. Type 1 diabetes occurs when an individual cannot produce enough insulin while type 2 diabetes occurs when an individual forms a level of insulin resistance (Fowler 2010). Both types experience prolonged exposure to high concentrations of glucose in the blood and general circulation. A higher concentration of blood-glucose is termed 'hyperglycaemia'. The World Health Organisation (WHO) has described diabetes based on hyperglycaemic values. The fasting plasma glucose and 2-hour plasma glucose (2 hours after ingestion of 75 g glucose) levels found in healthy non-diabetics are values up to 110 mg/dl (6.1 mM) and 140 mg/dl (<7.8 mM), respectively. There are two stages of development between the non-diabetic and diabetic conditions. The first stage is 'impaired fasting glucose' (IFG). The IFG fasting plasma glucose level is from 110 to 125 mg/dl (6.1 to 6.9 mM). The IFG 2-hour plasma glucose level are values up to 140 mg/dl (<7.8 mM). The second stage is 'impaired glucose tolerance' (IGT). The IGT fasting plasma glucose values are up to 126 mg/dl (<7.0 mM). The IGT 2-hour plasma glucose level is between 140-200 mg/dl (≥7.8-<11.1 mM). The fasting glucose level for Diabetes mellitus is above 126 mg/dl (≥7.0 mM). The 2-hour plasma glucose for diabetes is above 200 mg/dl (>11.1) (World Health Organisation 2006).

The condition both types of diabetes have in common is a decrease in the biochemical efficiency of the insulin hormone leading to hyperglycaemia. Insulin plays a role in the homeostasis of blood-glucose levels (Teuscher 2007). In healthy individuals, insulin is produced in β-cells of the pancreas and is released

into the circulation upon detection of glucose from digestion through membrane bound GLUT-2 receptors (Stolarczyk *et al.* 2007). The circulating insulin is targeted to insulin receptors on the cell membranes of adipocytes and striated muscle fibres. This triggers the translocation of GLUT-4 receptors from the cytosol to the membrane. Glucose can then enter through the GLUT-4 receptors and be processed for storage in glycogen molecules or catabolised to release its energy. The primary targets of insulin are muscle and liver tissue, while other tissue can obtain the required amounts of glucose through other channels (Livingstone *et al.* 1995; Winzell & Ahren 2007). The loss of insulin or a decrease in its effectiveness via degradation of itself or its receptors causes hyperglycaemia. The resultant increase in glucose concentration can cause glucose to diffuse through cell membranes at an unhealthy rate causing stress to all cell types. As pancreatic β-cells suffer during hyperglycaemia, decreases in their number exacerbate the insulin deficiency (Laybutt *et al.* 2002). This is the reason many type 2 diabetics eventually become type 1 suffering from the type 1 related β-cell loss. Chronic hyperglycaemia causes demoralising conditions such as blindness, kidney failure and tissue breakdown which can lead to either amputation or death (Fowler 2010).

The pancreas is an important organ of the human body which supplies enzymes for digestion and the hormones insulin and glucagon for glucose control. The head of the pancreas articulates with the duodenum, where it connects through a duct. The pancreas has been said to contain two different sections that are scattered throughout and in-between in a non-uniform pattern. These two sections are called the exocrine and the endocrine. The exocrine section contains the ability to produce digestive enzymes through its acinar cells. The endocrine section is responsible for producing insulin via β-cells. The type 1 diabetic

condition results from a lack of insulin being produced by diminishing β-cells. The type 2 diabetic condition is caused by insulin resistance which may be linked to inefficient production of insulin within the β-cells or a breakdown in glucose storage and management. In healthy individuals the β-cells are arranged into islets within the pancreas that surround interlaced capillaries connecting cells to the circulation. These islets are known as the islets of Langerhans and contain β-cells alongside the closely related α-cells, δ-cells and PP-cells. Though the β-cells make up most of the cellular component of these islets, the islets of Langerhans only equate to about 1-3% percent of the pancreas (Molina 2006).

1.1.2 β-Islet Cell Loss in the Diabetic Pancreas

After the pancreas has been compromised (due to injury or disease), or the β-cells have depleted, this insulin producing tissue is among the most difficult of tissues in the human body to grow *in vivo*. The complexity of the events leading to the post-natal regeneration of β-islet cells has eluded researchers for decades (Slack 1995). Reversing the decrease in β-cell mass has been addressed in many studies using many different approaches. Endogenous sources of β-cell renewal have included the manipulation of the transcription factor 3-Phosphoinositide-dependent protein kinase 1 (PDK1). PDK1 is an enzyme that is involved in intracellular signalling originating from hormones including insulin. Its dysfunction results in cell death. This enzyme was manipulated in order to understand premature apoptosis and improve the lifespan of β-cells within islets (Hashimoto *et al.* 2006). Some researchers have approached dedifferentiation of pancreatic acinar cells and then the subsequent reprogramming of these to redifferentiate into the β-cell phenotype. Different approaches have further

removed dedifferentiation steps using embryonic factors to bypass the long process and drive a phenotypic change from the neighbouring α-cells, δ-cells and PP-cells (all reside within the pancreas) (Tuch & Kannangara 2008).

The addition of islet neogenesis associated protein (INGAP) has resulted in pancreatic β-cell growth in tests using murine models but has been questioned as to how these data may benefit humans, after similar INGAP tests on humans did not carry the same success (research using the homologous human proislet peptide (HIP) has yet to be completed) (Lipsett *et al.* 2007). Techniques using transgenic mice has led to a greater understanding of the genes and proteins involved in β-cell regulation (both mitotic and apoptotic) but has not helped in determining the controlling factors of β-cell demise in the adult population (Levine & Ilkin-Ansari 2008; Tuch & Kannangara 2008). The next few sections review in greater detail some of the work that has been done recently to understand β-cell loss and regeneration.

1.1.2.1 β-Cell Loss Causes Hyperglycaemia

Hashimoto *et al.* (2006) used murine models to create a system where β-cells were genetically altered to produce a phenotype lacking in 3-Phosphoinositide-dependent protein kinase 1 (PDK1) from birth (β-cell-PDK1-/-). PDK1 is an enzyme that is involved in intracellular signalling originating from exogenous hormones (including insulin) which upon elimination results in cell death (Mora *et al.* 2004). The β-cell-PDK1-/- model was designed to highlight by deduction the importance of this gene (and subsequent protein) in β-cell subsistence, and consequently, the importance of β-cells in glucose homeostasis. *In situ* hybridisation indicated that the PDK1 gene was successfully eliminated from the

β-cells while leaving other tissues uncompromised (PDK1+/+). They found that all β-cell-PDK1-/- mice died within 6 months and that those kept under glucose control during that period showed excessive increases in blood glucose (above 500 mg dl-1; healthy β-cell-PDK1+/+ controls stayed at approximately130 mg dl-1). The β-cell-PDK1-/- mice also showed declining levels of insulin (below half of the control levels within 4 months; almost undetectable within 6 months). By compromising β-cells Hashimoto *et al.* (2006) showed that β-cell depletion causes reduced insulin levels and hyperglycaemia.

On a similar note, Foxo1, a downstream target of PDK1, has been associated with diabetic symptoms in humans. Studies on German and Finnish men showed correlations between certain Foxo1A mutations and altered insulin secretion and impaired glucose tolerance (Mussig *et al.* 2009). Future research into this area may prove valuable for understanding the onset of diabetes in human patients (Maedler *et al.* 2006; Cnop *et al.* 2011).

1.1.2.2 β-Cell Regeneration Research

A simple stimulus for pancreatic growth was found in pancreatectomised mice. The mice had 90% of their pancreas removed and Bromodeoxyuridine (Brdu) was added to monitor the following pattern of growth for the remaining 10%. Brdu is a uridine based nucleoside that can be introduced and incorporated into the DNA of proliferating cells. Its incorporation can then be assessed using immunohistochemistry (Wojtowicz & Kee 2006). A sham group which had 90% of its pancreas perturbed by rubbing was used to contrast the growth of the pancreatectomised group. By day 3 the pancreas of the pancreatectomised mice had grown 195% (75% more than the sham group) and by day 6 the

pancreaectomised model had grown 261%, which was more than 100% higher than the sham model (145%). The researchers observed a shifting occurrence of Brdu staining with time as the stain would diminish from earlier areas just as much as it increased in the newer areas. After two days the growth had started in the common duct then moved into the growing regions within another day. The growing regions housed the ductal branching and articulated with capillaries and connective tissue essentially growing a typical pancreas which included apparent islets of Langerhans. This technique may indicate that β-cell islets may depend on signals governing the mass of the total pancreatic organ thereby adding to autoinhibition or downregulation of the growth of the β-cell component (Bonner-Weir *et al.* 1993).

The Reg (regenerating) family of proteins was established about two decades ago in studies on pancreatitis. Reg proteins were known to be expressed during the disease and were believed to be responsible for regulating inflammation and reducing infection (Nata *et al.* 2006).

Recent studies of the Reg gene found that increasing Reg protein synthesis within β-cells resulted in their regeneration ameliorating experimental diabetes. By adding interleukin 6 (IL-6; an inflammation regulator) and dexamethasone (a synthetic steroid) researchers were able to induce the expression of Reg. It was also found poly(ADP-ribose) polymerase (PARP; a protein involved in DNA repair and apoptosis) could deter the transcription of the Reg gene. By adding PARP inhibiters in with the IL-6 and dexamethasone treatment, mRNA levels of Reg increased further, consequently improving β-cell growth (Akiyama *et al.* 2001). Islet neogenesis associated protein (INGAP), a RegIII protein (part of the Reg family), has been implicated as a major islet growth factor through stimulating the growth of β-cell mass in many individuals (and many species)

both diabetic and healthy (Lipsett *et al.* 2007). PARP inhibiters used alone are believed to have therapeutic effects on diabetics. The PARP inhibiters reduce the effects of hyperglycaemia by reducing the production of advanced glycation end-products (AGEs) and reactive oxygen species (ROS). Decreases in intracellular ROS can defer apoptosis and sustain healthier β-cell mass ratios (Brownlee 2005).

Freund's complete adjuvant (FCA; a mixture of oil, water and deactivated mycobacteria) has shown health improvements in diabetic KK-Ay mice (a murine strain highly susceptible to diabetes) (Muto *et al.* 1997) while others have used the same adjuvant to augment pancreatic tissue transplantation (Suri *et al.* 2006). Tests showed FCA significantly bolstered the return to glucose homeostasis in non-obese diabetic (NOD) mice after the transplants. The direct health benefits were believed to originate from the immunity responses to FCA introduction. They recorded upregulation of immunity proteins such as interleukin 1 (IL-1; drives immunity response) which when upregulated by other means (not FCA) results in the same benefits (Suri *et al.* 2006).

1.1.2.3 Stem Cell and Progenitor Cell Research

Experiments studying the lineage of pancreatic cells have found evidence that pancreatic ductal cells can act as progenitor or stem cells for islets in neonatal models. These progeny include β-cells, other endocrine cells and acinar cells (Xia *et al.* 2009). The cause of islet regeneration *in vivo* has been in debate for some time with some arguments suggesting that cellular replication is primarily responsible, while others have suggested *de novo* islet generation from nearby progenitor cells. Hanley and Rosenburg (2009) demonstrated that human islets

can be dedifferentiated into duct-like structures (indicative of pancreatic ducts) when treated with a peptide derivative of INGAP.

Bar-Nur *et al.* (2011) developed four sets of pluripotency-induced β-cells (BiPSCs) to study the expression profile and efficiency of growing further β-cells. Using pluripotent cells meant they could be used to grow any cell type from a single sourced cell, in this case a β-cell (Yu & Thomson 2008; Chan *et al.* 2009; Bar-Nur *et al.* 2011). They assessed the methylation status of the pancreatic and duodenal homeobox 1 (PDX1) gene. The PDX1 gene encodes for an essential transcription factor required for β-cell maturation. They noted that the degree of methylation was significantly lower than that found in non-beta pancreatic iPSCs. This was regarded as an artefact from the BiPSCs normal β-cell origin and demonstrated an advantage using BiPSCs for β-cell replacement therapies in patients. Previous iPSCs experiments yielded lower β-cell production, making them inefficient for clinical use, so this BiPSC finding was thought of as a successful alternative to be explored (Bar-Nur *et al.* 2011).

The potential for β-cell mass regeneration does not exclusively require the stimulation of stem cells within the gland. Data have shown increasing evidence that future treatments may benefit by targeting the accompanying α-cells within the pancreas to either redifferentiate or evolve into β-cells to compensate for the loss. Thorel *et al.* (2010) investigated the reported relationship between α-cells developing into β-cells via paired box 4 (Pax4) gene expression in mice. Pax4 is an essential gene involved in fetal development as well as pancreatic progenitor cell growth in adults (Sosa-Pineda *et al.* 1997). After ablation of almost all β-cell mass (more than 99%) they observed a 3-fold increase in β-cell mass between 15 to 30 days (using Pax4). After 5 months of good treatment (maintaining 20 mM blood glucose) the mice had recovered enough to forgo any treatment. Mice that

remained diabetic at this point still had a 10-fold increase in β-cell mass whereas recovered mice had a 44-fold increase. Due to discrepancies in the predicted rate of β-cell regeneration and the appearance of actual β-cell mass they made the conclusion that most of the regeneration had come from a different source. Using yellow fluorescent protein in new samples they performed lineage tracing of α-cell replication after nearly complete β-cell ablation and found that a small proportion of α-cells (1-3%) had become bihormonal expressing both glucagon and insulin. One month after ablation 65% of the β-cells had descended from α-cells and most still retained substantial degrees of glucagon expression (Thorel *et al.* 2010).

These observations support earlier work which used known embryonic pancreatic developmental factors Ngn3, Pdx1 and Mafa to induce mature pancreatic exocrine cells to develop a β-cell phenotype. These induced cells began producing insulin (and C-peptide; an indicator in insulin production) within 3 days and ameliorated hyperglycaemia. Despite the progress the manipulated cells failed to form islet structures. This technique showed the possibility of avoiding dedifferentiation and redifferentiation to improve the efficiency of β-cell induction but the failure to form islets may highlight the importance of epigenetic memory (genetic conditions that can be inherited by progeny) (Zhou *et al.* 2008).

Aristaless related homeobox (Arx) is an embryonic development gene involved in forebrain, testicular and pancreatic development (Gecz *et al.* 2006). It was found that overexpression of Arx in β-cells could induce a characteristic change to α-cells and pancreatic polypeptide cells (PP cells). These cell types usually neighbour β-cells within pancreatic tissue and are derived from the same progenitor cells. It was postulated that by manipulating the balance between Arx and Pax4, α-cells and PP cells could be used to source β-cells for patient therapy

(Collombat *et al.* 2007). Further work by Collombat *et al.* (2009) demonstrated that the consistent expression of Pax4 could stimulate pancreatic cells to form β-cell islets even to the detriment of having an absence of α-cells causing hypoglucagonemia and enlarged β-cell islets. A key factor required in the pancreatic cell metamorphosis observed was the expression of Ngn3, an embryonic factor which has been seen to increase in expression in studies on pancreatic stem cell activation and progenitor differentiation (Collombat *et al.* 2009).

The multitude of evidence shows that β-cell loss can indeed be reversed, even though most of the data comes from experiments using animals other than humans. Strategies involving transplantation and other exogenous sources have been embraced by many people, and have given reasonable success but β-cell loss has remained an issue leading to the return of medicinal insulin treatment. Besides β-cell loss the lack of donors and immunosuppressant difficulties in humans continue to direct the need for research into endogenous systems of β-cell regeneration. The stem cell induction approach has shown the most promise for future patients but remains a lifetime away from being an adequate answer for the diabetes pandemic as questions of efficiency and long-term side effects remain to be answered (Tuch & Kannangar 2008).

The development of treatments which can control the growth and phenotype of cells in the pancreas and elsewhere in the body has been, and will remain, at the forefront of research into diabetes and other metabolic disorders. In sight of a common goal, research must also be done into the biochemistry that governs cell plasticity and growth in order to gain an understanding of the metabolic memory that cells suffer after periods of conditioning.

1.1.3 Metabolic Consequences of Prolonged Hyperglycaemia

A protracted experiment studying the effects of glucose exposure in diabetics has found that individuals who experienced periods of hyperglycaemia were more at risk of developing severe pathologies resulting from the high glucose concentration. The intensity and duration of therapy given an individual affected the onset of pathology. Those who were under intense glucose control were those whose blood-glucose levels were maintained to levels similar in non-diabetics while those who were under poor control experienced chronic hyperglycaemia. Individuals who were switched to an intensive control of glucose after a period of months of poor control showed a tendency to develop severe diabetes related pathologies (as detected by inflammation, ischemia and tissue breakdown) even after a long period of intensive control. It was this unavoidable occurrence of pathology that led the researchers to coin the term 'metabolic memory' (Nathan *et al.* 2005).

Various other tests have contributed to the overall understanding of the metabolic memory phenomenon. The findings supported earlier studies which observed the same hyperglycaemic-induced recurrence of pathology after the reestablishment of glucose homeostasis. Much of the diseases seen in individuals with prolonged diabetes have been well studied but an overall correlation with hyperglycaemia was never satisfactorily identified until the Diabetes Control and Complications Trial (DCCT) and the United Kingdom Prospective Diabetes Trial (UKPDS). The DCCT and the EDIC (Epidemiology and Diabetes Complications; follow up to the DCCT) were large scaled tests which incorporated over 1,000 patients, searching for links between diet, diabetes and diabetic pathology. Findings from the UKPDS later supported and expanded the understanding of diabetes (Ihnat *et al.* 2007).

Enduring chronic hyperglycaemia leads to increased advanced glycation end-product (A.G.E. or AGE) formation, increased polyol and hexosamine pathway fluxes and an excess of activation of protein kinase C (PKC) isoforms. These biochemical alterations induced by prolonged hyperglycaemia are some of the factors responsible for the apparent metabolic memory seen in diabetic pathologies (Browlee 2001). These biochemical alterations, and others, will be discussed in the following sections.

1.1.3.1 Metabolic Memory Causes Retinopathy

In a study of the role of histone acetylation, Zhong and Kowluru (2010) performed an experiment using rats to determine whether histone acetylation could be contributing to the metabolic memory causing retinal pathogenesis. One treatment group was kept in poor glycaemia control (PC), a second group was kept in good glycaemia control (GC; urine glucose below 150 mg/24 hr), with a third group kept in poor control for six months and then good control for another six months (PC-GC).

The PC group was found to have significantly lower weight and higher glycated haemoglobin (GHb) values than the control group. The GC group had similar weight and GHb levels to the control group. The PC-GC group showed similar values to the PC group during poor control with their values becoming similar to a healthy control group after the initiation of good control. In order to quantify histone acetylation, histone deacetylase (HDAC) and histone acetyltransferase (HAT) activity was measured from samples in each group. As HDAC and HAT are directly involved in gene expression their quantification would help determine if a ‘memory’ had been created in the DNA of the PC-GC group (de Ruijter *et al.*

2003; Zhong & Kowoluru 2010). In the PC group HDAC was three times higher with HDAC1, 2 and 8 being at least 70% higher than the control. HAT activity decreased as inferred by the 30% (total acetylated histone 3 decreased 20-30%) decrease in histone 3 acetylation. In the PC-GC group HDAC activity was increased along with HDAC1, 2 and 8 while HAT activity remained reduced presumably from the PC period. The GC group showed limited increases in HDAC activity and HDAC expression and no decrease in HAT activity.

The results from their experiment showed that even after six months of poor glycaemia control, six months of (recuperative) good control could not avert certain effects of prolonged hyperglycaemia (Zhong & Kowluru 2010).

In a simultaneous study Kowluru *et al.* (2010) looked at the role of inflammation in the pathology of retinal pericyte loss due to metabolic memory. Retinal pericytes are responsible for regulating blood flow through the capillaries that support the retina (Allt & Lawrenson 2001). Bovine retinal pericytes were prepared from calves and randomly placed into one of three treatment groups. One group was assigned to 20 mM of glucose for two days followed by 5 mM (normal levels) of glucose for four days. Another group was assigned four days of 20 mM glucose and then four days of 5 mM glucose. The third group was put on 20 mM glucose for four days followed by 5 mM glucose for eight days. Between periods of glucose treatments the cells were rinsed and the media were changed often.

To investigate the effect of dexamethasone (a synthetic steroid) inhibiting the intracellular proinflammatory process another group was incubated with 1 mM in the presence of 5 mM glucose for four days after a high 20 mM glucose four day period. Appropriate controls were performed alongside the mentioned treatments. The results showed that pericytes incubated in 20 mM glucose for up to 4 days

had significant increases in all measured proinflammatory mediators from at least 30%. Cells incubated for four days of 5 mM glucose after two days of 20 mM show significant decreases in IL-1β, NF-κB, VEGF and TGF-β (cell proliferation proteins) expression and transcription while showing an increase in ICAM-1 (immunity cell adhesion protein; needed for immune response) compared to the control. The cells treated with four days of 20 mM showed that the following four days of normal glucose did not bring about any benefit and that all proinflammatory mediator levels remained high. Extending the good glucose control period to eight days showed decreased levels in all but TGF-β but the other mediators were still well above normal. Four days of 5 mM glucose after four days of 20 mM glucose failed to stop pericyte apoptosis but dexamethasone proved to be a powerful regulator of high glucose by inhibiting pericyte apoptosis and maintaining normal levels of VEGF and NF-κB even when incubated for eight days in 20 mM glucose (Kowluru *et al.* 2010).

It is because of these experiments and many others that we now have an improved understanding of the epigenetic and metabolic memory which gives rise to the pathologies seen in diabetics (particularly Type 2 diabetics). Hyperglycemia causes an influx of glucose derived metabolites which leads to AGE formation, intracellularly and extracellularly, and higher ROS production. The AGE formation on mitochondrial proteins as well as strained glycolytic pathways causing excessive electron donation create the first half of a vicious loop ending with glyceraldehydes 3-dehydrogenase (GAPDH) inhibition. GAPDH is important for the complete catabolises of glucose within cells (Nicholls *et al.* 2012). Its inhibition can cause unhealthy downstream effects. The first by-product of prolonged hyperglycaemia, AGE formation, will be discussed in detail next.

1.1.3.2 A.G.E. Formation Driven by Hyperglycaemia

The hyperglycaemic cytosol facilitates an increased formation of glyoxal from the auto-oxidation of glucose. This increase is a direct result of the unhealthy influx of glucose which the cell is not designed to accommodate. It has been shown that the spontaneous nature of glyoxal formation increases within hyperglycaemic conditions (Thornalley *et al.* 1999). Another product resulting from this glucose backlog is methlglyoxal (MGO). MGO can be formed by the uncontrolled fragmentation of glceraldehyde-3-phosphate and dihydoxyacetone. 3-deoxyglucosone is another glucose by-product that can be produced through passive, non-enzymatic pathways (Thornalley 1990 as cited by Brownlee 2001). In normal cellular conditions the glyoxalase system is responsible for processing glyoxal and MGO into less reactive products. The glyoxalase system is comprised of two enzymes and reduced glutathione. When the amount of MGO and glyoxal exceeds the activity of the glyoxalase system, much of these unprocessed substrates go on to adversely affect the cell (Xue *et al.* 2001). Aldehyde reductase has also been found to reduce AGE production in tests on PC12 cells from rats (by convert glucose to sorbitol, thereby reducing available glucose). Hyperglycaemia can overwhelm these protective enzymes leading to more AGE production (Suzuki *et al.* 1998). Much of the interaction that forms the resultant AGE products occurs through Maillard reactions (the non-enzymatic binding of sugars with amino acids in the presence of heat) (Reddy & Beyaz 2006).

Extracellular AGE is known to react with various matrix proteins such as collagen. AGEs can form cross-links between proteins in the matrix increasing stiffness. Sims *et al.* (1996) as cited by Beilin *et al.* (2001) described histological studies where AGE tissue accumulation and aortic stiffness were correlated. There are

various receptors which ligand with AGEs, most notably RAGEs. RAGEs, upon ligation can induce vascular lesions causing disease.

Park *et al.* in 1998 studied the effects of a truncated RAGE receptor (sRAGE) in atherosclerosis. ApoE-null mice (susceptible to atherosclerosis by way of a lipid transfer gene deletion) usually develop atherosclerosis earlier than their normal counterparts. A group of these mice were diabetically induced with streptozotocin. Streptozotocin is a toxin similar in structure to glucose and as such the GLUT-2 receptors on β-cells almost exclusively take in the toxin causing damage to the β-cells (Szkudelski 2001; Bolzan & Bianchi 2002). After six weeks of diabetes there were discrete lesions at common points in the thoracic aorta and aortic arch and had 5.3 times more area affected by lesions than the control.

The diabetic group had a 2.3 fold increase in AGE from kidney extracts and a 2.5 fold increase in plasma AGE than in the control group. sRAGE was administered intraperitoneally once a day into hyperglycaemic mice and euglycemic mice. Another group received mouse serum albumin (MSA). sRAGE treated diabetic ApoE-null mice had decreases in aortic lesion area and complexity relative to the doses received. The diabetic mice treated 40 μg/day showed the same clear results as the non-diabetic mice treated with 40 μg/day MSA (both groups were ApoE-null). It was suggested that introducing sRAGE into the vascular system may compete for binding with free AGE having an inhibitory effect (Park *et al.* 1998).

1.1.3.3 Biochemical Pathways Overloaded in Hyperglycaemia

The polyol pathway flux has been implicated with various pathways to pathology in a cell. The polyol pathway (non-flux) is involved in converting glucose into

sorbitol via the enzyme aldose reductase and then turning sorbitol into fructose via the enzyme sorbitol dehydrogenase (Lee & Chung 1999; Chung *et al.* 2003). Much of the connections between the flux and pathology have now been attributed to the excess activation of protein kinase C (PKC) which has its own pathways. Aldose reductase converts glucose into sorbitol, with low affinity, using NADPH. NADPH is used to reduce glutathione (GSH) by glutathione reductase. It is the decrease in NADPH used by aldose reductase which brings about the decreased levels of GSH (Browlee 2001). Sorbitol dehydrogenase turns sorbitol into fructose using NAD+ and turning it into NADH causing further channelling of glucose down the polyol pathway. This loop exacerbates the GSH decrease causing potential oxdative stress to the cell and reducing its role as an antioxidant (Lee & Chung 1999).

Hyperglycaemia can cause an increase in the flux of the hexosamine pathway. The pathway is incorporated into a sensing mechanism that triggers the synthesis of cell stress proteins (Hanover *et al.* 2010). Having high glucose within the cell may cause the simultaneous production of glucosamine-6-P from fructose-6-P (instead of producing high fructose-1,6-bisP) by glutamine:fructose-6-phosphate amidotransferase (GFAT). The excess glucosamine is then converted to N-acetylglucosamine (GlcNAc) which is then attached by the O-GlcNAc transferase enzyme to transcription factors such as Sp1 as O-GlcNAc-Sp1. The binding of glycosylated transcription factors is believed to generate more expression of their corresponding genes than normal phosphorylated transcription factors (Brownlee 2001).

An experiment on glucosamine concentration within mesangial cells (smooth muscle cells that regulate blood flow through the kidneys) showed that low concentrations allowed the cells to proliferate but that higher glucosamine

concentrations induced increases in proapoptotic proteins. An amount of glucosamine (10 mM) administered for four hours showed a three to four fold increase in p53 (which regulates many genes including proapoptotic genes) which was sustained for eight hours. Other proapoptotic changes were observed with increased levels of Bax and decreased levels of Bcl-2 (Le *et al.* 2010).

1.1.3.4 Excessive PKC Activation by Hyperglycaemia

Hyperglycemia can increase the production of diacylglycerols (DAG) from glycerol-3-phosphate, which is produced from dihydroxyacetone phosphate. This increase in DAG activates nine of the enzymes in the PKC family (Assert *et al.* 2001; Lori *et al.* 2003). Activated PKC-beta and delta isoforms increase NADPH oxidase activity leading to increased ROS production. NADPH oxidase is an enzyme that uses reduced nicotinamide adenine dinucleotide phosphate (NADPH) to bind with oxygen to form superoxide, one of the ROS species (Bedard & Krause 2007).

Further capillary occlusion coupled with AGE formation can be due to increased PKC giving rise to increased TGF-β. It is through increased TGF-β that an increase in collagen and fibronectin can occlude capillary blood flow (Brownlee 2001). An experiment researching the effects of a PKC beta inhibitor in diabetic db/db mice showed promising therapeutic properties for the inhibitor. The db/db mice had a 400% increase in mesangial extra cellular matrix (ECM) contributed largely by fibronectin and type IV collagen. Subjects treated with the inhibitor had approximately half the mesangial area than subjects not treated showing evidence that PKC beta is involved in the overexpression of proteins for the ECM. Increased TGF-β expression was observed in the glomeruli of the db/db mice.

This expression was attenuated along with excessive ECM area in subjects treated with the PKC-beta inhibitor (Koya 2000).

1.1.3.5 ROS Production Due to Hyperglycaemia

Du *et al.* (2003) have performed many experiments providing an abundance of data, about the role of ROS and diabetic pathology. They treated bovine aortic endothelial cells with different treatments, two in particular, 5 mM glucose or 30 mM glucose. The cells with 5 mM glucose were used to simulate normal glycemic conditions while the 30 mM glucose was used to simulate diabetic conditions. GADPH activity in the 30 mM group was highly inactivated, as is believed to occur in diabetics in vivo. Normal GAPDH activity was observed in the group treated with 5 mM glucose.

Another group treated with 5 mM glucose and a GAPDH inhibitor (GAPDH antisense oligonucleotides) showed similar GAPDH inactivity to the 30 mM group. This evidenced the understanding that GAPDH can be regulated by glucose levels. They further found that GAPDH inhibited 5 mM cells expressed approximately the same increased levels of PKC activation, intracellular AGE formation and nuclear factor kappa-light-chain enhancer activated of B cells (NF-κB) activation as the 30 mM group. NF-κB is responsible for activating many cell stress response genes (Li & Stark 2002). Its activation is indicative that the endothelial cells were under stress during exposure to hyperglycaemia. These findings further supported GAPDH as being glucose regulated. They inhibited poly(ADP-ribose) polymerase (PARP) and observed a correlation in continued GAPDH activity in 30 mM cells which showed the opposite level of activity to GAPDH in normal PARP 30 mM cells (Du *et al.* 2003).

1.1.3.6 Glycation of Mitochondrial Proteins

It is believed that an increase in cellular glucose saturates the electron transport chain (ETC) with electron donors from the citric acid cycle (TCA). The saturation of the ETC unbalances the electrochemical potential allowing for prolonged existence of intermediates (ubisemiquinone etc.) which gives rise to ROS. As this perturbed ETC system continues to produce ROS the levels of ROS escape the super oxide dismutases and cause damage to the DNA. Poly (ADP-ribose) polymerase (PARP) is activated by this DNA damage and uses NAD+ to create nicotinic acid and ADP-ribose. Excessive amounts of ADP-ribose cause some to bind to GAPDH inactivating it. Inactivated GAPDH gives rise to further increases in ROS via a backup of glycolytic metabolites. High glyceraldehydes-3-P contributes to increased PKC activation and MGO production which causes AGEs. High fructose-6-P contributes to the increased hexosamine pathway flux and high glucose contributes to the increased polyol pathway flux. This is the vicious cycle created by excessive glucose which causes much of the pathogenesis in diabetes (Brownlee 2005).

Rosca *et al.* (2005) studied the effects of glycation of mitochondrial proteins. They extracted mitochondria from the kidneys of Lewis rats which had been diabetically induced and kept in pathogen-free conditions. Appropriate controls were set up. The mitochondria was subjected to several experiments looking at glycaemia control, oxidative stress, carbonyl-induced modification of mitochondrial proteins and the effects of aminoguanidine on compromised ETC.

They observed the usual hyperglycaemic symptoms of higher Hb glycation in streptozotocin induced diabetic rats than the controls. After 12 months the mitochondria from diabetic rats experienced significant inhibition of state 3 respiratory activity and increased state 4 activity. A NADH oxidase assay tested

the integrity of the ETC. The ETC was significantly inhibited by 19% after 12 months of diabetes. They further investigated the ETC components to find that Complex III was the primary effected component in the ETC by hyperglycaemia.

Inhibition or interference with Complex III is thought to increase the output of ETC derived ROS by prolonged exposure of ubisemiquinone to oxygen. The research team then diverted to discovering whether there had been earlier mitochondrial protein modification putatively caused by hyperglycaemia. Western blotting and immunoprecipitation revealed that two of the eleven Complex III components are modified by MGO (AGE formation). Aminoguanidine (a drug used to inhibit AGE formation from 3-deoxyglucosone (Nilson 1999)) administration decreased the MGO-induced modifications (Rosca *et al.* 2005).

The onset of a metabolic memory, in cases of diabetes, is believed to be driven primarily by a build-up of glucose in the circulation. The methods where this build-up occurs can be different, but after long periods of suffering the end result of this build-up is the same. The deposition of AGE products, and the constant release of ROS in the system causes stress to the tissue and affects the individual cells. In response the cells undergo programmed cell death, or apoptosis, which is evident in cases of retinopathy and pancreatitis where cellular breakdown has caused organ dysfunction (Kowluru 2010; Zhong & Kowluru 2010).

In order to appreciate the contribution that cellular breakdown plays in diabetes we must understand the role that apoptosis and programmed cell death play in regulating tissue growth. Controlled cellular breakdown is as important as cellular growth. This system ensures the avoidance of constant tumours and unnecessary biomass in healthy individuals.

1.1.4 Apoptosis and Programmed Cell Death

The word apoptosis is used to describe the organised breakdown and loss of cells. It is sometimes used variably with the term 'programmed cell death' coined by Lockshin and Williams (1964: as quoted in Pearce 2008). Early research into biological systems witnessed the occurrence of cell growth and proliferation while recording the occurrence of organised cell loss. This cell loss was initially thought to be controlled by necrotic events but overtime and by the assistance of ever-increasingly powerful technology, it became more evident that cell loss was being controlled not just by necrosis but by innately-programmed biological pathways (Kerr *et al.* 1972). Apoptosis is now understood to be a part of a larger scheme of cell regulation that occurs in developing animals as well as their aged counterparts. This regulation occurs alongside mitosis (cell growth by dividing) to bring about the precise organisms living today (Elmore 2007).

A robust model of apoptosis was devised using the nematode *Caenorhabditis elegans*. Due to its ease of cultivation and simple cell structure (1,090 cells in hermaphrodites; 1,179 cells in males) *C. elegans* provided a simple platform where cell growth could be monitored alongside developmental apoptosis. The number of cells that undergo programmed cell death (131 cells in hermaphrodites; 148 cells in males) during the organism's development was also an easier task comparative to more complex organisms. Researchers found that at least 13 genes were associated with the apoptotic events and that most of these had conserved homologues to more complex species including humans (Horvitz 1999).

Three major pathways have been described that can initiate programmed cell death, each of which lead to the activation of pro-apoptotic caspases. The perforin/granzyme pathway is used by cytotoxic T cells and natural killer (NK)

cells to target other neighbouring cells for apoptosis. The perforin protein binds and inserts into the target membrane forming oligomeric pores that allow the next piece of the pathway, granzyme, to pass through into the cytosol of the target cell (Law *et al.* 2010). Granzyme A activates the SET complex (a group of proteins containing the 'SET' protein that are involved in DNA cleavage), which then brings about DNA cleavage via the release of DNase NM23-H1 while granzyme B activates caspase 3 and caspase 10 (Fan *et al.* 2003). The extrinsic pathway relies on the ligand-activation of target cell-surface death receptors. There are multiple receptors identified but some better understood versions are FasR and TNFR1. FasR binding immediately recruits Fas-associated protein with death domain (FADD) while TNFR1 binding recruits tumour necrosis factor type 1-associated death domain (TRADD), FADD and RIP (a protein kinase needed for apoptosis (Barcia *et al.* 2003)). These factors come together to produce the death inducing-signalling complex (DISC) which with procaspase-8 triggers activity of caspase 3. Activated caspase 3 is a master switch for apoptosis (Kischkel *et al.* 1995). The last pathway is the intrinsic pathway. Cellular stress from invasive chemicals, such as toxins and ROS, as well as conditions like hypoxia, brings about mitochondrial stress. The release of cytochrome c from stressed mitochondria into the cytosol forms the apoptosome with Apaf1 and procaspase-9. The apoptosome then activates caspase 3 (similar to the extrinsic pathway) which is a key switch in committing the cell to undergo apoptosis (Elmore 2007).

Cells can endure different types of stress for varying periods. It has been found that the Hsp60 protein can be released by these cells as a potential indicator of stress. Elevated levels of Hsp60 have been found in diabetic patients (Devaraj *et al.* 2009; Yuan *et al.* 2011) and it is thought that this quandary may provide pivotal information to understanding the prevalence of tissue breakdown in

diabetes. By first understanding Hsp60 we may make better judgements about its role in diabetes.

1.2 Heat Shock Protein 60

1.2.1 Biological Importance of Hsp60

Hsp60 is a 60 kD protein most often found within healthy mitochondria. As a member of the chaperonin family it is involved with the transportation of polypeptides originating from the cytosol into the mitochondrial matrix. It is further involved with the successful folding of those same polypeptides into their tertiary states. Hsp60 is not only found in the mitochondria but as a functioning protein in the cytosol as well, acting as a chaperone and partner in other reactions (Gupta & Knowlton 2005; Quintana & Cohen 2011).

The Hsp60 protein has at least 150 homologues in various species including some that closely describe our world's biological origins such as archea. Many of these homologues are between 40 to 100% conserved in amino acid sequence similarity (Brocchieri L & Karlin S 2000). The most commonly studied homologue to human Hsp60 is GroEL from *E. coli* strains. In early research GroEL was characterised by studies that analysed the synthesis of bacteriophages in *E. coli* colonies. By adding inhibitive mutations to the genes for GroEL and GroES (Hsp10 homologue) the bacteriophages were not synthesised leading researchers to postulate that GroEL and GroES were important factors in protein synthesis. Further research showed these same mutations rendered the cells incompatible with heat stress at 42^{o}C (Zeilstra-Ryalls *et al.* 1991). Later research on GroEL showed that translated polypeptides, for a number of essential proteins, as well as the non-bacterial human ornithine transcarbamylase (OTC) protein failed to fold

into their tertiary states when the mutant GroEL was rendered useless by heat shock (using a mutant GroEL produced with heat sensitive mutations). The polypeptides were instead found to fold spontaneously into other forms or aggregate and precipitate (Horwich *et al.* 1993; Fenton *et al.* 1994).

As evolution had already indicated the immense importance of Hsp60 it has been found that a number of diseases that affect the human condition have been linked to deficiencies in this chaperone. Several mutations to the HSPD1 gene encoding human mitochondrial Hsp60 (mitoHsp60) have been linked to hypomyelination and concomitant neurodegenerative disorders (Magen *et al.* 2008). Deletions and substitutions of various amino acids in the mitoHsp60 protein have proven overwhelming to the health of the hosts' mitochondria. A missense mutation, D29G, is implicated with a complicated spastic paraplegia (SPG) while a V89I mutation leads to (SPG13), a latent version of the disease with high penetrance. It has been postulated that patients that live with these allelic mutations subsist on the mitoHsp60 produce by the alternate allele ergo suffering from hypomyelination (Magen *et al.* 2008).

1.2.2 Hsp60 Form and Function

In order for these Hsp60 related processes to take place, the Hsp60 must first be incorporated into a 14 member oligomer consisting of identical Hsp60 proteins. The complex forms in the shape of two rings. Both rings contain seven proteins and these rings bind together to form the cylindrical quaternary structure. This quaternary complex was initially named GroEL after its characterisation in *E. coli* and dominates the titles of past research into chaperonins. This Hsp60 complex, hereafter referred to as chaperonin60, is still not complete without the partnership

of Hsp10. Hsp10 forms a polymer from seven identical proteins which has been described as a cap that articulates with the quaternary Hsp60 complex. Like GroEL, the initial name given for the seven member complex was GroES in *E. coli* hereafter referred to as chaperonin10 (Horwich *et al.* 2007). Three domains have been described in the chaperonin60 structure, each being distinct in function from the other domains. The apical domain houses the binding sites for substrates and the chaperonin10 cap. The intermediate domain provides flexibility to the complex needed during the binding of ATP. The equatorial domain provides the site for ATP binding and as indicated by its name provides the articulation sites for binding with the partnering ring structure to form the quaternary chaperonin60. During the chaperonin60s hydrophobic-surface state a polypeptide substrate can bind to the apical domain via a hydrophobic groove between two helices, H and I. ATP then binds to the equatorial domain changing the chaperonin60 conformation which in turn changes the hydrophobic-surface state to a hydrophilic one. This releases the polypeptide into the chaperonin cavity while also priming the apical domain to bind with chaperonin10. Inside the cavity hydrophobic and hydrophilic interactions between the polypeptide and the chaperonin play a role in accommodating the desired folding. As ATP is turned to ADP chaperonin10 is also released and the newly folded protein is released into the intracellular space (Feltham & Gierasch 2000; Ranford *et al.* 2000; Horwich *et al.* 2007). Due to the serious requirement for cells to produce viable proteins functioning in the correct location Hsp60 is one of the most conserved genes in evolution.

Hsp60 is one of several proteins that form the heat shock protein family. Like other heat shock proteins (Hsps) Hsp60 can assist in protein folding and chaperoning of the protein structures to maintain their stability within cells. Heat shock treatment causes increased expression of Hsps which has been used to

demonstrate the arrest of cellular apoptosis after mild heat shock (Calderwood *et al.* 2007). Other forms of stress can cause increases in the expression of Hsps, many of which have yet to be elucidated.

The Hsp60 protein has been the focus of some 'chicken and egg' research in the past. Cheng *et al.* (1990) used a mif4 yeast strain containing a temperature-sensitive Hsp60 to determine if introduced wild-type Hsp60 could rescue the heat stressed cells from inhibition and death. At 37^{o}C the growth of mif4 is inhibited and can only be redeemed if the temperature is lowered to 23^{o}C within 6 hours. By growing the mif4 at 37^{o}C they found that the only cells growing were transfected mif4 (containing the wild-type Hsp60) (Cheng *et al.* 1990).

1.2.3 Hsp60/Caspase Mediated Apoptosis

Hsp60 has been shown to form a sequestration complex with the pro-apoptotic protein Bax in the cytosol of cardiomyocytes. This has been confirmed by electron paramagnetic resonance (EPR) and immune-electron microscopy which have shown a colocalisation of the two proteins while others have also observed the anti-apoptotic Bcl-XL protein colocalising with Hsp60. Experiments testing the effects of cellular stress due to hypoxia or by decreasing the amount of cellular ATP (similar end-result to hypoxia) have shown translocation of Hsp60 to the plasma membrane and the concomitant translocation of Bax to the mitochondria. The molecular reason for the division between Hsp60 and Bax is not fully understood but dose dependant administration of antisense Hsp60 has further confirmed that reductions in Hsp60 lead to increased degradation of Bcl-XL and increased synthesis of Bax. Administration of Hsp60 to previously Bax administered cells also inhibits apoptosis. Bax proteins form oligomers which

install into the mitochondrial membranes as pores. Any free cytochrome c can then leech out through these pores into the cytosol and combine with Apaf-1 and caspase 9 to form the apoptosome. This then stimulates caspase activity ensuring the apoptotic determination of the cell (Gupta & Knowlton 2005). Hsp60 has been implicated as a target of the autoimmune response seen in β-cells. The transgenically induced expression of an auto immune-sensitive Hsp60 epitope in the thymus reduced the occurrence of diabetes in NOD mice from 76% to 27%. In normal individuals it is thought that T-cells target specific Hsp60 epitopes that are expressed on the surface of the β-cells while tolerating the expression of many other Hps60 epitopes expressed in other tissues (Birk *et al.* 1996).

1.2.4 Extracellular Hsp60 Activity

Ghosh *et al.* (2008) demonstrated that elevated levels of Hsp60 can be found in adenocarcinoma cells of human breast and colon tissue. By using interfering siRNA designed to ablate Hsp60 (both the cytoplasmic and mitochondrial) they observed a decrease in the amount of the IAP (inhibitor of apoptosis) family protein survivin that could be extracted using western blots. This decrease in survivin is thought to be evidence contributing to a theory that Hsp60 actively sequests survivin protein in ‘pools’ within mitochondria that allow for survivins quick release to inhibit apoptosis in times of cellular stress. The cytoplasmic survivin is understood to prevent the activation of caspase-9 by binding with it inherently reducing caspase-9s binding with the apoptosome (Dohi *et al.* 2004). Within healthy cells this role is an acceptable occurrence prolonging cellular viability whereas in cancer cells the increased Hsp60 my actually help propagate cancerous growth by unnecessarily halting apoptosis. Further research in the

same study by Ghosh *et al.* (2008) showed that the ablation of Hsp60 correlated with an increase in p53 expression which is thought to induce Bax related apoptosis. By regulating the levels of Hsp60 in the tumours of cancer patients it is postulated that the tumour regulating proteins described can be reinstated to their normal healthy roles.

The term 'metabolic memory' has been used to describe the state of vascular breakdown occurring in long-time diabetic patients. The major contributing attribute of patients with apparent metabolic memory is hyperglycaemia which can be brought about by a prolonged high glucose diet, insulin resistance or β-cell deficiency. Higher levels of blood-serum Hsp60 have been observed in most cases of the disease and when considering the latest research into Hsp60 and inflammation, it becomes clear that an understanding of Hsp60s role in potentially propagating diabetes needs to be specifically investigated (Jax 2010). A recent clinical study has highlighted the state of serum Hsp60 and anti-Hsp60 expression in diabetic patients before and after intensive glycaemic control. Researchers found that despite seeing significantly reduced glycosylated haemoglobin, and decreases in BMI (body mass index), waist circumference and HOMA (homeostatic model assessment) figures, the levels of serum Hsp60 and serum anti-Hsp60 did not change. Even the levels of variance in Hsp60 sampling showed little change. A significant decrease in IL-6 was also recorded suggesting a small, potential decrease in inflammation but the levels of IL-8, IL-10, IL-12 and TNFα were unchanged. This observation may add to our understanding of the correlation between Hsp60 and metabolic memory (Blasi *et al.* 2012).

A study on children suffering from clinically diagnosed septic shock (a whole body inflammatory disease due to microbial infection) used ELISA techniques to investigate the levels of Hsp60 in the blood serum of 63 children suffering from

sepsis, 10 critically ill children not suffering from sepsis, and 24 healthy control children. They found that 24 hours after entry those with sepsis had significantly higher amounts of serum Hsp60 than those who were compromised with other illnesses. This was also apparent when comparing the sepsis patients with the healthy controls. The median Hsp60 levels in sepsis patients were 16.7 ng/ml whereas the levels in the other groups were 0 ng/ml (Wheeler *et al.* 2007).

Hsp60 has been well characterised as an important factor in many types of heart disease. Patients suffering from arterial fibrillation (irregular heart beat) were compared with healthy controls with regular heart beats (sinus rhythm). The researchers used samples of myocardial cell samples excised from the right atria in patients undergoing cardiac surgeries and found that the levels of Hsp60 were significantly higher with a 2.5-fold increase in patients with arterial fibrillation (Shafler *et al.* 2002). Earlier work on the hearts of patients suffering from dilated cardialmyopathy (DCM) showed similar patterns of increased Hsp60 expression in stressed cells excised from hearts during surgeries. They witnessed a 5-fold increase Hsp60 expression in tissue with DCM than the healthy donor hearts. Another observation recorded by the researchers was that the DCM heart samples contained much higher development of type I and III collagen in the form of fibrosis, another indicator of substantial tissue stress (Latif *et al.* 1999). Studies on murine hearts have illustrated well the movement of Hsp60 from intracellular locations to the surface of stressed myocytes. From nine to twelve weeks after LAD ligation of the rat hearts, data showed localisation of Hsp60 to the membrane of cells, with some treated samples having Hsp60 on the outside surface of the membranes. TNF-α, LVDD, BNP and ANP were increased confirming high levels of stress and the propagation of inflammation. By using fluorescently labelled indicators that bind to caspase 3, 7 and 8 that fluoresce

during caspase activation the researchers observed that in cells with Hsp60 localising to the membrane also had a correlated increase in caspase 3, 7 and 8 activation. By using propidium iodide to stain for ruptured membranes they found that cells with membrane located Hsp60 had no greater inclination to accept the PI stain than other cells without the same Hsp60 profile, indicating that the localisation of the Hsp60 to the membrane correlated well with apoptotic events in those respective cells (Lin *et al.* 2007; Knowlton & Uma 2008).

Hsp60 has been found to hold extracellular roles differing from the protein-chaperoning it is primarily responsible for inside host cells. Recent research from the past decade has given evidence that Hsp60 is an important node in the immune network. Research into monocytes and dendritic cells has revealed that Hsp60 present in the corresponding media can cause these innate immunity cells to mature and activate their immune responses. This can result in the release of various pro-inflammatory molecules such as IL-1β, IL-6, IL-12, IL-15 and TNFα into the extracellular space (Henderson *et al.* 2010; Quintana & Cohen 2011). Hsp60 has also been found to interact with B cells and T cells. Cohen-Sfady *et al.* (2005) used murine B cells to test the immunicological interactivity of human Hsp60. They found that dose dependant exposure to Hsp60 could be correlated with respective increases in B cell proliferation, a consequence not seen before in other immune cells exposed to Hsp60. B cells also released a differing profile of cytokines to other immune cells. These B cells were secreting higher levels of IL-10 and lower levels of IL-6. Once placed in the presence of T cells the B cells drove the T cells to release IFN-ϒ and IL-10. By comparing B cells between wild-type, mutant TLR4 receptor and knockout MyD88 (myeloid differentiation primary response gene) cell variants it was deduced that Hsp60 interaction with B cells used TLR4 receptors (Cohne-Sfady *et al.* 2005).

1.3 Mitochondria

1.3.1 The Mitochondrial Organelle

Mitochondria are eukaryotic cell organelles that are responsible for the production of ATP energy within their host cells. Mitochondria range from 0.5 µm to 1 µm in size and are believed to be derived from a symbiosis between ancient eukaryotic and bacterial cells. This relationship has landed mitochondria with many roles in cellular growth, adaptation and death. Mitochondria have retained a small amount of DNA where genes for a variety cellular growth and regulation genes can be found. Most important genes for growth and adaptation still reside within the cells' chromosomes. As such, the analysis of mitochondria has become a means of understanding this observed cell plasticity under stress, and a means of analysis of programmed cell death (Henze *et al.* 2003).

1.3.2 Mitochondria and Hsp60 in Disease

By comparing the expression and profile of Hsp60 and mitochondria researchers have ascertained ways to understand and predict stress under certain conditions. Hsp60 has been found useful in predicting the onset of desired apoptosis in tumours in human bladders. The usefulness of Hsp60 expression analysis exceeded that of p53 analysis, the next trigger in the apoptotic pathway, much closer kinetically to the apoptotic event. By improving the awareness of Hsp60 expression future patients needing chemoradiotherapy to treat the cancer may be better managed, avoiding excessive exposure to the aggressive treatment (Urushibara *et al.* 2007). A study on murine myocytes used an adenoviral vector incorporated with Hsp60 and Hsp10 (AdvHsp60 and AdvHsp10) to increase the

said proteins' expression in the host cells' mitochondria. It was found that during ischemia and reperfusion cells with increased levels of AdvHsp60 and AdvHsp10 were able to avoid apoptosis by 40% compared to the controls. The overexpressing cells were also better maintained during reoxygenation having mildly lower caspase-3 activation initially but substantially lower activation after 4 hours. These data provide a means to use and develop Hsp60 clinically to improve patients' outcomes after physically stressful injuries (Lin *et al.* 2001).

In order to develop protocols for medical professionals to diagnose and assess patients suffering from diabetes and metabolically related diseases more research needs to be completed into using Hsp60 as a marker for cellular stress. Transfection of cells offers an effective way to introduce fluorescently labelled Hsp60 and other genetic information into living eukaryotic cell lines. The labelled Hsp60 can then be followed using fluorescence microscopy to ascertain the degree of stress that certain conditions produce.

1.4 Cell Transfection

1.4.1 Various Transfection Events

The term transfection describes a procedure where foreign genetic material is introduced into a living eukaryotic cell. As a result of differing parameters such as cell type, transfection method and environmental condition, the transfection protocols implemented in different experiments can be very disparate. The physiological results of the introduced nucleic acids may also play an important part in dictating what kind of transfection should be performed (Kim & Eberwine 2010).

Stable transfections are performed when introduced nucleic acid is incorporated into the chromosomes of the host cell. This incorporation requires that the genes encoding new mRNA be accompanied by selection markers such as specific-drug resistance genes. After one to three days the original cell media is replaced by selective media. Approximately two to three days after this exchange the remaining culture growing in the presence of the stressor drug is believed to be due to cells that have incorporated the foreign nucleic acids into their chromosome (Recillas-Targa 2006).

Transient transfections are performed when introduced nucleic acid is brought into regions of the cell that allow for the processing and transcription of the genetic code. Cells can be successfully transfected (transiently) by introducing mRNA into the cell cytosol. mRNA located in the cytosol can be directly translated by the host ribosomes into the concluding protein. Transient transfection with DNA requires the foreign DNA to be brought into the host cells nucleus where it can be processed and transcribed by the host cells transcription apparatus. Transient transfections may last from 1 to 3 days in common cases before the genetic material is lost (Recillas-Targa 2006).

1.4.2 Transfection Methods

There are many transfection protocols used which have inherent advantages and disadvantages dependant on the cell type, time and cost involved. The calcium phosphate method is comparatively cheaper than any other approach. It relies on the binding between molecules of calcium phosphate and adsorbing DNA molecules in the transfection solution. The method of DNA uptake by the cells is not fully understood but endocytosis and phagocytosis of the calcium phosphate-

DNA complex are thought to be possible pathways for the DNA uptake. A disadvantage of relying solely on chemical methods is that transfection efficiencies can be as low as 1% in certain cell lines (Jordan *et al.* 1996; Salozhin & Bolshakov 2009).

A similar method to the use of calcium phosphate includes the cationic lipid driven lipofection. Despite the differing names and structures of these lipid agents they all have similar elements that characterise the fundamental quality of transfection lipids. They have a positively charged head group which interacts electrostatically with the negatively charged sugar-phosphate backbone on the nucleic acid. The lipid molecules themselves can interact together to form approximately 100 nm liposomes which, being positively charged, migrate towards the negatively charged cell membranes. It is believed that the complex is taken up by similar means seen with other chemical transfection reagents such as calcium phosphate. The pathway from the cytosol to the nucleus remains elusive but it is postulated that the entire lipid-DNA complex may be brought into the nucleus where the nucleic acid is then processed. Despite the improvement in transfection efficiency when compared to non-lipid reagents the same disadvantage remains for certain cell types that still produced as little as 1% transfection efficiency. Lipofectamine 2000 is among the most commonly used lipofection agents available (Dalby *et al.* 2004).

Physical methods for transfection have been increasingly popular overtime as the technologies that govern these protocols have become more refined. There are many different physical approaches that omit cationic molecules and biological vectors and still achieve substantial transfection efficiency. A major dividing factor between these approaches is whether the protocol is predominantly mechanical or physical in nature. Mechanical protocols can use either

microinjection or ‘gene-gun’ apparatus. Microinjections have been known to produce nearly 100% transfection efficiency in target cells (Zhang & Yu 2008). Though the advantages are obvious the disadvantages include labour intensive single-filed cell manipulation. To achieve a maximal outcome requires consistency and copious amounts of time, even after the cost of the apparatus has been considered. The gene-gun or ‘biolistic’ approach is similar in demand for financial investment but has a wider application. Shallow cell cultures or tissue surfaces are the limit to the current generation of devices but are sufficient to warrant the use of the gene-guns for many research applications and topical treatments on patients. A comparative study showed slightly higher transfection efficiencies for gene-gun transfections than transfections performed using Lipofectamine 2000 on mammalian cells (Uchida *et al.* 2009).

Predominantly physical protocols include electroporation, sonoporation and laser irradiation. Electroporation and sonoporation rely on the same premise that pulsating cells with electricity or ultrasound can cause a disruption in the cell membrane resulting in pores that allows the DNA to diffuse in with or without aid from chemical reagents. Laser irradiation, or ‘phototransfection’, has shown much promise in recent years. The protocol requires the pulsation of a cell membrane with a laser for as short as one femtosecond that can create a pore large enough for the DNA to diffuse into. The transfection efficiency has been seen as high as 100% (Tirlapur & Konig 2002). The other advantage to using laser irradiation is that sections of cells can be targeted specifically, so in the case of neuronal cells, a dendrite or axon could be transfected deliberately without interfering directly with the soma. The major disadvantage again is a high financial threshold and an additional level of training required to operate the device (Mehier-Humbert & Guy 2005).

Magnetofection has been considered a mechanical approach to transfection but is best used in conjunction with chemical reagents and viral vectors. By precipitating DNA onto electrolyte coated, magnetic nanoparticles of iron oxide Christian *et al.* (2003) performed successful transfections on a range of eukaryotic cells using various transfection reagents and vectors. They observed increased transfection by up to four orders of magnitude among the treatments. Another improvement noted was that the time taken to achieve substantial transfection numbers was reduced from hours to mere minutes.

Transfection and transformation have been used in conjunction with various other protocols to analyse the efficiency and result of the genetic fission. An increasing number of researchers have turned to immuno-staining and integrated fluorescent proteins to label the organelles and proteins of interest. By attaching an Hsp60 to a GFP label through genetic manipulation, a cell can be observed from the outside through fluorescence microscopy without needing to add invasive labelling chemicals during the time of testing. In order to understand the affect florescence can have on a sample we need to understand first what the fluorescence phenomenon is.

1.5 Fluorescence in Cell Culture Analysis

1.5.1 Fluorescence in Problem Solving

The use of fluorescent chemicals to analyse biological systems was pioneered around the 1980s. The original fluorescent probes were at first too inefficient to produce consistent and reliable data. Often the wavelength was too short and the extinction coefficient was poor. These short comings often resulted in cellular autofluorescence and a fleeting signal. More complicated problems involved

compromising cellular integrity to achieve a significant signal (Grynkiewicz *et al.* 1985). Grynkiewicz *et al.* (1985) were the first to present data showcasing a, then, new generation of advantageous fluorescent probes. These were stilbene chromophores attached to chelating molecules that targeted primarily Ca^{2+} in red blood cells.

The benefits of fluorescent imaging and processing have encouraged the further development of the technology and it has expanded into many different applications. Photo induced electron transfer (PET) is based on a system where a fluorophore becomes excited by electron donation from an adjacent receptor. In practise, a sample is placed in the presence of a receptor which binds to target molecules and then excites the fluorophore to emit a conformation signal. Internal charge transfer (ICT) is similar to PET, except that the fluorophore is integrated firmly with the receptor and can demonstrate degrees of change. Fluorescence resonance energy transfer is used to detect the energy states of pairing molecules and the transmission of energy between them (Callan *et al.* 2005).

1.5.2 Fluorescence-Assisted Research

Since studies began on the genome we have been able to characterise biological systems as well as define the codes of life. Further studies produced the transcriptome which gave us insights into how DNA is used in cells. Research on the proteome has shown us how the DNA is translated into cells while the newly described toponome will illuminate the interactions between all of these cellular components (Golzhauser *et al.* 2010, Schubert 2010).

Understanding the factors which make up the toponome have allowed researchers to understand the workings of healthy and compromised cells alike. Wang *et al.* (2008) introduced a GFP tagged Hsp70 to bovine aortic endothelial cells. They treated the cells on a heat perfusion stage by temporarily heating the cells to 42^{o}C and continuously observed the expression of the Hsp70-GFP. The natural Hsp70 was stained with red fluorescence and the colocalisation of the red and green fluorescence was observed. This approached gave the researchers evidence that the GFP tagged Hsp70 was incorporated correctly and that heat shock had caused a small amount of Hsp70 to migrate from the cytoplasm to the nucleus. They postulated that Hsp70 may be involved in alleviating stress in the nucleus, in addition to its known cytoplasmic duties.

The maturation of Golgi apparatus cisternae in yeast was eluded using a GFP and RFP attached to various Golgi structural proteins. Secretory cargo proteins are usually moved through the Golgi and are processed with glycosylation and phosphorylation. By viewing the fluctuations of the two fluorescent proteins inside the cisternae during post translation of cargo proteins, Losev *et al.* (2006) provided evidence that the cisternae mature as the cargo proteins move through the Golgi suggesting that the maturation is a result of post translational processing.

A caveat must be heeded when using certain fluorescent approaches, especially when inserting genetic material designed to create a house keeping gene augmented with a fluorescent protein. Wang *et al.* (2008) noted during treatments that the Hsp70-GFP used resulted in an Hsp70-GFP expression seven times lower than the natural Hsp70. Earlier research has given evidence that adding a GFP to a fundamental protein can redirect the state of the host cell. Aokage *et al.* (2004) found that adding a Bcl-2 family protein with a GFP caused mitochondria to aggregate at the cell membrane and initiate apoptosis.

1.6 Aims and Objectives

Diabetes Mellitus has proven to be a complicated disease that has adversely changed the lives of millions of people around the world. Looking at the biochemistry of diabetics has shown intriguing signs leading researchers to conclude that key proteins may be involved in the development and pathology of the disease. Hsp60 typically has been implicated with intercellular signalling during inflammation and has elevated levels in diabetic circulation.

In this study we will look to transform the *E. coli* strain, DH5α, with a vector containing the gene for human Hsp60 (HSPN1) which is at the 3' end of a green fluorescent protein (GFP). The vector will then be multiplied within the growing DH5α. Methods for the vector DNA extraction will then be looked at and then an effective method employed to produce endotoxin-free DNA (endotoxin, also known as lipopolysaccharide, is produced by DH5α and can cause altered Hsp60 expression in mammalian cells). We will then investigate the transfection of the human cervical cancer cell line 'HeLa' with the extracted DNA. The transfection efficiency will be investigated and an effective method of transfection determined.

Lastly, we will use laser-scanning confocal microscopy to image live transfected HeLa cells. Hsp60 has a role in the cellular stress response so the expression and location of the attached GFP signal will be imaged alongside fluorescently labelled mitochondria. Transfected cultures will be put through treatments to test the movement of the Hsp60-GFP. Sodium azide will be used to stress mitochondria which concomitantly can alter Hsp60 expression. A high glucose concentration will also be used to stress the transfected cells as hyperglycaemia has been implicated in the translocation of circulating Hsp60 in diabetics.

Overall this study aims to investigate the colocalisation between the Hsp60-GFP and mitochondria. We aim to determine if using the Hsp60-GFP and examining it through confocal microscopy can provide insight into the movement of Hsp60 out of mitochondria during cellular stress.

2 Materials

2.1 Media, Reagents and Common Solutions Prepared

Name	Composition
LB Broth	10 g Tryptone 5 g yeast extract 10 g NaCl Dissolve in 800 ml RO H_2O and adjust to pH 7 Bring volume to 1 L then autoclave Store at 4^{o}C
LBamp Broth (containing ampicillin)	0.5 g ampicillin Bring volume to 5 ml with RO H_2O to make 292 mM ampicillin Filter sterilise through a 0.2 µm filter Take 500 µl of 292 mM ampicillin Add with LB broth to make 500 ml Store at 4^{o}C, use within 3 days
LB agar	5 g tryptone 2.5 g yeast extract 5 g NaCl Dissolve in 450 ml RO H_2O and adjust to pH 7.5 Add 7.5 g agar and heat in microwave to nearly boiling Autoclave then pour into approximately 30 petri dishes Store at 4^{o}C

LBamp (containing ampicillin) agar	0.5 g ampicillin Bring volume to 5 ml with RO H_2O to make 292 mM ampicillin Filter sterilise through a 0.2 µm filter Take 500 µl of 292 mM ampicillin Add with 60^oC autoclaved LB agar to make 500 ml pour into approximately 30 petri dishes Store at 4^oC
TE pH 8.0	10 ml 100 mM Tris-HCl pH 8.0 10 ml 10 mM EDTA pH 8.0 80 ml RO H_2O
0.2 M NaOH + 1% SDS	0.8 g NaOH Dissolve in 50 ml RO H_2O 1g SDS Bring volume to 100 ml with RO H_2O
3 M K acetate pH 5.2	29.44 g K acetate 70 ml RO H_2O and adjust to pH 5.2 Bring volume to 100 ml with RO H_2O
0.1 M $CaCl_2$ + 1% PEG8000	1.10 g $CaCl_2$ 1 g PEG8000 Bring volume to 100 ml with RO H_2O then autoclave Store at 4^oC

Phosphate Buffered Saline (PBS)	8 g NaCl
	0.2 g KCl
	1.44 g Na_2HPO_4
	0.24 g KH_2PO_4
	Dissolve in 800 ml RO H_2O and adjust to pH 7.4
	Bring volume to 1 L
HeLa DMEM media	0.011 g pyruvic acid
	0.45 g glucose
	2.5 ml 4.5 mM $NaHCO_3$
	2 ml 5000X penicillin/streptomycin
	1 ml 100X amino acid solution
	Bring volume to 100 ml with 1X DMEM
	Remove 10 ml and replace with 10 ml FBS
	Filter sterilise through a 0.2 µm filter
	Store at 4^oC
HeLa DMEM media 100 mM glucose	0.135 g glucose
	Make up to 10 ml with HeLa DMEM media
	Filter sterilise through a 0.2 µm filter
	Store at 4^oC

HeLa DMEM media 25 µM sodium azide	0.065 g sodium azide 1 ml HeLa DMEM media, mix to make 1 M sodium azide Take 10 µl 1 M sodium azide Add with 990 µl HeLa DMEM media 10 mM sodium azide Take 100 µl 10 mM sodium azide Add with 900 µl to make 1 mM Take 1 ml of 1 mM sodium azide Add with 9 ml HeLa DMEM media to make 100 µM Filter sterilise through a 0.2 µm filter Store at $4^{o}C$ Dilute aliquot by 4X to make 25 µM sodium azide before use
4.5 mM $NaHCO_3$	1.5 g $NaHCO_3$ Bring volume to 100 ml with RO H_2O Store at $4^{o}C$
0.5 M EDTA	14.61 g EDTA Dissolve in 80 ml RO H_2O and adjust to pH 8.0 Bring volume to 100 ml
10 mM EDTA pH 8.0	0.292 g EDTA Dissolve in 80 ml RO H_2O and adjust to pH 8.0 Bring volume to 100 ml

100 mM Tris-HCl pH 8.0	0.121 g Tris Dissolve in 80 ml RO H_2O and adjust to pH 8.0 Bring volume to 100 ml
5X Tris-borate (TBE)	54 g Tris base 27.5 g boric acid 20 ml 0.5 M EDTA pH 8.0 Bring volume to 1 L with RO H_2O
1X Tris-borate (TBE)	200 ml 5X TBE Bring volume to 1 L with RO H_2O
1% agarose gel in 1X TBE	1 g agarose Bring volume to 100 ml with 1X TBE Heat in microwave on high for 1 min 30 sec Stir contents Heat in microwave on high for another 1 min 30 sec Bring volume to 100 ml with 1X TBE Add 2.5 µl 25 mM ethidium bromide Pour into gel tray at 50^{o}C and leave to set for 30 min

1 µM Mitotracker CMX Ros (CMX Ros) stock solution	50 µg CMX Ros Dissolve in 94 µl DMSO to make 1 mM CMX Ros Take 10 µl of 1 mM CMX Ros Add with 9.99 ml to make 10 ml 1 µM CMX Ros Store both solutions below -20^{o}C
50 nM Mitotracker CMX Ros (CMX Ros) working solution	500 µl 1 µM CMX Ros Add with 500 µl HeLa DMEM media to make 500 nM CMX Ros Take 100 µl of 500 nM CMX Ros Add with 900 µl HeLa DMEM media to make 50 nM CMX Ros Use immediately
Propidium iodide (PI) working solution	2 µl 1.5 mM PI Add with 198 µl HeLa DMEM media to make 150 µM PI Use immediately

2.2 Statistical Analysis

All statistical analyses in this project were calculated using Microsoft Excel. The mean values for the data were processed as necessary and the standard error of the mean (S.E.M.) was calculated by the Excel equation displayed in **Equation 2.1**.

```
=STDEV(A1:A2)/SQRT(COUNT(A1:A2))
```

Equation 2.1 – The equation used to calculate the standard error of the mean in Microsoft Excel.

Single-tailed and two-tailed student's *t*-tests were used to compare and determine significance between data sets. The accepted level of significance was $p < 0.05$. Significant differences were indicated using "*".

3 Transformation and Purification of RG224428 from *E. coli* DH5α Cells

3.1 Introduction

The RG224428 plasmid used in this study was purchased from Origene in a 10 µg aliquot. It contains a Homo *sapiens* HSPD1 gene at the 3' end of a green fluorescent protein (GFP) gene (**Figure 3.1**). These genes are located at the 5' end of a eukaryotic CMV promoter which is crucial to their transcription within eukaryotic cells. The GFP protein has a 26 kDa, 232 amino acid structure and is referred to in the literature as TurboGFP (Evdokimov *et al.* 2006). The GFP protein originated from *Pontellina plumata* (a Copepoda species) as the ppluGFP2 protein. The TurboGFP is an optimised version of its derivative and is designed to avoid aggregation within the cytosol. Upon correct folding the GFP has an excitation maximum at 482 nm and an emission maximum at 502 nm (Evdokimov *et al.* 2006).

Another important gene incorporated into the plasmid is Amp, an ampicillin resistance gene. This gene will be used to select out transformed bacterial cells growing in competitive media (laced with ampicillin). Upon transcription the mRNA is translated to form a human Hsp60 protein with a GFP protein connected to the C-terminus. The sequencing for this plasmid was performed previously (personal communication, Martinus). In order to produce the necessary quantity and quality of RG224428 plasmid required for our study transformation and extraction protocols were employed to assess their effectiveness on DH5α *E. coli*. This section describes the successful protocols used to produce viable RG224428 plasmid. The transformation and extraction experiments were analysed on petri

dishes and agarose gels respectively. A NanoDrop was further employed to test the quantity and quality of the extracted DNA.

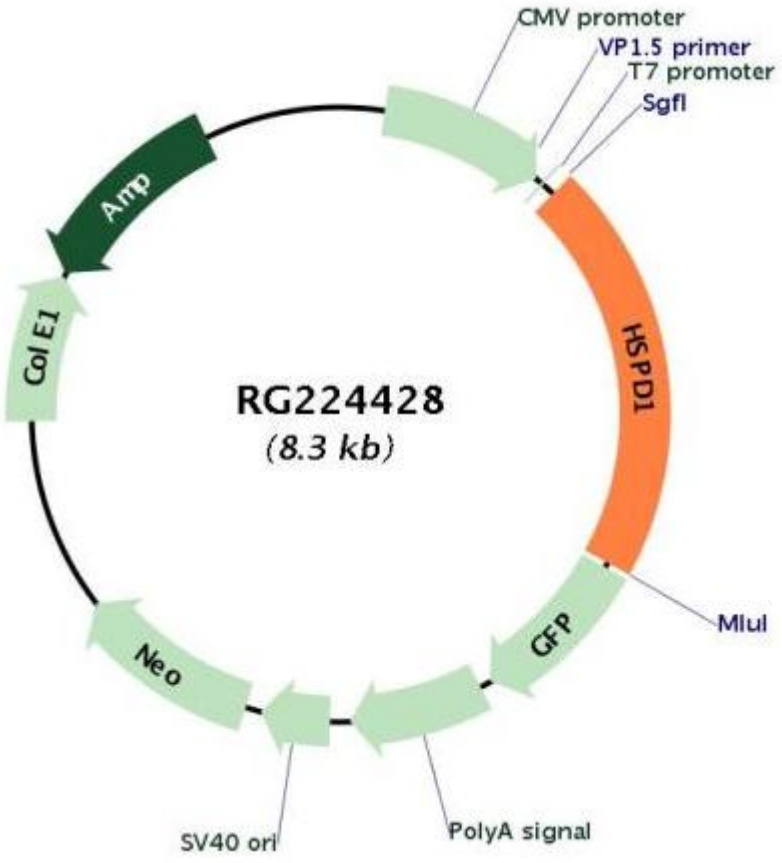

Figure 3.1 – Gene map for RG224428. The HSPD1 gene encodes for the human Hsp60 (obtained from Origene website: www.origene.com/Human_ORF_Clone/RG224428.aspx)

3.2 Methods

3.2.1 Growing DH5α *E. coli* Cells

The *E. coli* strain DH5α was purchased from Invitrogen. The advantage of using DH5α cells are they yield a high copy number of the cloned plasmid after transformation. The cells were grown in LB broth at 37^{o}C in an incubator. A colony was taken from a previously streaked LB agar plate and placed in 100 ml LB broth, mixed periodically and grown overnight. The following day 100 µl of inoculated LB broth was streaked onto newly prepared LB agar plates. The inoculated plates were stored at 4^{o}C. When a culture was required for research, 1 to 2 colonies would be removed from the plates and grown overnight in LB broth at 37^{o}C. An aliquot for research would be taken from the resultant growth.

3.2.2 Generation of Chemically Competent DH5α *E. coli* Cells

DH5α was grown overnight on an LB agar plate at 37^{o}C. A resulting colony was added to 10 ml LB broth and placed in a shaking incubator at 37^{o}C for 3 hr 30 min at 10 rpm. A 1.5 ml aliquot of culture was then centrifuged at 14,000 rpm for 2 min to pellet the cells. All supernatant was discarded and the pellets were resuspended in 100 µl of 0.1 M $CaCl_2$ containing 1% PEG8000 to make the cells competent (ready to take up external DNA from the environment). $CaCl_2$ was used in order to improve the permeability of the cell membranes and therefore improve the uptake of the introduced plasmid (Aich *et al.* 2012). Polyethylene glycol 8000 (PEG8000) also improves the permeability of cell membranes by forming pores and by adding it to a cell permeabilising media ($CaCl_2$) can

increase the transfection efficiency by 100-300 fold (Tu *et al.* 2005; Tostado *et al.* 2012).

3.2.3 Transformation of PUC19/Hsp60-GFP into DH5α *E. coli*

Competent cells were incubated on ice for 5 min were upon an aliquot of plasmid suspended in TE (pH 8.0) was added. PUC19 had a concentration of 29.4 ng/µl and RG224428 had a concentration of 434.3 ng/µl (see **3.2.4**). No plasmid was added to the control samples and their volume was brought up to match the volume of the treated samples with TE (pH 8.0). The tubes were mixed by inversion and the sample was further incubated on ice for 20 min with periodic gentle mixing (every 5 min). Immediately after the 20 min incubation the sample was placed into a thermomixer at 42^{o}C for 45 sec at 900 rpm. The sample was removed and 900 µl of pre-warmed (37^{o}C) LB broth was added and the sample placed again into a shaking incubator at 37^{o}C for 1 hr. The sample was centrifuged at 14,000 rpm for 2 min to pellet the cells and the supernatant was discarded. The cells were then resuspended in 100 µl of pre-warmed (37^{o}C) LB broth and aliquots of 30 µl were pipetted on to LB agar plates and spread with a sterile spreader. Treated samples were aliquoted onto two LB agar plates and four LB ampicillin agar plates. Control samples were added to LB agar and LB ampicillin agar plates. The inoculated plates were incubated overnight at 37^{o}C. Once the growth became substantial the plates were then stored at 4^{o}C. When a culture was required for research, 1 to 2 colonies would be removed from the plates and grown overnight in their respective LB broth systems (eg. with

ampicillin if taken from an ampicillin plate) at 37^{o}C. An aliquot for research would be taken from the resultant growth.

3.2.4 Quantification of DNA

DNA was quantified using a NanoDrop 2000 spectrophotometer (NanoDrop). Using the NanoDrop relies on the principle that DNA absorbs light at peak 260 nm. This absorption is due to interaction between 260 nm light and the aromatic nature of the pyrimidine (thymine and cytosine) and purine (guanine and adenine) bases (Markovitsi *et al.* 2010). The amount of light that is absorbed is subtracted from the light that is emitted to generate an absorbance curve. The quality of the DNA can also be assessed since many other by-products of DNA extraction peak at different wavelengths (ie. phenol peaks at 270 nm). By calculating the 260/280 and 260/230 ratio the purity can also be assessed as other non-DNA products (such as protein which peaks a 280 nm) peak within these regions. A 260/280 ratio between 1.8 and 2 and a 260/230 ratio higher than 1.5 indicate highly pure DNA.

The concentration of extracted PUC19 was calculated as 142.4 ng/µl with a 260/280 ratio of 2.03. The 260/230 ratio was 2.17. The concentration of extracted RG224428 was calculated as 30.7 ng/µl with a 260/280 ratio of 1.87 and a 260/230 ratio of 3.13.

3.2.5 Restriction Digestion of DNA

A single digest was performed adding 2 µl restriction enzyme buffer (Roche), 7 µl MQ water, 1 µl *EcoR1* or *NdeI* restriction enzymes (Roche) and 10 µl DNA. *NdeI* contains a restriction site CATATG found on PUC19. *EcoR1* cuts at the restriction site GAATTC, which is contained on RG224428. By using a single digest the DNA is cleaved in to single bands that can run through agarose gel and be compared with a DNA ladder (graded with single band DNA). Samples were incubated in a thermomixer at 37^{o}C for 1 hr at 900 rpm. The digested samples were immediately prepared for analyses on agarose gel.

3.2.6 Detecting DNA on Agarose Gel Electrophoresis

To assess the size of the extracted DNA aliquots the samples were analysed by agarose gel alongside samples of either pure PUC19 or RG224428, respectively. A 100 bp ladder (Dnature) was used to assess the size of PUC19 fragments. The ladders maximum size was 3000 bp which was adequate for the 2,686 bp PUC19. A 1,000 bp ladder (Dnature) was used to gauge the size of the RG224428 DNA. The ladders maximum size was 10,000 bp, adequate for the 8,300 bp RG224428.

Digested samples and undigested samples (20 µl each) were mixed with 5 µl loading dye, 20 µl of which were pipetted into the wells of 1% agarose gel in 1X TBE. Upon initial agarose gel analyses the pure RG224428 proved to be too high a concentration for efficient gel analyses. The DNA needed to be diluted to achieve better parity with the extracted DNA samples and ladder. The pure RG224428 (suspended in TE pH 8.0; 868.6 ng/µl) 1 µl was diluted with 27 µl of TE pH 8.0 to bring the concentration down to a similar level as the extracted DNA

(diluted pure RG224428 was approximately 31.02 ng/µl while the extracted DNA in similar TE was 30.7 ng/µl).

3.2.7 Purification of DNA

3.2.7.1 Purification of PUC19 DNA

One colony of DH5α+PUC19 was taken from LB ampicillin agar plates and used to inoculate 200 ml LB ampicillin. The culture was incubated overnight at 37^{o}C. A 1.5 ml sample of the culture was pipetted in a tube and centrifuged for 13,000 rpm for 1 min. The supernatant was discarded and pellet resuspended in 200 µl ice cold GTE. Fresh 0.2 M NaOH containing 1% SDS buffer (300 µl) was added and the sample mixed gently by inversion. Next, 300 µl of 3 M K acetate pH 5.2 was added and the sample was again gently mixed by inversion for 30 sec. The tube was incubated on ice for 10 min and then centrifuged at 13,000 rpm for 10 min. The resulting supernatant was transferred to a new sterile, unused tube. RNase (2 µl; 2 mg/ml) was added and the sample incubated at 37^{o}C for 10 min in a thermomixer at 900 rpm. Chloroform (600 µl) was then added and the tube mixed by inversion for 30 sec. The tube was then centrifuged at 13,000 rpm for 1 min and a 500 µl aliquot of aqueous supernatant was transferred into another new sterile, unused tube. Chloroform (600 µl) was added to this latest sample and mixed by inversion for 30 sec where upon it was centrifuged at 13,000 for 1 min. The aqueous supernatant (400 µl) was then transferred to a new sterile, unused tube along with 600 µl of absolute isopropanol. The sample was centrifuged at 13,000 for 10 min to precipitate the DNA. The supernatant was carefully removed and the pellet was washed in 500 µl of 80% ethanol by centrifugation at

13,000 rpm for 1 min after which the ethanol was removed and the pellet left to air dry for 5 min. This final pellet was resuspended in 25 µl TE pH 8.0 and left to dissolve for 30 min.

The DNA was quantified using a NanoDrop 2000 spectrophotometer (NanoDrop) as discussed in **3.2.4**. The concentration was calculated as 142.4 ng/µl with a 260/280 ratio of 2.03. The 260/230 ratio was 2.17.

3.2.7.2 Purification of RG224428 DNA

In order to purify RG224428 cloned in DH5α cells a plasmid extraction was performed using a QIAGEN EndoFree Plasmid Maxi Kit (QIAGEN Cat. no. 12362) and performed closely to the manufacturer's protocol with slight alterations. By using the kit we could ensure that the plasmid was extracted and purified to produce endotoxin free DNA. The need for endotoxin free DNA is due to the later transfection of eukaryotic HeLa cells (**4.2.2**). Endotoxin (also called lipopolysaccaride (LPS)) is produced by bacteria and usually resides in their cell walls. LPS has the ability the ligand with the TLR4 receptor found on eukaryotic cells including HeLa. Activation of the TLR4 receptor results in an immune response leading to inflammation (Raetz & Whitfield 2002). In order to use RG224428 cloned in DH5α bacteria for mammalian transfection the LPS needs to be removed to avoid false reading in our treatments. LPS exposure to mammalian cells causes upregulation and translocation of Hsp60 (Davies *et al.* 2006; Li *et al.* 2009).

LB ampicillin broth (100 µl) was inoculated with a transfected cell colony and incubated overnight at 37^{o}C. The entire 100 µl culture was then split into 25 µl

aliquots, each placed into a 50 ml tube. The tubes were centrifuged in a refrigerated (4^{o}C) centrifuge at 6,000 g for 15 min. The supernatant was discarded and the pellets were systematically resuspended in 10 ml buffer P1, collecting each pellet until all the cells and the 10 ml buffer were contained in one tube. Next, 10 ml of buffer P2 was added and the tube was mixed by inversion and incubated at RT for 5 min. Immediately 10 ml of pre-chilled (in fridge, 4^{o}C) buffer P3 was added mixed by inversion. The resulting lysate was poured into a QIAfilter cartridge (cap on) and incubated at RT for 10 min. The lysate was filtered through the cartridge using the plunger into a sterile, unused 50 ml tube. Buffer ER (2.5 ml) was added to the filtrate and then the contents were mixed by inversion and incubated on ice for 30 min. Buffer QBT (10 ml) was added to an endotoxin free QIAGEN-tip 500 to calibrate the filter and was emptied by gravity flow. The filtered lysate was then added to the QIAGEN-tip 500 and allowed to empty via gravity flow into a separate 50 ml tube. The QIAGEN-tip 500 was further washed using two aliquots of buffer QC (30 ml) and emptied by gravity flow. To elute the DNA 15 ml buffer QN was added to the filter tube and a new sterile, unused 50 ml tube was placed in order to catch the DNA filtrate. At this point the DNA extraction sample was stored overnight in a fridge at 4^{o}C. The following day 10.5 ml of isopropanol was added to the DNA sample and mixed by inversion. Immediately the sample was centrifuged in a refrigerated (4^{o}C) centrifuged at 5,000 g for 1 hr. The supernatant was decanted and 5 ml endotoxin free 70% ethanol was added and the sample centrifuged again at 5,000 g for 1 hr (4^{o}C). The ethanol was decanted and the pelleted left to air-dry for 30 min. Endotoxin free buffer TE (2 ml) was added and the pellet gently resuspended by stirring and inversion. The sample was left undisturbed to dissolve in the buffer TE for 30 min in the fridge at 4^{o}C.

The DNA was quantified using a NanoDrop 2000 spectrophotometer (NanoDrop) as discussed in **3.2.4**. The concentration was calculated as 30.7 ng/µl with a 260/280 ratio of 1.87. The 260/230 ratio was 3.13.

3.3 Results

3.3.1 Transformation of DH5α *E. coli*

Various chemical methods were used to transform DH5α cells but one method alone proved effective for our study. In order to ensure success before using the RG224428 plasmid (contains human Hsp60 with a GFP at the C-terminus) (**Figure 3.1**), PUC19 was used as the treatment plasmid. The ineffective methods were all chemical based and relied on incubating the treated cells on ice and at approximately 37^{o}C. All of these resulted in an absence of growth on competitive media. The first ineffective method used super optimal broth containing super optimal broth with catabolite repression (SOC) media accompanied by 2M $MgCl_2$ (cell permeabilisation) and 1M glucose and after incubation on ice was incubated at 37^{o}C for 45 min. The second ineffective method used transformation & storage solution (TSS)(Iiiumina), PEG 6000, dimethyl sulphoxide (DMSO) and $MgSO_4$. After incubation on ice the treated cells were placed in a 42^{o}C waterbath and incubated at 37^{o}C for 45 min.

The successful method (shown in **3.2.3**) which yielded generous numbers of colonies growing on competitive media used 0.1M $CaCl_2$ and PEG 8000. After incubation on ice the treated cells were placed into a thermomixer at 42^{o}C and and incubated at 37 ^{o}C for 60 min. **Figure 3.2** and **Figure 3.3** shows the different growth rates between the control samples and the treated samples. **Figure 3.2**a shows non-treated control DH5α grown to confluence, on standard LB agar. **Figure 3.2**b yielded no growth of non-treated DH5α on LB ampicillin competitive media. **Figure 3.2**c shows generous but non-confluent growth for DH5α transformed with the PUC19 growing on the same LB ampicillin. Since PUC19

contains a gene for ampicillin resistance it was deduced that the transformation was successful.

Due to the successful results of this protocol it was employed for use with RG22428. RG224428 also contains a gene for ampicillin resistance and the pictures in **Figure 3.3**a-c shows similar results to that seen with PUC19.

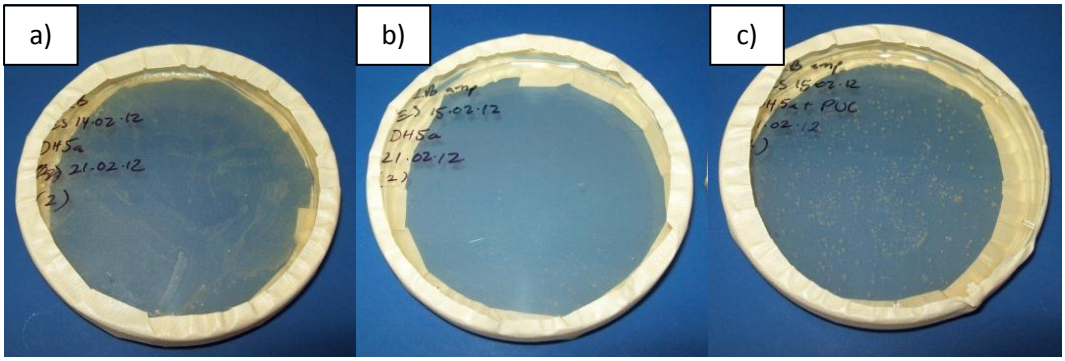

Figure 3.2 – DH5α *E. coli* PUC19 transformation plates. a) Confluent DH5α grown on LB agar plate. b) DH5α grown on LB ampicillin agar plate. c) DH5α transformed with PUC19 (contains ampicillin resistance gene) grown on LB ampicillin agar.

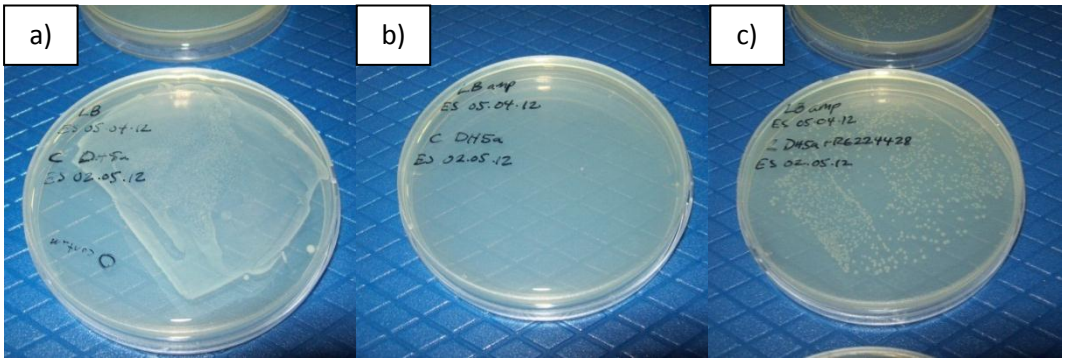

Figure 3.3 – DH5α *E. coli* RG224428 transformation plates. a) DH5α grown on LB agar plate. b) DH5α grown on LB ampicillin agar plate. c) DH5α transformed with RG224428 (contains ampicillin resistance gene) grown on LB ampicillin agar.

3.3.2 Plasmid Extraction from DH5α *E. coli* Cells

The initial method used to extract the PUC19 plasmid from transformed DH5α incorporated TENS pH 8.0 and 3M NaOAc pH 5.2 into the protocol. The resultant supernatant was washed in a 1:1 phenol/chloroform solution. When analysed under a NanoDrop, the data revealed potential contamination of the isolated DNA with phenol as indicated by a second peak at approximately 270 nm (the peak absorption of phenol; pure DNA peak absorption is 260 nm). Phenol/chloroform is used in the protocol to help precipitate the DNA from the supernatant. An aqueous phase is developed which contains the DNA with the phenol/chloroform in the lower supernatant. **Figures 3.4-3.6** show our attempts to wash the phenol from the DNA. The different lines indicate the differing quantities of DNA that resulted from various different washing steps. The extraction samples at this stage contain DNA, phenol, chloroform and isopropanol (to separate the DNA). Centrifugation is used to separate the DNA from the phenol/chloroform.

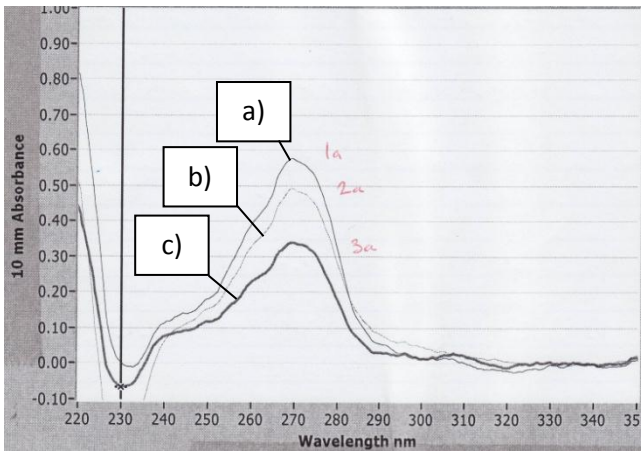

Figure 3.4 – Graph of PUC19 DNA samples extracted using phenol on a NanoDrop spectrophotometer. The lines show UV light absorption on PUC19 extraction samples extracted. Samples were centrifuged at the phenol/chloroform step for various times. a) Sample was centrifuged for 10 min. b) Sample was centrifuged for 20 min (10 min twice). c) Sample was centrifuged for 30 min (10 min thrice).

Figure 3.4a, b and c were centrifuged for 10 min, 20 min and 30 min, respectively (b and c were performed in consecutive 10 min rounds). The concentrations declined with increased centrifugation time. The concentrations were 19.63 ng/µl, 16.49 ng/µl and 11.56 ng/µl for a, b and c, respectively. **Figure 3.5**a, b and c show data from the same protocol using the same centrifugation times (10, 20 and 30 min, respectively) but the samples were refrigerated overnight (4^{o}C). The concentrations were more similar to each other with figures of 24.48 ng/µl, 20.69 ng/µl and 20.50 ng/µl for a, b and c, respectively. **Figure 3.6** is produced from a slightly different protocol. The phenol/chloroform centrifugation step was set to 10 min but the aqueous DNA was washed in progressively more chloroform (with intentions to remove the phenol). As more chloroform steps (200 µl chloroform each) are employed there is a decline in phenol but also a decline in DNA. **Figure 3.6**a, b, c and d show this decline (a had 1 wash; b 2 washes; c 3 washes; d 4 washes). The concentration of DNA was calculated as 111.24 ng/µl, 42.20 ng/µl, 9.78 ng/µl and 8.49 ng/µl for a, b, c and d, respectively. All of the figures

show the same 270 nm peak indicative of phenol contamination. As more phenol was removed, DNA was lost.

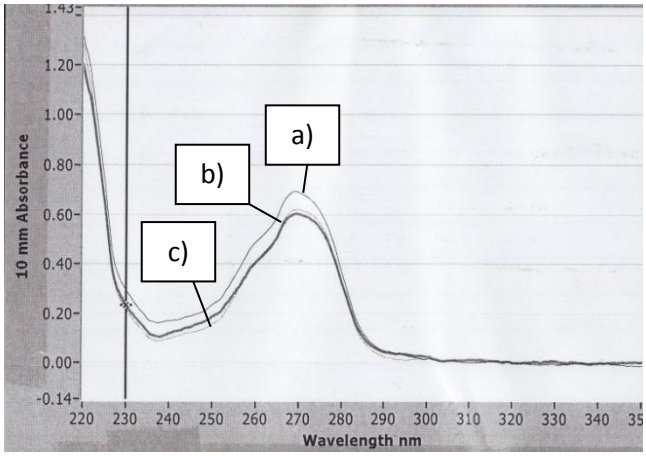

Figure 3.5 – Graph of PUC19 DNA samples extracted and incubated overnight using phenol on a NanoDrop spectrophotometer. The lines show UV light absorption on PUC19 extraction samples. Samples incubated at 4°C overnight and then centrifuged at the phenol/chloroform step for various times. a) Sample was centrifuged for 10 min. b) Sample was centrifuged for 20 min (10 min twice). c) Sample was centrifuged for 30 min (10 min thrice). The lines for b) and c) overlap.

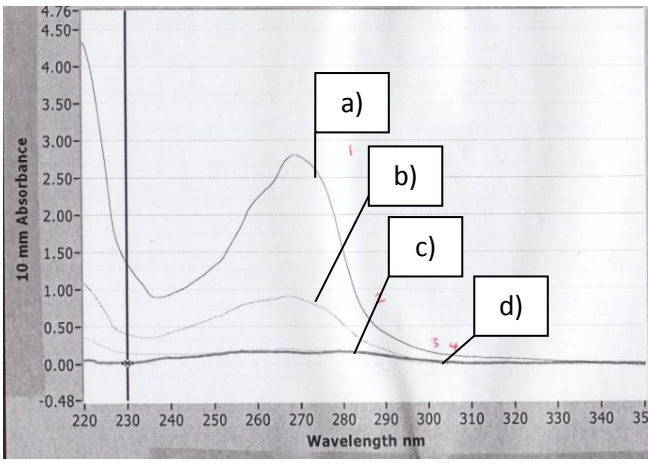

Figure 3.6 – Graph of PUC19 DNA samples extracted using phenol and washed various times with chloroform on a NanoDrop spectrophotometer. The lines show UV light absorption on PUC19 extraction samples. Each DNA sample washed in 200 µl chloroform a different amount of times. a) Sample was washed once. b) Sample was washed twice). c) Sample was washed three times). d) Sample was washed four times. The lines for c) and d) overlap.

Due to the difficulty of phenol removal we moved to a new protocol that incorporated glucose/tris/EDTA (GTE), 0.2 M NaOH/1% SDS and K acetate pH

5.2. No phenol was used in the protocol. The NanoDrop results showed a pure sample with a 260/280 ratio of 2.04 and a 260/230 ratio of 2.38 as shown in **Figure 3.7**. The concentrations recorded were 142.4 ng/µl and 149.9 ng/µl. The extracted PUC19 DNA was analysed on agarose gel electrophoresis alongside pure PUC19 DNA.

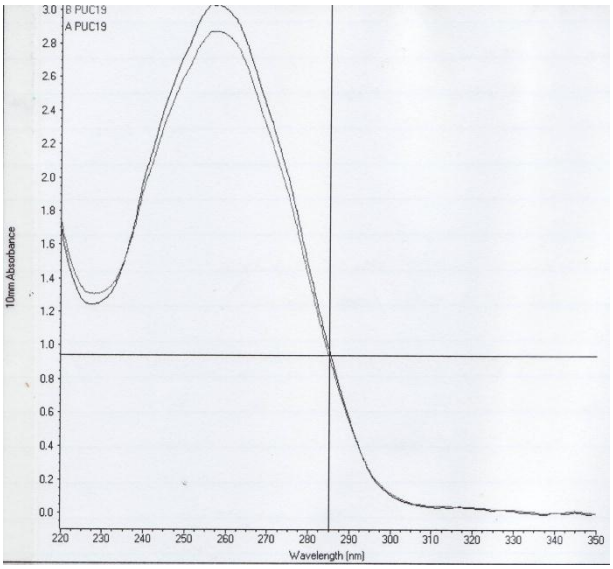

Figure 3.7 – Graph of relatively pure PUC19 DNA extraction samples analysed on a NanoDrop. The lines show a considerably pure plasmid DNA sample with singular peaks at 260 nm. The highest peak shows a concentration of 149.9 ng/µl. The lower peak is 142.4 ng/µl.

The pure uncut DNA in **Figure 3.8** lane 3 reveals multiple banding. This is indicative of the different forms that pure DNA plasmid can be found in (multimeric, circular, linear and supercoiled). Supercoiled DNA can be seen as the lowest band as it is more compact and has run further through the gel than linear strands. Circular DNA can be seen above with the multimeric strands (DNA strands bound together) at the top. The single-digested pure DNA can be seen in lane 4. It is linear and has lined up with the ladder DNA (also linear) to show a band between 2,000 bp and 3,000 bp (PUC19 is 2,686 bp). Lane 5 and 7 shows uncut extracted DNA (circular) while lane 6 and 8 reveal faint bands that

line up with the pure cut PUC19 DNA. Double banding occurred on the gel and it is thought this was due to a shorter-than-usual incubation time between the DNA and ethidium bromide. Carlsson *et al.* (1995) reported this occurrence with tests they performed. They found that short incubation times with *bis*-intercalating dyes (including ethidium bromide) could cause multiple banding. They postulated that it was due to uneven staining of DNA strands. Strands with more dye would run slower while bands with less dye would run ahead causing either a second band or a smear. The DNA quantities were calculated to be > 14.7 ng/µl in extraction samples that were put through a single digest with *NdeI* (**Figure 3.8**). Despite the comparatively low DNA yield seen on the gel (spectral analyses showed up to 149.9 ng/µl) this protocol was considered a worthy alternative to the more expensive extraction kit protocol we would use on the RG224428.

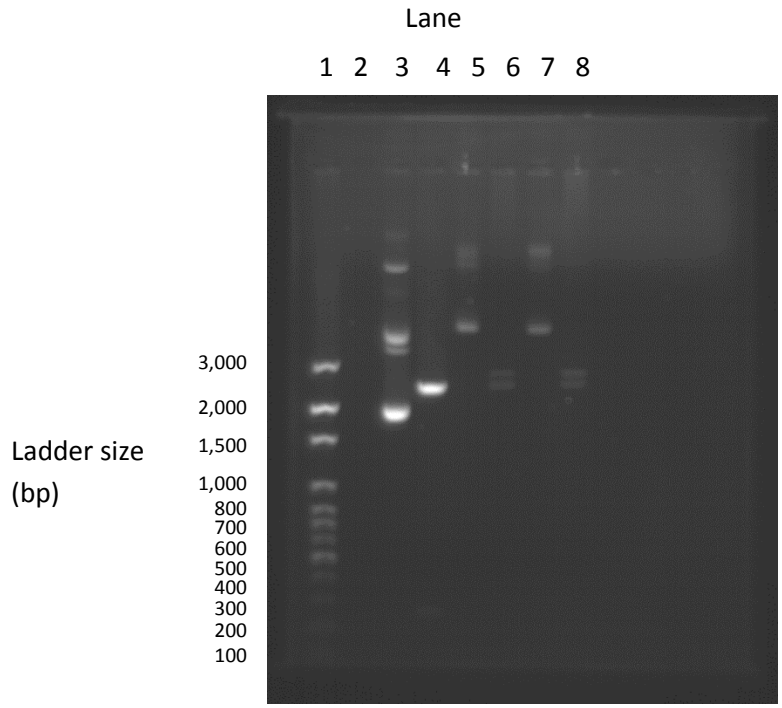

Figure 3.8 – Agarose gel electrophoresis of PUC19 extracted from DH5α. Double banding is evident due to a shorter than usual incubation time for the DNA and ethidium bromide. The pure plasmid was 25 ng/µl. The spectral analysis calculated the extracted plasmid as 149.9 ng/µl. Lane 1: 5 µl 100 bp DNA ladder (100-3000 bp). Lane 2: empty. Lane 3: 20 µl pure PUC19 uncut. Lane 4: 20 µl pure PUC19 cut. Lane 5: 20 µl extracted PUC19 uncut. Lane 6 20 µl extracted PUC19 cut. Lane 7: 20 µl extracted PUC19 uncut. Lane 8: 20 µl PUC19 cut.

The use of the QIAGEN plasmid maxi kit proved successful. A NanoDrop analysis confirmed the extraction sample had a good level of purity with a 260/280 ratio of 1.87 and a 260/230 ratio of 3.13 as seen in **Figure 3.9**. The concentration was calculated as 30.7 ng/µl. **Figure 3.10** shows an image of extracted RG224428 analysed using agarose gel electrophoresis. Lane 2 shows the multiple banding of pure uncut RG224428. Lane 4 shows single-digested pure RG224428 at approximately 8,000 bp (RG224428 is 8,300 bp). Lane 5 shows the multiple banding of extracted RG224428. Lane 7 shows a band of extracted RG224428 which is in line with the pure cut sample.

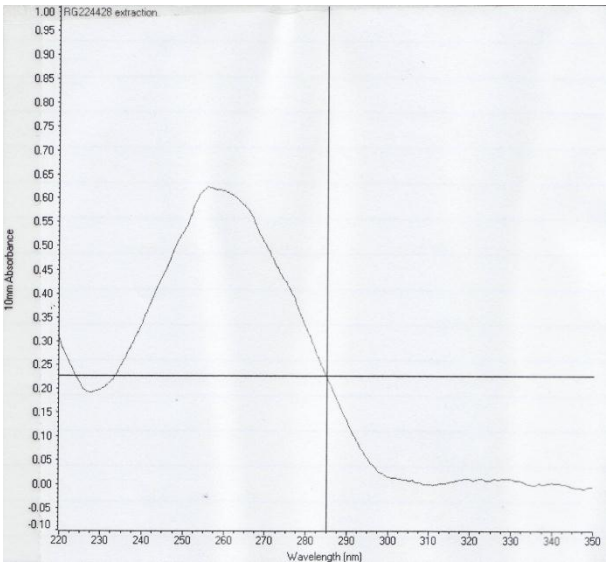

Figure 3.9 – Graph of RG224428 DNA extraction samples using QIAGEN plasmid maxi kit analysed on a NanoDrop. The lines show a considerably pure plasmid DNA sample with a singular peak at 260 nm. The calculated concentration of the DNA is 30.7 ng/µl.

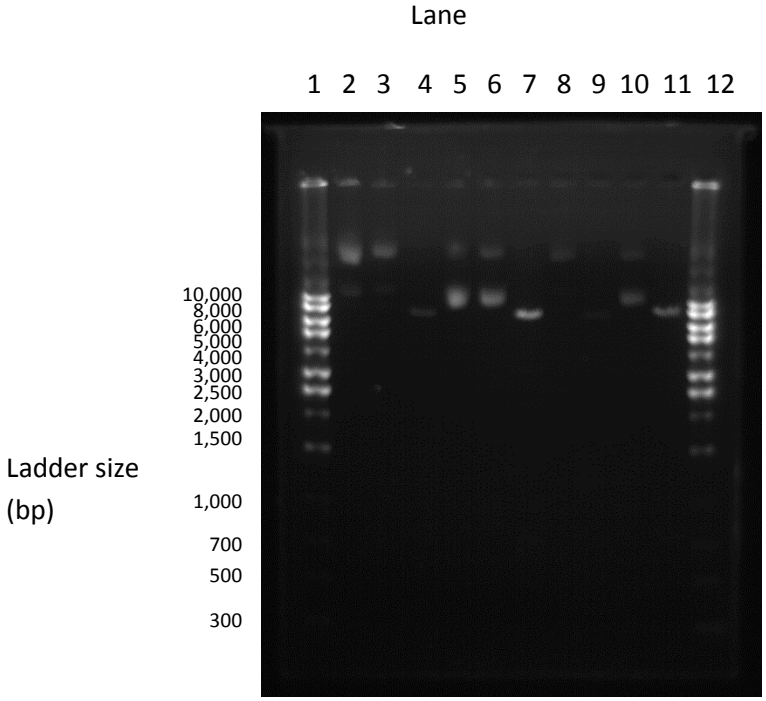

Figure 3.10 – Agarose gel electrophoresis of RG224428 extracted from DH5α. The pure DNA was diluted to a concentration of 30.7 ng/µl to match the extracted DNA (30.7 ng/µl). Lane 1: 5 µl 1,000 bp DNA ladder (1,000-10,000 bp). Lane 2: 5 µl pure RG224428 uncut. Lane 3: 5 µl pure RG224428 cut with *Hind III* (obsolete). Lane 4: 5 µl pure RG224428 cut with *EcoR1*. Lane 5: 5 µl extracted RG224428 uncut. Lane 6: 5 µl extracted RG224428 cut with *Hind III* (obsolete). Lane 7: 5 µl extracted RG224428 cut with *EcoR1*. Lane 8: 2.5 µl pure RG224428 cut with *Hind III* (obsolete). Lane 9: 2.5 µl pure RG224428 cut with *EcoR1*. Lane 10: 2.5 µl extracted RG224428 cut with *Hind III* (obsolete). Lane 11: 2.5 µl extracted RG224428 cut with *EcoR1*. L. Lane 12: 5 µl 1,000 bp DNA ladder (1,000-10,000 bp).

3.4 Discussion

The objective of this study was to clone and purify RG224428 plasmid DNA into a state suitable for mammalian cell transfection. As the initial quantity of RG224428 was low (10 µg) the PUC19 plasmid was used to optimise transformation and purification procedures. The gram-negative bacteria DH5α *E. coli* (DH5α) was used for the transformation and cloning of both of the plasmid vectors. The method used to perform the transformation incorporated $CaCl_2$, a known cell permeabilising agent (Aich *et al.* 2012), with polyethylene glycol 8000 (PEG8000). PEG8000 can create pores in cell membranes and it is thought that the combination of $CaCl_2$ and PEG8000 improve the chances of DNA uptake (Tu *et al.* 2005; Tostado *et al.* 2012). Transformed DH5α cells were then grown and plasmid DNA extractions were performed. The concentration and quality of the extracted DNA was assessed using a NanoDrop 2000 spectrophotometer (NanoDrop). The extracted plasmids were then processed with restriction enzymes (single-digest) to produced single bands of DNA which were measured on agarose gel electrophoresis.

The *Escherichia coli* strain DH5α has been successfully used many times in research to clone plasmid vectors containing genes of interest. Contemporary studies have used DH5α's 'high-copy number plasmid' properties to clone genes for industrial applications. Ariff *et al.* (2009) used DH5α to clone the gene for the xylanase enzyme, an enzyme unnatural to *E. coli* strains. Xylanase is used to break down hemicellulose in plants (an increasingly important reaction for fuel production). Karthikeyan *et al.* (2011) transformed DH5α with a vector containing the gene for penicillin G acylase (naturally found in B. *Badius pac*). Penicillin G acylase is an important enzyme in producing 6-amino penicillanic

acid (6-APA), a key molecule used to produce semi-synthetic penicillins. DH5α has been used to produce fluorescent indicator proteins in the past. DH5α was transfected with arsenate resistance (arsR) gene regulators attached to a GFP. The model was used to design a system where *E. coli* can be used to detect arsenic (a toxin) in the environment. In the presence of arsenic the DH5α would fluoresce under UV light (Tani *et al.* 2009). In our study DH5α was effectively transformed with the plasmids PUC19 and RG224428 (seen in **Figures 3.2-3.3**, respectively). The PUC19 plasmid was used to optimise transformation and extraction protocols before using RG224428. The RG224428 plasmid was used because it contains genes for a human Hsp60 with a GFP protein attached at the C-terminus. The cloned plasmid would then be used to transfect human HeLa cells to detect Hsp60-GFP movement under stress (chapter **4**).

The extraction of plasmid DNA was initially performed on DH5α transformed with PUC19. One of the protocols used first employed phenol. Phenol is used in plasmid extractions because it has a lower polarity than water. This molecular property means that it can repulse DNA into the adjacent water (the aqueous phase) during centrifugation (Morales & Zhan 2010). Phenol also binds with proteins causing them to separate out of the aqueous phase. It is in this aqueous phase that pure plasmid DNA should reside (Wang & Rossman 1994). In our study, spectral analyses revealed that the phenol used to separate the plasmid DNA from cellular proteins was contaminating the purified DNA. Different methods were used to rid the DNA of the phenol. Longer centrifugation periods (centrifugation of samples containing phenol/chloroform and DNA) and extra washes with chloroform did not remove the phenol contamination but instead decreased DNA yields. The contamination may have been caused by phenol binding to protein trapped in the aqueous phase. Proteins, such as the 16 kDa

C1D (a pro-apoptotic protein) and the serpin proteins (Spi-1, Spi-2 and Spi-3; involved in DNA repair), have been known to bind tightly with DNA after deproteinisation (Sjakste *et al.* 2010). If protein had been bound tightly to our DNA, or had a net polar charge, this may have contributed to the phenol contamination (as phenol also binds to proteins). Despite the possibility of tightly binding protein being linked to the phenol contamination no other contaminants were detected or were as obvious as phenol in our spectral analyses. Future extractions using phenol may need to incorporate a filter system to further remove particles that may contribute to phenol contamination. Due to the difficulty in removing phenol we employed a different DNA extraction protocol which provided uncontaminated purified DNA.

In order to purify the RG224428 plasmid for use in mammalian cells we used the QIAGEN Endo Free Plasmid Maxi Kit (QIAGEN). The advantage of using this kit is that it incorporates filters that could effectively remove endotoxin, naturally a part of the DH5α cells. Endotoxin-free solutions were also supplied. Endotoxin-free methods were required because the RG224428 plasmid DNA was to be used later to transfect mammalian HeLa cells (**4.2.2**). Endotoxin (also called lipopolysaccharide (LPS)) is produced by bacteria (including DH5α) and usually resides in their cell walls. LPS has the ability to ligand with the TLR4 receptor found on mammalian cells including HeLa. Activation of the TLR4 receptor results in an immune response leading to inflammation (Raetz & Whitfield 2002). LPS has been shown to induce an immune response in HeLa cells. Mineshiba *et al.* (2005) added LPS with HeLa cells to induce the synthesis of human beta-defensin-2. Millan-Mendoza *et al.* (2007) showed that LPS derived from Chlamydia trachomatis could cause apoptosis in HeLa cells. Our research was designed to investigate the movement of the Hsp60-GFP encoded by RG224428.

The cells were to be induced by controlled cellular stressors which control could not be achieved if the HeLa cells were already contaminated with LPS (detailed in **4.2.5**). LPS would not only affect the viability of the HeLa cells but could generate false-positive results for Hsp60 translocation. Davies *et al.* (2006) demonstrated that LPS introduced into peripheral blood mononuclear cultures causes the release of Hsp60 into the extracellular space. Li *et al.* (2009) also demonstrated that LPS administered to pancreatic tissue from mice causes significant increases in Hsp60 expression. By avoiding contamination of RG224428 plasmid DNA with LPS the plasmid can be used to transfect HeLa cells effectively.

4 Transfection of Hsp60-GFP into HeLa Cells and Colocalisation Analysis

4.1 Introduction

The human Hsp60 protein has many vital roles in human biology. In order to induce the transcription and subsequent translation of the Hsp60-GFP contained on RG224428 a human cell line HeLa (or HeLa) cells, was purchased from the American Tissue Culture Collection (ATCC number: CCL-2). The important component of this cell type is that RG224428 only contains a eukaryotic CMV promoter for the Hsp60-GFP gene (HSPD1-GFP)(**Figure 3.1**), which is naturally contained in virtually all eukaryotic cells including HeLa. HeLa cells are also a feasible option for this developmental study.

In order to perform a successful and adequate transfection of HeLa cells with RG224428 a chemical approach was used in the form of lipofectamine 2000 (Invitrogen). Lipofectamine 2000 reagent was purchased as a working solution of 1 mg/ml. Lipofectamine is a cationic lipid based transfection agent that forms liposomes in the transfection media (media design specifically for transfection). The positively charged (cationic) liposomes bind to negatively charged (anionic) DNA. This creates a colloid of lipofectamine and DNA (lipofectamine/DNA complex). The lipofectamine provides the ability to overcome the electrostatic repulsion that would usually inhibit naked DNA uptake. The lipid properties also allow the lipofectamine to bind and pass through cell membranes (Dalby *et al.* 2004). This system provides a way for transfection vectors to be introduced to target cells.

Opti-MEM (Gibco, Life Technologies) is a reduced-serum media used during the transfection process to optimise transfection yields. Protein content in normal growth media (in the presence of oxygen) can block the liposomal activity necessary for transfection (Fordada *et al.* 1997). By using a reduced-serum media the effects of protein:liposome interaction are negated (Cheung *et al.* 2001).

Laser scanning confocal microscopy has proven useful at examining biological systems in great detail. The advantage of a confocal microscope is due to the confocal component which reduces the amount of scattered light passing through the lens. This also helps process very thin images (in the Z-dimension) which are useful for colocalisation. The introduced Hsp60-GFP is visible as a group of GFP emitting at 502 nm. The grouping of the GFP is thought to be due mostly to the collection of GFP into the larger chaperonin60 complex (one GFP bound to each of the 14 Hsp60 proteins). As the larger chaperonin60 complexes are broken down the Hsp60-GFP may be grouped into vesicles and remain visible or dissipate below the resolution of the microscope as singular GFP signals.

A powerful feature of the confocal approach is found in its accompanying software which can be used to determine colocalisation of up to four different fluorescent signals. This section looks at the transfection of HeLa cells with an Hsp60-GFP and then investigates the colocalisation of the GFP signal with the signal emitted by Mitotracker. It further looks at the possibilities of using this technique to detect variance between known stressors of mitochondria, where the Hsp60 protein is predominantly stored in healthy cells.

4.2 Methods

4.2.1 HeLa Cell Culture

The human epithelial cancer cell line, HeLa, was purchased from the American Tissue Culture Collection (ATCC number: CCL-2). The cells were grown in DMEM (1x) (Gibco, Life Technologies) with additional 25 mM glucose and 1mM pyruvate. The media was also supplemented with 4.5 mM $NaCOH_3$, 2 ml 1x penicillin/streptomycin and 1% MEM-NEAA (100x) amino acid solution (Gibco, Life Technologies). Fetal bovine serum (FBS) was added to make a 10% FBS DMEM media. Cells were grown in a humidified incubator at 37^{o}C, 5% CO_2 using standard incubation conditions. Cells were passaged every 7 days by centrifugation (Megafuge 1.0) at approximately 400 rcf and resuspended in pre-warmed HeLa media.

4.2.2 Transfection of HeLa Cells with RG224428

Lipofectamine 2000 reagent (Invitrogen) was purchased as a working solution of 1 mg/ml. Opti-MEM (Gibco, Life Technologies) is a reduced-serum media used during the transfection process to optimise transfection yields (as discussed in **4.1**).

HeLa cells were grown in wells on 4-well glass chamber slides (Lab-Tek) with initial seedings of approximately 7,800 cells per ml in pre-warmed HeLa DMEM media. When the cells reached approximately 50% confluence (or approximately 168,000 cells per ml) they were considered ready for transfection.

The general transfection protocol was adopted from the manufacturer's instructions for transfection with lipofectamine 2000. An aliquot of 20 µl opti-

MEM was added to tubes in row 1 and 25 µl opti-MEM was added to tubes in row 2. RG224428 DNA (1 µg) in endotoxin-free TE (QIAGEN) was added to each tube in row 1 while 1 µl Lipofectamine 2000 was added to each tube in row 2. The samples were incubated for 5 min at room temperature (RT). The contents of the tubes in row 1 were added to the matching tubes in row 2, respectively (tube A from row 1 added with tube A in row 2), to make transfection media. The newly mixed samples were incubated at RT for 20 min.

HeLa growth media was removed from each well and the cells washed in 200 µl pre-warmed PBS pH 7.4 (37^{o}C). The cells were washed again in 200 µl pre-warmed opti-MEM (37^{o}C). 50 µl of transfection media was added drop-wise to each well covering the cells. Another 150 µl pre-warmed opti-MEM (37^{o}C) was added to each well to ensure desiccation was avoided during incubation. The cells were incubated at 37^{o}C for 3 h under normal incubator conditions.

The transfection media was removed and the cells were washed in 200 µl pre-warmed DMEM (37^{o}C) where then 1 ml pre-warmed DMEM (37^{o}C) was added and the cells incubated at 37^{o}C under normal incubator conditions.

Transfection efficiency was analysed using a Nikon Eclipse TS100 inverted microscope with a UV block and appropriate filters. Imaging was performed using a Nikon Coolpix 4500 digital camera. 20X magnification was used to view transfected cell cultures. In each frame, the number of transfected cells were counted and divided by the amount of total cells. They were then multiplied by 100 to bring it to a percentage.

Transfected cells were characterised by a distinct green fluorescence being emitted under UV light excitation. Many cells would emit this green fluorescence but only those that had a ‘stencilled-cell’ appearance were counted as ‘transfected’.

This ‘stencilled-cell’ appearance can be seen in **Figure 4.8**. The reason for this high standard was due to the use of colocalisation in later experiments (sub-section **4.2.5**). Hsp60-GFP would be imaged alongside fluorescently stained mitochondria. By avoiding weakly fluorescent cells we could determine to best transfection ratios (DNA:lipofectamine etc.) to produce the most fluorescently ‘stencilled-cells’. A key problem with imaging live cells is that particles in the media can refract the light used to calculate colocalisation. This creates enough background noise that it can overwhelm the detection of weakly emitting cells. High background noise causes researchers to increase the thresholds of fluorescent signal detection. Higher thresholds of detection eliminate much of the information in all cells. It can also give false-positive readings to non-transfected cells as they appear to have GFP signals (generated by noise). By selecting a transfection method that produced very bright ‘stencilled’cells’ on top of a dimmer green background (made up of transfected cells that weakly emit fluorescence) it would benefit the more time-intensive confocal microscopy (colocalisation). **Equation 4.1** was used to calculate the relative transfection efficiency of RG224428 in HeLa cells.

$$\% \text{ Transfection efficiency} = (\text{Hsp60-GFP cells} / \text{cells}) * 100$$

Equation 4.1 – Calculating relative transfection efficiency of RG224428 in HeLa cells

4.2.3 Propidium Iodide Staining of HeLa Cells

In order to test if the Hsp60-GFP transfection was toxic to HeLa cells propidium iodide was used. Propidium iodide binds to nucleic acids and can be used to detect specific cell necrosis in cultures. The peak absorption is at 535 nm and the

peak emission is at 617 nm. Propidium iodide was stored as a stock solution of 1.5 mM (commonly 1 mg/ml) in sterile water. A 'working solution' of 150 µM was made by diluting 2 µl propidium iodide in 198 µl DMEM.

The growth media was removed from HeLa cells and the cells were washed in pre-warmed PBS pH 7.4 (37^{o}C), before adding 200 µl of propidium iodide working solution. The cells were incubated at RT for 5 min and the staining solution was removed and the cells were again washed in 200 µl PBS pH 7.4. **Equation 4.2** was used to calculate the relative toxicity of the Hsp60-GFP in transfected cells.

$$\% \text{ Cytotoxicity} = (\text{PI stained Hsp60-GFP cells} / \text{Hsp60-GFP cells}) * 100$$

Equation 4.2 – Calculating relative cytotoxicity of Hsp60-GFP in transfected cells

4.2.4 Mitotracker RED CMX Ros Staining of HeLa Cells

Mitotracker RED CMX Ros is a fluorescent dye that has peak absorption at 578 nm and a peak emission at 599 nm, producing a strong red fluorescence. The fluorescence of Mitotracker CMX Ros is dependent on actively respiring mitochondria where it then becomes oxidised and binds to the mitochondria (Lemasters & Ramshesh 2007; Terai & Nagano 2008). A stock solution of 1 mM was made according to the manufacturer's manual by adding 94 µl DMSO to 50 mg Mitotracker RED CMX Ros. A 'working solution' of 500 nM was made by diluting 10 ml stock solution in 9.99 ml to make 1 µM where upon the 1 µM solution was diluted to 500 nM with an equal aliquot of pre-warmed (37^{o}C) HeLa DMEM media.

The growth media was removed from HeLa cells and the cells washed in pre-warmed PBS pH 7.4 (37^{o}C), before adding 200 µl of Mitotracker RED CMX Ros working solution. The cells were incubated at 37^{o}C for 10 min, and then the staining solution was removed and the cells were washed in 200 µl of PBS pH 7.4.

The cells were viewed under a Nikon Eclipse TS100 inverted microscope with a UV block and appropriate filters. Images were collected with a Nikon CoolPix 4500 digital camera. An Olympus FV1000 laser scanning microscope (LSCM) was used to collect higher resolution images using the Olympus FluroView software (ver1.6a).

4.2.5 Stressing Transfected HeLa Cells

After transfection had been performed on the cells (**4.2.2**) a number of treatments were employed to stress the cells in order to investigate the movement of the Hsp60-GFP out of mitochondria. Treatments of 100 mM glucose and 25 µM sodium azide were chosen to stress the cells as they have been known to induce increased Hsp60 expression (personal communication, Hall). The control group was grown in normal HeLa DMEM media (**4.2.1**). The '100 mM glucose group' was grown in HeLa DMEM media laced with added glucose. The concentration of glucose was brought to 100 mM by adding 0.135 g of glucose with HeLa DMEM media to make 10 ml. The '25 µM sodium azide' treatment was made using sodium azide and HeLa DMEM media. Sodium azide (0.065 g) was diluted with HeLa DMEM media until it was at a concentration of 25 µM sodium azide in 10 ml HeLa DMEM media (detailed in **2.1**). The transfected cells were grown in 2 ml of each treatment and incubated at 37^{o}C with 5% CO_2 under normal incubator conditions. When confocal imaging was performed the flourodish

being analysed was kept in an incubator built around the confocal microscope at 37^{o}C and 5% CO_2.

4.3 Results

HeLa cells were grown successfully in HeLa DMEM media as shown by **Figure 4.1**. At four days the growth begins to curve off and plateau. This corresponds with the cells reaching confluence in the flask. Each week the cells were passaged and a new flask seeded with approximately 80,000 cells.

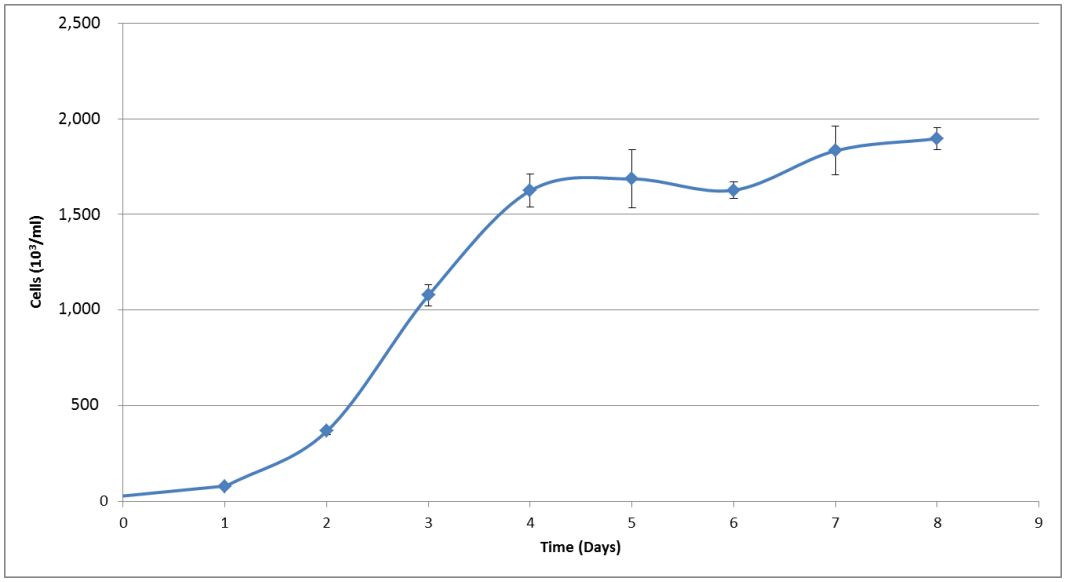

Figure 4.1 – Growth chart for HeLa cell culture over 8 days. Error bars showing S.E.M.

The picture in **Figure 4.2** shows a standard image of HeLa cells while the pictures in **Figure 4.3** show the effect of transfection with RG224428. In this visual comparison the bright green in **Figure 4.3**b represents HeLa cells synthesising the GFP bound Hsp60 protein from RG224428. The GFP is fluorescing light at approximately 550 nm (green) in response to excitation with UV light.

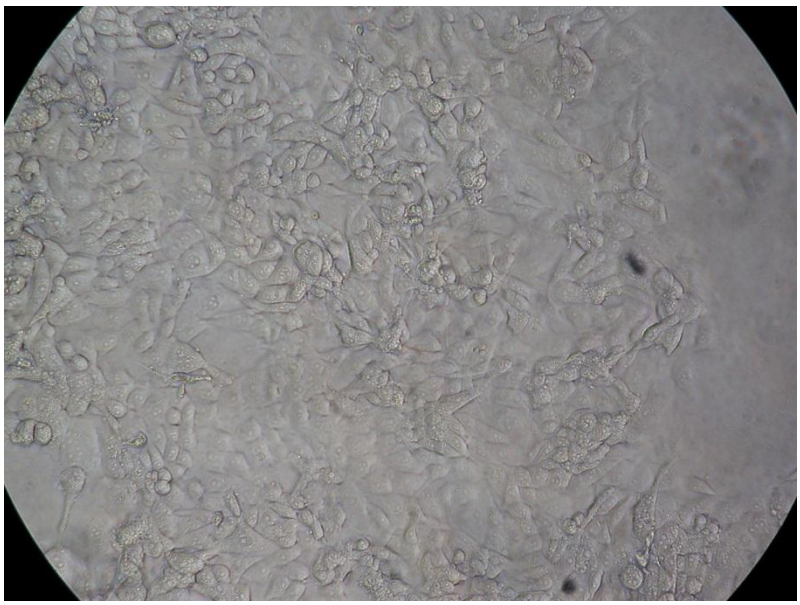

Figure 4.2 – HeLa cells grown in HeLa DMEM. 20X magnification on inverted wide field microscope.

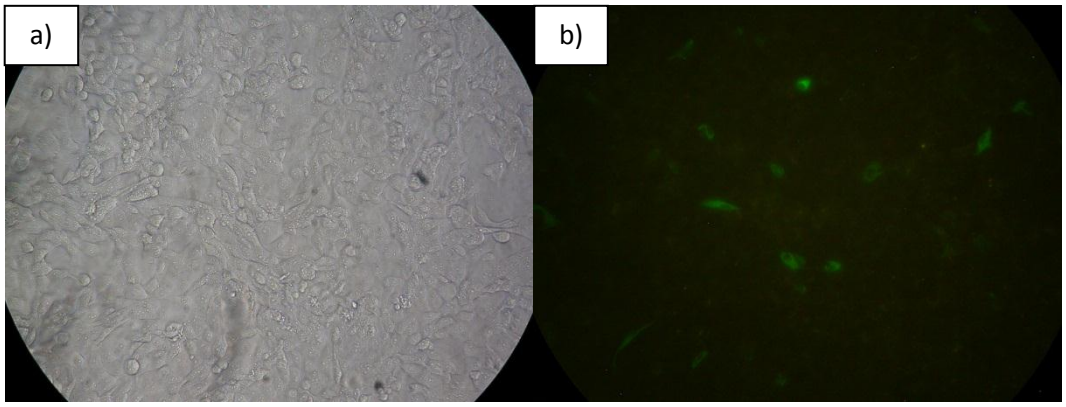

Figure 4.3 – HeLa cells transfected with RG224428 24 h after transfection. a) A frame of transfected HeLa cells under normal light. b) The same frame of transfected fluorescent HeLa cells under a UV light with a 550 nm filter. Both photos performed using 20X magnification on inverted wide field microscope. Transfected cells were characterised by a bright green 'stencilled-cell' appearance (**4.2.2**).

The transfection times were analysed to obtain data on transfection efficiency. The threshold of inclusion was relatively high for transfected cells (as detailed in **4.2.2**). By varying the time that the HeLa cells spent in the transfection media we were able to detect a steady decrease in the rate of transfection. A time of 3 hours registered a mean of 2.07 ± 0.43% transfection efficiency, while 4 hours saw a

slight decline to 1.67 ± 0.21%. The longest time of 5 hours saw a reduction in transfection efficiency by nearly half at 1.13 ± 0.08% (**Figure 4.4**). Upon further inspection student's t-tests revealed that there was no statistical significance between the three times. This occurred despite the S.E.M. showing substantial differences in boundaries between '3 hours' time and the other two time varients. The difference between the '4 hours' and '5 hours' times did approach significance ($p < 0.05$) but still showed insignificant differences with the 3 hour time. According to our data, a transfection time of 3 hours is possibly the best as it uses the least amount of time and it achieves a transfection efficiency just as substantial as longer times.

The ratio of DNA and lipofectamine 2000 in the transfection media was investigated to assess what ratio could produce the best transfection efficiency. As lipofectamine 2000 is expensive the ratios were kept within feasible boundaries. Ratios are designated as DNA:lipofectamine 2000 in µl sized aliquots. The ratio of 1:0.5 had a transfection efficiency of 1.64 ± 0.24% while 1:1 had the highest success with a ratio of 4.02 ± 1.41%. There was a substantial drop in the mean transfection efficiency when moving up to higher lipofectamine 2000 ratios. The 1:2 ratio samples had a mean of 1.50 ± 1.16% while the ratio for 1:3 had a mean of 21.3 ± 1.03% (**Figure 4.5**). Despite the observable difference in mean transfection efficiency there were no statistically significant differences between any DNA to lipofectamine 2000 ratios. The 1:1 ratio showed near significant differences between 1:1 against both 1:0.05 and 1:2 but failed to gain significance. Due to the relatively high mean the 1:1 ratio was used in future transfections. Even though using 0.05 µl and 2µl of lipofectamine proved a similar efficiency, it was decided that the irregularly high transfection efficiencies (1:1 as high as

7.56%; the highest 1:0.05 was 2.31%) that contributed to the insignificantly high mean were worth our attention.

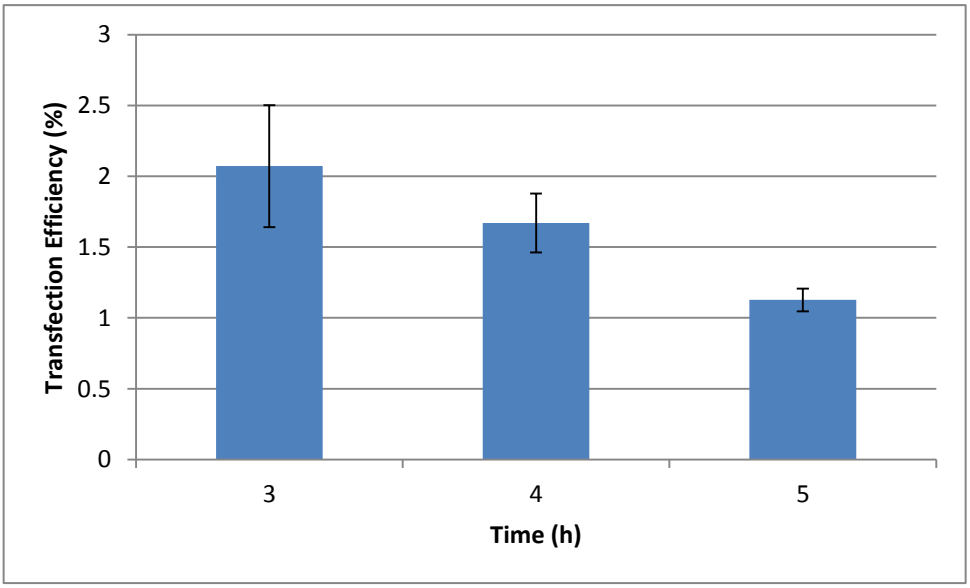

Figure 4.4 – Transfection efficiency of HeLa cells left in RG224428 transfection solution over different times. Bar graph showing the mean ± S.E.M.

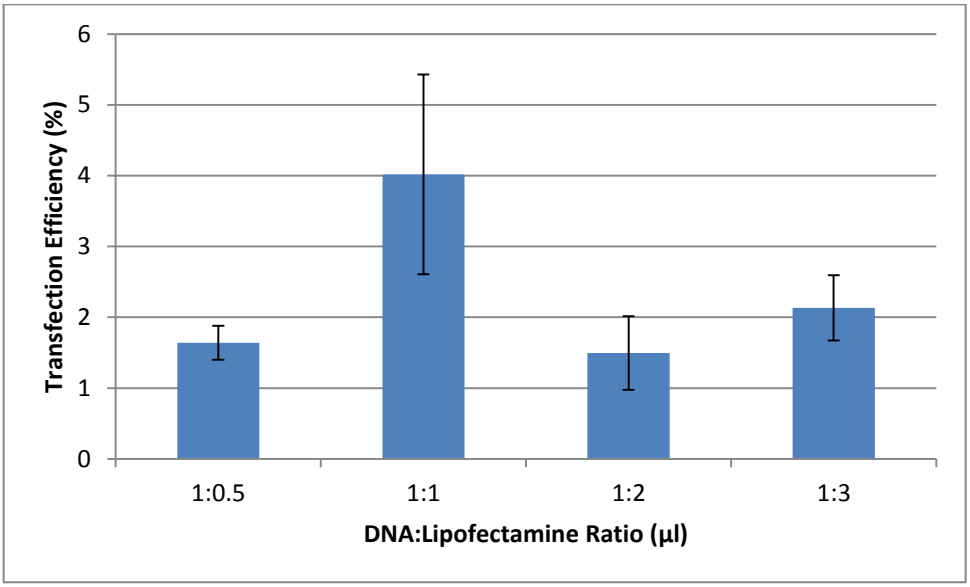

Figure 4.5 – Transfection efficiency of HeLa cells with differing RG224428 transfection solution ratios. Bar graph showing the mean ± S.E.M.

To assess whether the transfected cells were causing unwanted necrotic damage, propidium iodide (PI) was used to stain exposed nucleic material (**Figure 4.6**b). Assessing the control group showed the average amount of transfected cells that had PI staining within their vicinity was 3.76 ± 0.53%. There was no significant change in PI staining over the three days. The glucose treatment showed a similar trend with an average of 2.13 ± 1.93% and no significant changes over the three days. The sodium azide group had a significantly higher mean at 11.3 ± 4.3% which was due to a spike at 48 h ($p < 0.05$).

In order to detect successful colocalisation between the Hsp60-GFP and the HeLa cell mitochondria, Mitotracker RED CMX Ros (commonly referred to as mitotracker or CMX Ros) was used to stain the mitochondria cell culture. **Figure 4.7**a shows HeLa cells stained with mitotracker while **Figure 4.7**b shows the Hsp60-GFP simultaneously stained with mitotracker. Mixing of the two fluorescent signals can be seen clearly on the left of **Figure 4.7**b.

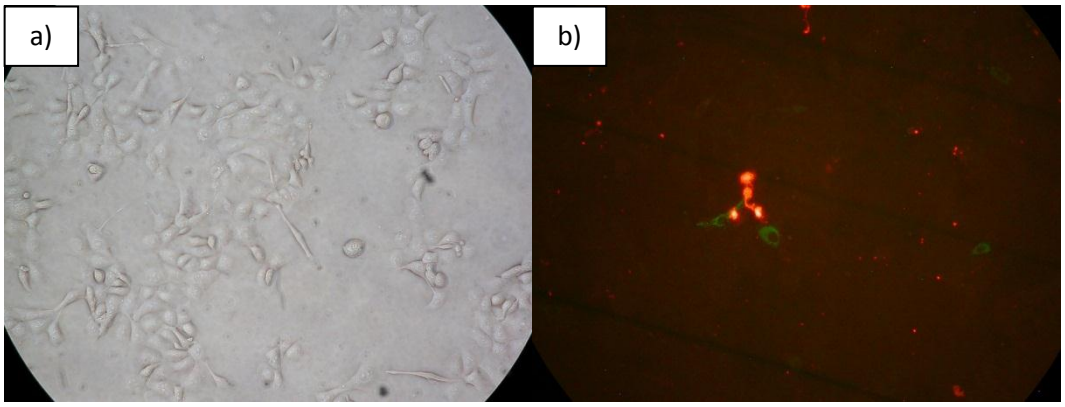

Figure 4.6 – HeLa cells transfected with RG224428 and stained with propidium iodide. a) A frame of transfected HeLa cells under normal light. b) The same frame of transfected fluorescent HeLa cells under a UV light with a 550 nm filter. Both photos performed using 20X magnification on inverted wide field microscope.

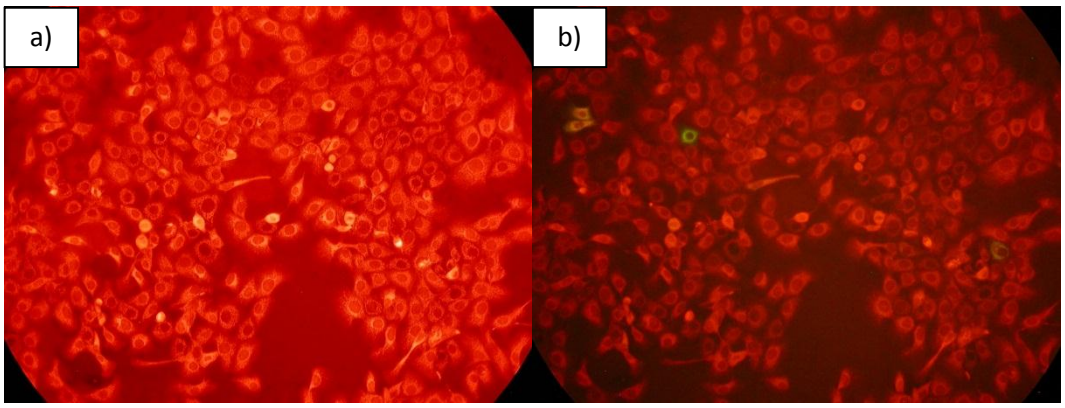

Figure 4.7 – HeLa cells transfected with RG224428 and stained with Mitotracker CMX Ros. a) A frame of transfected HeLa cells under a UV light with a 700 nm filter. b) The same frame of transfected fluorescent HeLa cells under a UV light with a 550 nm filter. Both photos performed using 20X magnification on inverted wide field microscope.

The colocalisation between the GFP signal emitted from the Hsp60-GFP (green; transcribed from RG224428) and Mitotracker CMX Ros (red; used to label host mitochondria) was analysed using an Olympus FV1000 inverted laser scanning confocal microscope. The degree of colocalisation was calculated using Olympus FluroView software (ver1.6a). The statistic of interest used to determine colocalisation was the overlap coefficient (r), derived from Pearson's coefficient (used to detect overlapping signal intensities per pixel). Due to variance in the signal intensities in our work, r is used as it ignores signal intensity. The r statistic calculates the degree of overlap from 0 to 1, 1 being a perfect 1:1-overlap between signals (0 being no overlap). Three different treatments (explained by their names) were used to detect differences in Hsp60-GFP-mitochondria colocalisation, 'control', '100mM glucose' and '25μM sodium azide' (hereafter referred to as control, glucose and sodium azide, respectively).

Figure 4.8-4.9 show images captured by us on a laser scanning confocal microscope (60X magnification). The imaged cells are HeLa cells transfected with RG224428. **Figure 4.8** has an r value of 0.78 indicating a high degree of colocalisation. **Figure 4.8**a-c shows the multiple layers of the image being placed

over each other. False colours have been used to highlight the different channels (the confocal detect signals as different shades of grey). a) shows the fluorescent GFP signal. b) shows the mitotracker signal and c) shows the two signals superimposed. The yellow pixels indicate sites of colocalisation. **Figure 4.8**d shows the cell being imaged under normal light. e) shows the GFP signal superimposed over the normal light image. f) shows the two fluorescent signals superimposed over the cell. **Figure 4.9**a-f show the same properties as mentioned for **Figure 4.8**a-f but the cell has much less colocalisation as calculated by the r value (r = 0.54).

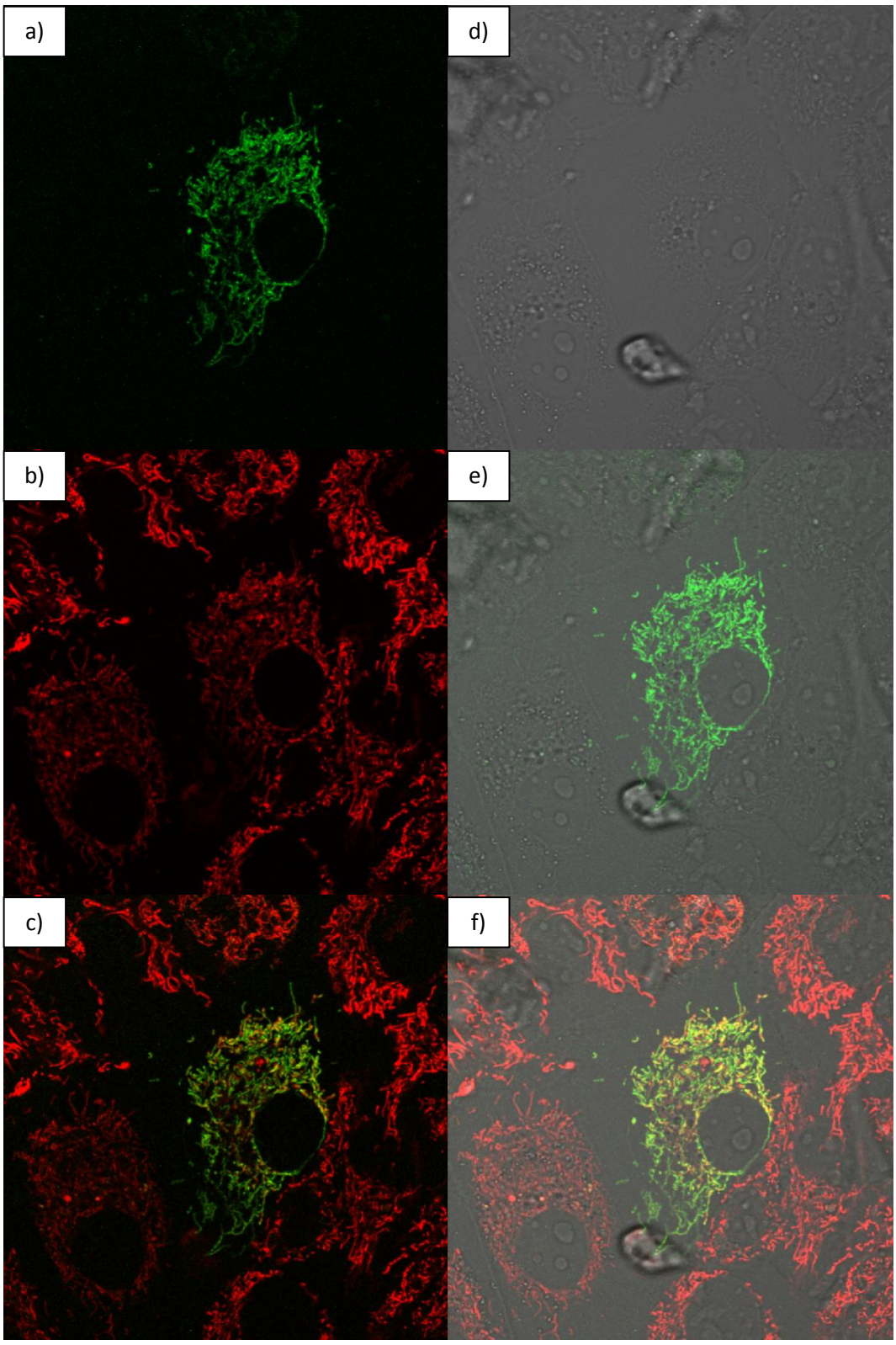

Figure 4.8 – Confocal laser scanned image of a transfected HeLa cell in false colour (green represents the Hsp60-GFP signal; red represents Mitotracker RED CMX Ros). Cell transfection in control group after 24 h. The cell in the images has an r value of 0.78.

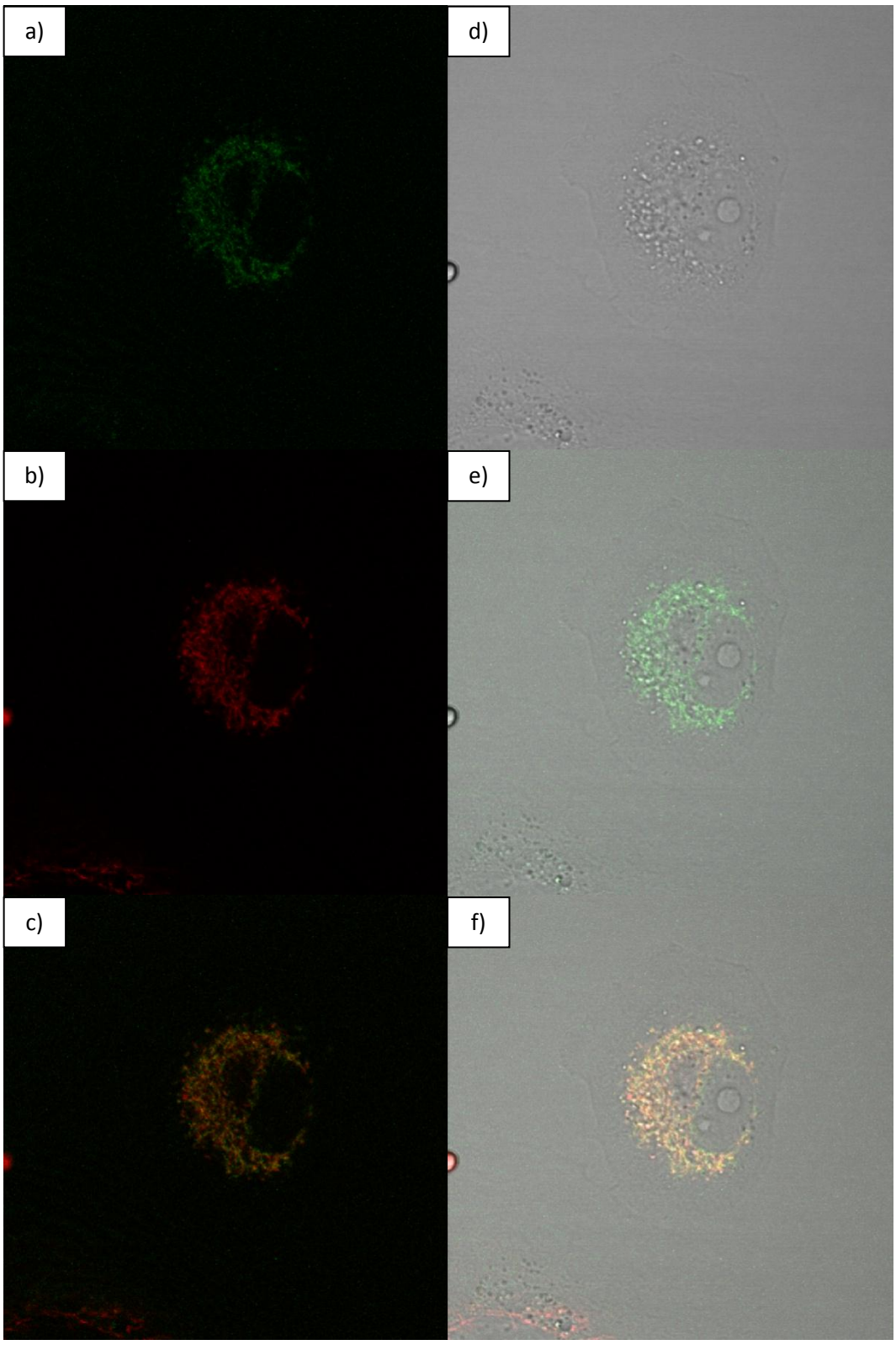

Figure 4.9 – Confocal laser scanned image of a transfected HeLa cell in false colour (green represents the Hsp60-GFP signal; red represents MitotrackerREDCMX Ros). Cell transfection in glucose group at 48 h. The cell in the images has an r value of 0.54.

The following figures (**Figure 4.10; Figure 4.11; Figure 4.12**) show images of transfected cells in the control, glucose and sodium azide groups, respectively. Each figure shows images of cells within each group taken at the time points 24, 48 and 72 h (a), b) and c), respectively). In each series of pictures the signal for mitotracker (left) is shown followed by the Hsp60-GFP signal (middle). The images are then overlaid, 1:1, to reveal points of colocalisation in yellow (right). An increase in colocalisation is shown in **Figure 4.10** between a) and c) as evidenced by the r values 0.70 and 0.75, respectively. The images in b) appear to capture 3 different cells expressing Hsp60-GFP. **Figure 4.11** shows the decrease in colocalisation over time in glucose group cells (0.76, 0.67 and 0.58 for a), b) and c), respectively. The image in c) appears indicative of a cell under stress. Large vesicles of mitochondria (red) and Hsp60-GFP (green) can be seen around the nuclei. **Figure 4.12** shows the state of colocalisation for the sodium azide group at 24, 48 and 72 h (a), b) and c), respectively). The r values for a), b) and c) are 0.68, 0.69 and 0.73, respectively.

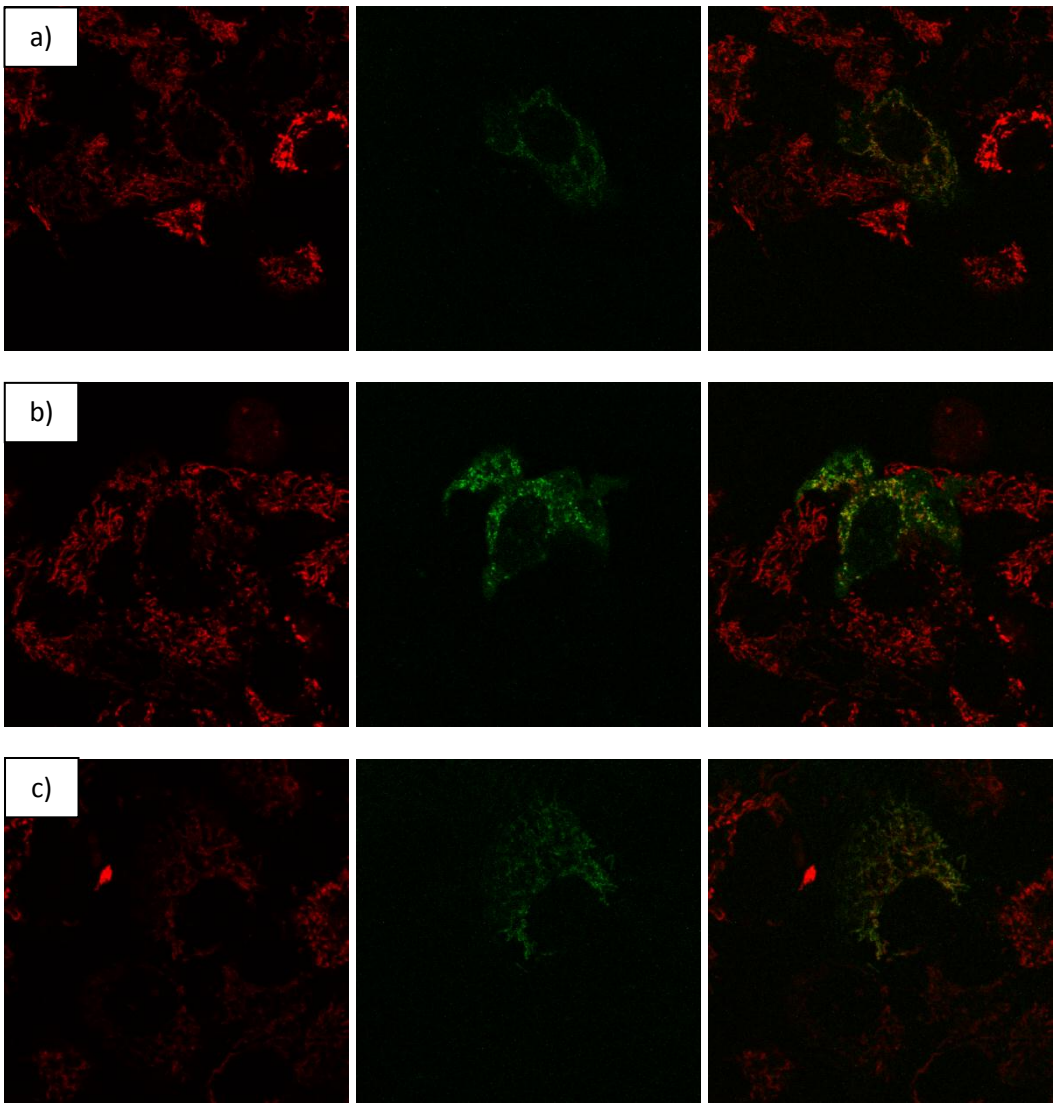

Figure 4.10 – Colocalisation of Hsp60-GFP with mitotracker in control group using false colour (red = mitotracker; green = Hsp60-GFP; yellow = colocalisation between the two signals). a) 24 h; r = 0.70. b) 48 h; r = 0.65. c) 72 h; r = 0.75.

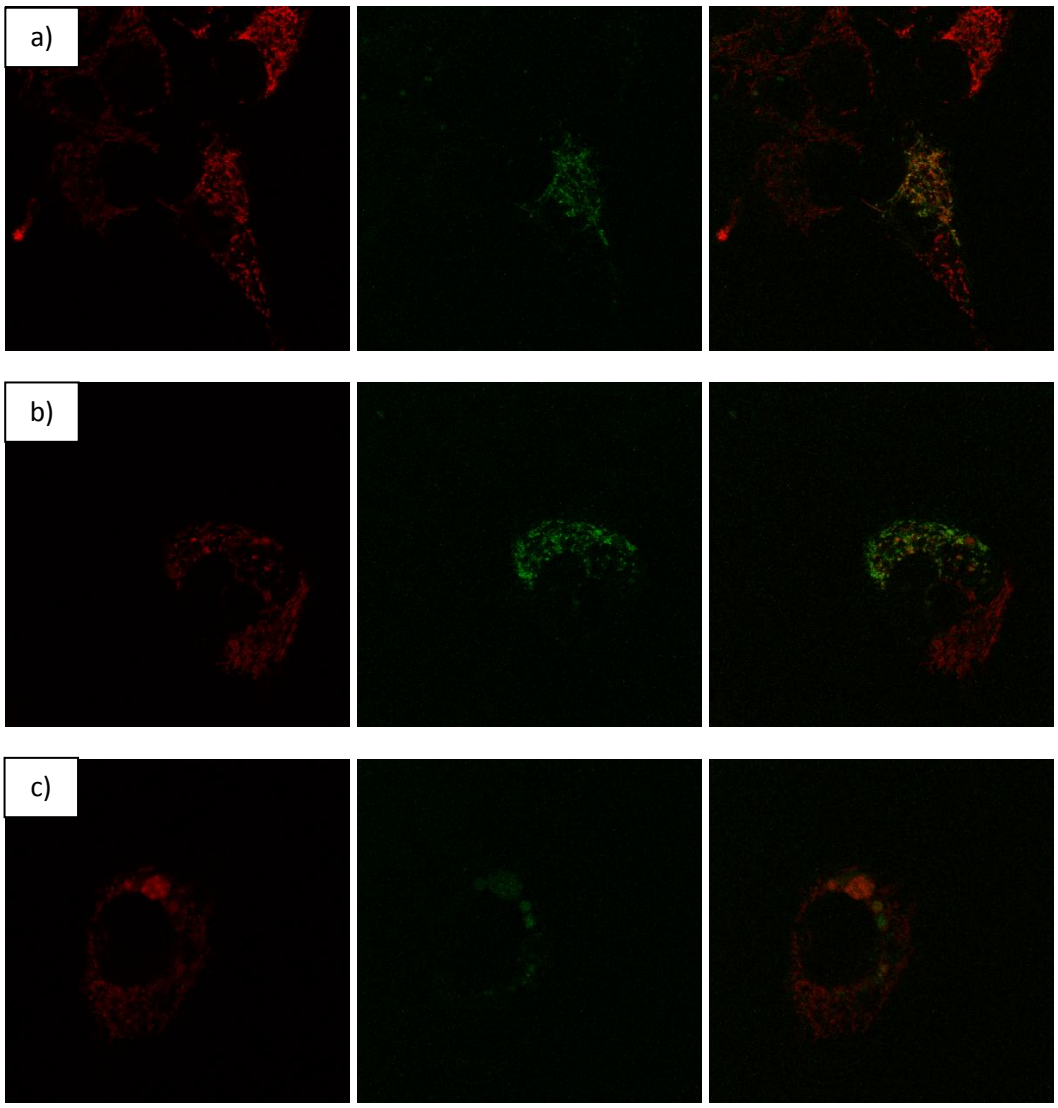

Figure 4.11 – Colocalisation of Hsp60-GFP with mitotracker in glucose group using false colour (red = mitotracker; green = Hsp60-GFP; yellow = colocalisation between the two signals). a) 24 h; r = 0.76. b) 48 h; r = 0.67. c) 72 h = 0.58.

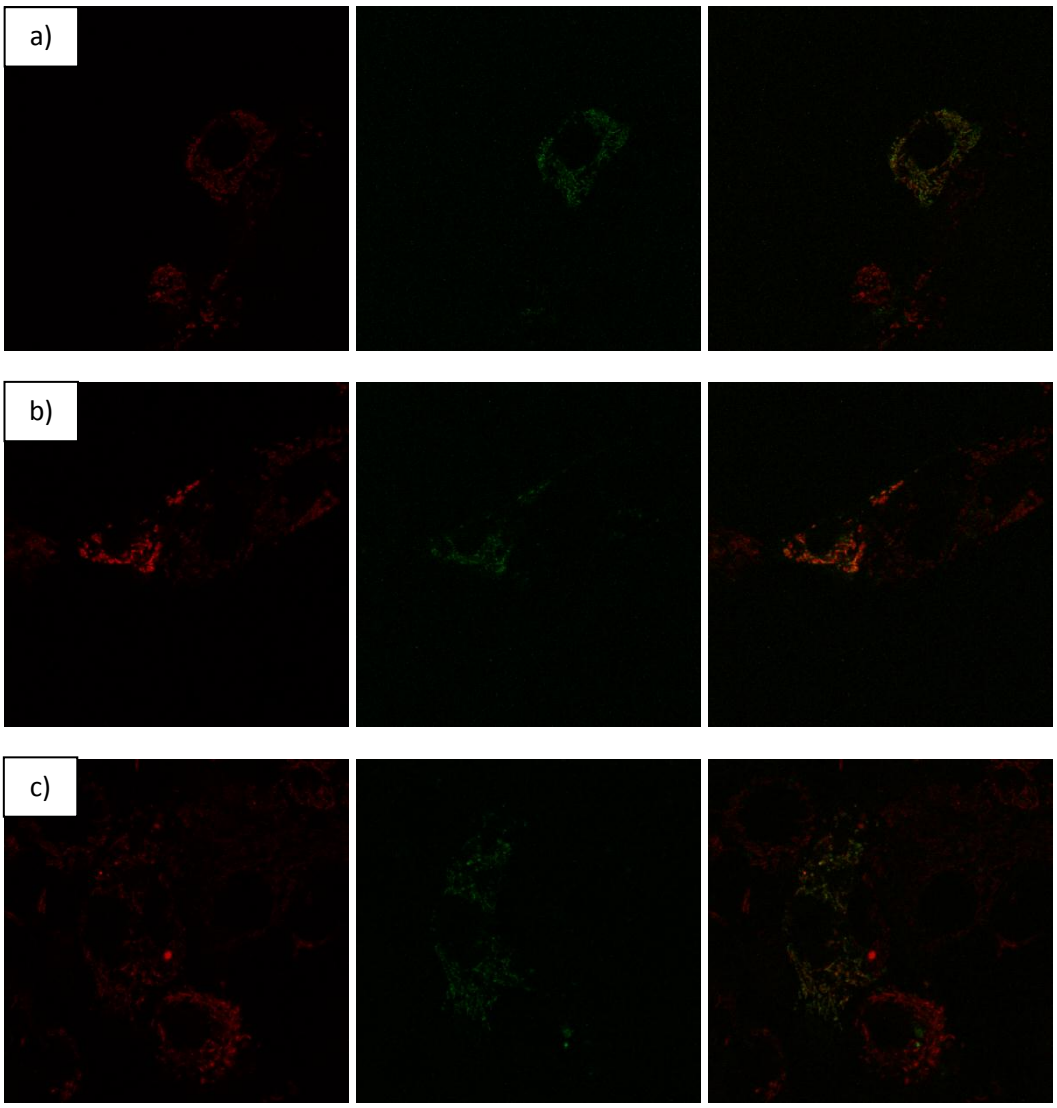

Figure 4.12 – Colocalisation of Hsp60-GFP with mitotracker in sodium azide group using false colour (red = mitotracker; green = Hsp60-GFP; yellow = colocalisation between the two signals). a) 24 h; r = 0.68. b) 48 h; r = 0.69. c) 72 h; r = 0.73.

Figure 4.13 shows the changes in the mean overlapping values for the control group. At 24, 48 and 72 h the varied means are 0.65 ± 0.02, 0.69 ± 0.02 to 0.72 ± 0.01 respectively. The increased overlap between 24 h and 72 h was significant ($p < 0.05$). It shows an increase in colocalisation by approximately 7% from 24 h to 72 h. **Figure 4.14** shows the changes in the mean overlapping values for the glucose group. A different pattern could be seen immediately when compared to the control group. There appeared to be a decline in the colocalisation of Hsp60-GFP and Mitotracker CMX Ros signals. At 24, 48 and 72 h the varied means are 0.69 ± 0.03, 0.66 ± 0.03, 0.60 ± 0.04 respectively. Using a two-tailed student's t-test revealed no significance differences between the means of 24, 48 and 72 h ($p > 0.05$). However, a single tailed test showed that there was a significant decrease from 24 to 72 h ($p < 0.05$), the significance being between 24 and 72 h specifically (by approximately 9%). The graph in **Figure 4.15** shows the mean overlap coefficient for the sodium azide treatment. Using the overlap coefficient revealed no significant differences between the means of 24, 48 and 72 h ($p > 0.05$). Scaling down to a single tailed student's t-test showed change to significance. The differences between the means however still showed varied colocalisation. Data from 24 h had a mean of 0.69 ± 0.02 with a 48 h mean of 0.66 ± 0.02 while 72 h had a mean of 0.73 ± 0.03 There appeared to be a sudden (but insignificant) spike in colocalisation at 72 h.

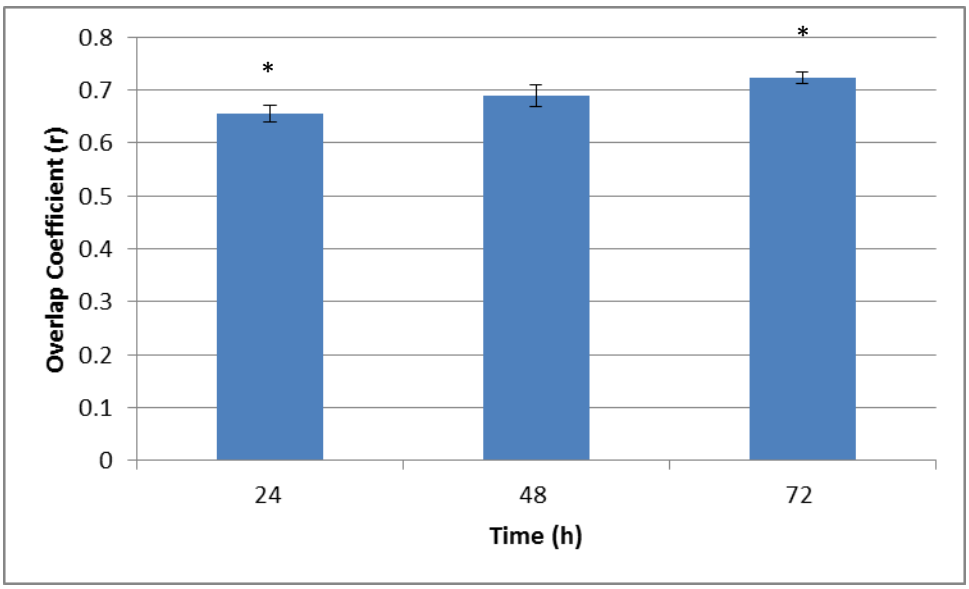

Figure 4.13 – The overlap coefficient (r) means for the control group at 24, 48 and 72 hours. Bar graph showing the mean ± S.E.M.

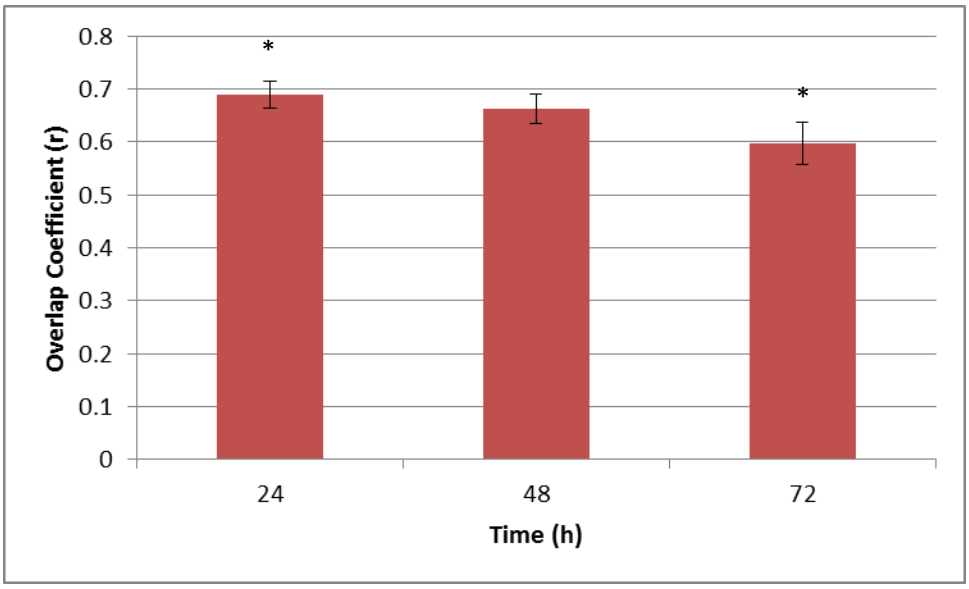

Figure 4.14 – The overlap coefficient (r) means for the 100mM glucose group at 24, 48 and 72 hours. Bar graph showing the mean ± S.E.M.

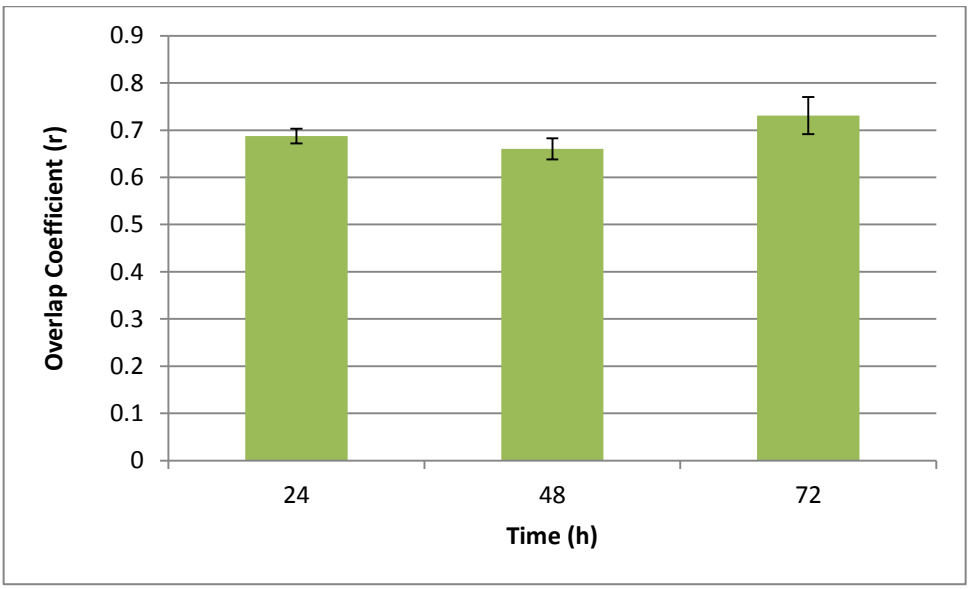

Figure 4.15 – The overlap coefficient (r) means for the 25µM sodium azide group at 24, 48 and 72 hours. Bar graph showing the mean ± S.E.M.

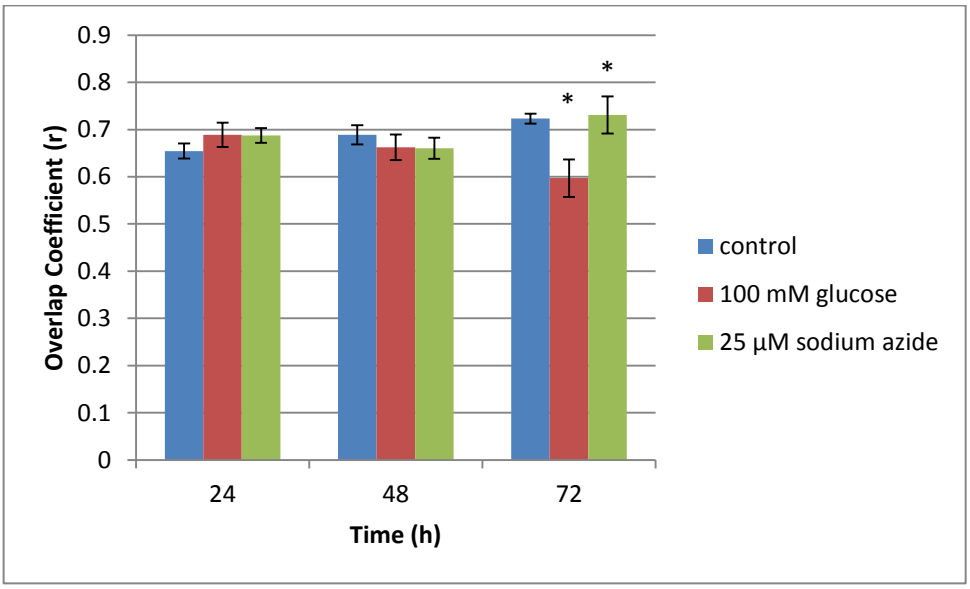

Figure 4.16 – The overlap coefficient (r) means for the all three treatments at 24, 48 and 72 hours. The blue, red and green bars show means for control, 100 mM glucose and 25 µM sodium azide, respectively. Bar graph showing the mean ± S.E.M.

The data seen in **Figure 4.16** shows all three treatments assessed side-by-side. At 24 h were no significant differences between the degrees of colocalisation between Hsp60-GFP and mitotracker for all treatments. The same was found for the 48 h time point. All the treatments revealed similar levels of overlap. At 72 h

a significant, and relatively substantial, difference was observed between the control and the glucose treatments. This same significance was observed between the sodium azide and glucose treatments. The 72 h figures for the control and glucose treatments were 0.72 ± 0.01 and 0.60 ± 0.04. This indicates a difference in colocalisation of approximately 12%. The 72 h figure for sodium azide was 0.73 ± 0.03 indicating an approximate difference with the glucose treatment of 13%.

4.4 Discussion

The human Hsp60 is an important protein that resides in the mitochondria of human cells. It has roles in protein folding, chaperoning denatured proteins and in the intracellular stress response (Gupta & Knowlton 2005; Quintana & Cohen 2011). Hsp60 has been more recently implicated in intercellular signalling and that it shares receptors with cell stressors such as LPS (Cohne-Sfady *et al.* 2005). It was also found that diabetic patients had elevated levels of Hsp60 in saliva and serum samples (Yuan *et al.* 2011). In this chapter HeLa cells were transfected with RG224428, a plasmid encoding a human Hsp60 with a GFP protein attached to the C-terminus. Transfected cells were treated with high glucose (to simulate hyperglycaemia) and sodium azide (a mitochondrial stressor). The Hsp60-GFP was then analysed on a confocal microscope and its colocalisation with Mitotracker CMX Ros (used to stain actively respiring mitochondria) was calculated.

Modern day HeLa cells are derived from a human cervical cancer cell line originating from 1951 (Ursano 2012). As such, they are mammalian and possess a phenotype similar to normal human cells (though immortalised). They can be grown in media designed to emulate a human biological system and due to their robust nature they are useful for scientific studies. Some researchers have used HeLa cells to study mitochondrial diseases such as mitochondrial encephalomyopathy (Isobe *et al.* 1997). HeLa cell nuclei were replaced with nuclei from patients suffering mitochondrial diseases in order to establish if the complications were caused by mutations in mitochondria (or chromosomal DNA). Bouvard *et al.* (2002) transfected HeLa cells with the tat gene from human immunodeficiency virus 1 (HIV1). This caused a reduction in the cells' ability to cope with glucose. Their work showed that Mn-dependant superoxide dismutase

(Mn-SOD; reduces superoxide to O_2 and H_2O_2) was impaired with a 50% reduction in activity causing glucose cytotoxicity. Recently HeLa cells were transfected to produce a pH sensitive protein which fluoresces in acidic conditions. This was used to understand the acidic properties of intracellular organelles. Diseases such as cancer and Alzheimer's disease have been linked to abnormal cellular pH conditions (Lv *et al.* 2013).

In our research HeLa cells were transfected with the plasmid RG224428 (**Figure 3.1**) which encodes a human Hsp60-GFP. A lipid based transfection agent, Lipofectamine 2000 (Invitrogen), was used to deliver the plasmid into the cytosol of the HeLa cells (detailed in **4.2.2**). The highest average transfection efficiency we could achieve with our methods was ~4%. This result is considerably very low to what has been reported in the literature. Susa *et al.* (2008) reported transfection efficiencies in fluorescence emitting cells as high as 20% using Lipofectamine 2000. This represents a 5-fold increase over our results. Some key differences were they used the gonadotrope cell line LβT2 and they achieved this efficiency using much less DNA (10 ng). β-galactosidase transfection assays have been used to detect transfection efficiencies. These assays require that the gene for β-galactose be translated by cells in order to digest galactose products usually linked with a marker that changes colour upon digestion (Li *et al.* 2012). Using β-galactosidase assays, Yomano *et al.* (2010) tested the transfection efficiencies of various cell types with various different transfection reagents. HeLa cells transfected using lipofectamine 2000 were among their tests. Out of six different transfection reagents (Arrest-In (Thermo Scientific); ExpressFect (Denville Scientific); FuGENE HD(Roche); jetPEI(Polyplus-Transfection); Lipofectamine 2000 (Invitrogen); Superfect (Qaigen)) Lipofectamine 2000 showed the lowest efficiency for β-galactosidase methods excluding serum. It was the second lowest

when 10% serum was used. Their data also show that efficiency changes between cell lines. In C2C12 mouse myoblasts Lipofectamine 2000 had a ~4-fold lower efficiency than jetPEI (Yomano *et al.* 2010). Variables such as cell type and transfection reagent may need to be reconsidered in future tests using our methods. There may be other cells that can incorporate the Hsp60-GFP more readily. Despite low transfection efficiency HeLa cells were successfully transfected and proved useful for our study.

Propidium iodide (PI) is a fluorescent probe used to detect cellular damage by binding to exposed DNA (Lin *et al.* 2007; Knowlton & Uma 2008). We stained transfected HeLa cells with PI and found that an average of ~4% of transfected cells were colocalising with PI (on a wide-field microscope; 20X magnification). This suggested that the Hsp60-GFP posed very low-to-no toxicity to the cells.

Hsp60 expression is upregulated with many types of cellular stress. Upregulation can be as high as 10% in stress induced cells. The increased Hsp60 is thought to deal with protein denaturation and misfolding (Pockley 2002). Increases in heat from 25^{o}C to 46^{o}C have seen 30-40% increases in polypeptide binding with Hsp60 (Martin et al. 1992). Sarri *et al.* (2009) found that Hsp60 expression is significantly increased after cardiac allograft rejection events in heart transplant patients. Data collected from biopsies showed Hsp60 levels of 8.94 pg/ml and 14.92 pg/ml for samples taken during rejection and recovery, respectively. Hsp60 in blood serum samples from type 2 diabetic patients showed dramatic increases. Non-diabetics had levels as high as 7 ng/ml while diabetics had levels as high as 75 ng/ml (Yuan *et al.* 2011). Hsp60 has been found expressed on the surface of various cell types. Hsp60 expressed on the surface of pancreatic β-cells has been linked with T-cell mediated insulitis (Birk *et al.* 1996). Since Hsp60 predominantly resides in mitochondria and is released in times of stress, we

wanted to investigate the changes in colocalisation between Hsp60 and mitochondria. In our study we used HeLa cells transfected with an Hsp60-GFP. Mitochondria were stained with Mitotracker CMX Ros. Where many have used fixed-cell preparations we employed three conditions on live cells growing in media. The colocalisation analyses were performed using and Olympus FV1000 laser scanning microscope. The overlap coefficient ('r value'; derived from Pearson's correlation) was used to calculate the degree of colocalisation. The overlap coefficient was used instead of Pearson's correlation because the Pearson correlation requires the fluorescent signals to be of equal intensity. We found that the intensity of the chemically based mitotracker was consistent between cells but the biologically derived Hsp60-GFP was not. When colocalising the two signals it was clear that the intensities were very different.

We found that the control group had a significant ~7% increase ($p < 0.05$), from 24 h to 72 h in the colocalisation between the mitotracker and Hsp60-GFP signals. This change over time may be due to our induced Hsp60-GFP competing for mitochondrial uptake with the endogenous Hsp60. At 24 h there may be GFPs attached to the pre-peptide Hsp60s that emit fluorescence in the cytosol while the Hsp60 is still in a peptide form awaiting uptake into mitochondria. This increase overtime has been observed in other studies. Jayakumar *et al.* (2001) waited 4 days to allow for transfected cells to produce optimal levels of Hsp70 before testing isheamia and reperfusion stress in rat hearts.

An important aspect of our methods to consider is that inducing overexpression of Hsp60 may alter the cells ability to cope with stress. A study using a viral vector containing Hsp72 to transfect porcine renal tubular epithelial cells (LLC-PK1 cells) showed that the introduced vector caused overexpression of Hsp72. The 3-fold increase in Hsp72 expression was correlated with a significant increase in

resistance to H_2O_2 and cisplatin (a pro-apoptotic drug) stress (Komatsuda *et al.*1999). This type of response would be difficult to avoid in our methods but insuring the controls are well represented alongside the treatments would provide the necessary clarity.

The glucose (100 mM) treatment showed a decline in colocalisation by ~9% ($p < 0.05$) after 72 hours. Relative to the control group the glucose group had a total decline of ~12% ($p < 0.05$) in colocalisation between the Hsp60-GFP and mitotracker signals. In normal healthy cells 80 – 85% of Hsp60 is found within mitochondria leaving 15 – 20% in the cytosol (Knowlton & Srivatsa 2008). Hsp60 has been found to be upregulated by up to 10% during stress (Pockley 2002). More research would be required to investigate a connection between the ~12% change we observed in Hsp60 expression with the similar levels of upregulation in other studies (Pockley 2002). Another factor to consider is that Hsp60 has been found to accumulate in the cytosol without disrupting mitochondrial Hsp60 levels (Chandra *et al.* 2007).

Sodium azide is a highly toxic substance that has been used to stress mitochondria in earlier research (Leary *et al.* 2002; Ishikawa *et al.* 2006). The toxic properties of sodium azide arise from its interaction with complex IV of the electron transport chain in mitochondria. It binds to the Fe^{3+} in cytochrome c oxidase (complex IV) which in turn cancels the oxidative phosphorylation vital to sufficient ATP production (Ishikawa *et al.* 2006). Concentrations as low as 10 µM have been found to adversely affect mammalian cells by reducing complex IV activity (Leary *et al.* 2002). Ishikawa *et al.* (2006) found that different tissues can have differing levels of tolerance to sodium azide. They found myocardial and nerve cells to be more sensitive than fibroblast, liver and kidney epithelial tissue. They also noted that mitochondria stressed with sodium azide had atrophied. We

initially expected to see a reduction in mitotracker uptake in cells stressed with sodium azide as well as a disruption in mitochondrially-bound Hsp60-GFP. As these conditions were not apparent future sodium azide treatments will need to be tested using MTT assays to ensure mitochondrial activity is being inhibited.

Further testing will be required to establish by what means the colocalisation declines in high glucose concentrations. Fluorescent probes for lipid rafts may prove useful in detecting the movement of Hsp60 out of mitochondria. Lipid rafts can translocate around the cytosol and bind with membranes. The inhibition of lipid raft creation has reduced Hsp60 translocation in studies before (Merendino *et al.* 2010). It may be found that a decrease in Hsp60-GFP and mitotracker colocalisation my lead to an increase in Hsp60-GFP colocalisation with probes bound to lipid rafts. Assays calculating mitochondrial Hsp60 and cytosolic Hsp60 may provide the information needed to establish whether the observed decrease in colocalisation is by Hsp60-GFPs translocation out of mitochondria or the translation, modification and application of Hsp60-GFP straight to the cytosol.

5 Final Summary and Future Directions

In this study, live HeLa cells were transfected with an Hsp60-GFP to determine if they could be used to study the colocalisation between the Hsp60 protein and mitochondria. The plasmid RG224428 containing the Hsp60-GFP was successfully cloned and purified, in and from DH5α *E. coli*.

Using Lipofectamine 2000 HeLa cells were transfected with a transfection efficiency of ~4%. In order to improve the transfection efficiency a control plasmid (GFP only) may need to be employed to test the interaction between the Hsp60-GFP and the HeLa cells. By varying the conditions HeLa is grown in we may find that an additional Hsp60 gene source may be treated differently to the chromosomal gene. Diabetic hyperglycaemia has been linked to an increase in Hsp60 expression in the circulation (Jax 2010; Yuan *et al.* 2011) and other studies have found that Hsp60 can be upregulated during stress (Shafler *et al.* 2002; Gupta & Knowlton 2005). The growth media we used to grow HeLa cells had a glucose concentration of 25 mM. This higher glucose concentration was several times higher than the >11.1 mM concentration that describes diabetes (World Health Organisation 2006). The high glucose environment in the growth media that preceded the transfection media may have altered or upregulated the chromosomal Hsp60. This may have had a negative effect on the expression of the introduced Hsp60-GFP. Future studies may need to test transfection efficiencies in cells grown in media with lower glucose concentrations. Different transection reagents may also provide greater efficiencies. Tests have shown that transfection reagents can achieve different transfection yields. Other cell types may also provide more efficient platforms to transfect with an Hsp60-GFP (Yomano *et al.* 2010).

Despite the low transfection efficiency staining with propidium iodide determined that the transfection imposed very low-to-no toxicity in the HeLa cells. Staining cells with Mitotracker CMX Ros revealed the successful uptake of Hsp60-GFP to mitochondria. Using laser scanning confocal microscopy it was shown that growth media adjusted to hyperglycaemic conditions (100 mM glucose) caused ~12% of the Hsp60-GFP signal to translocate out of the mitochondria and into the cytosol after 72 hours. Our research suggests that hyperglycaemic stress my cause a disruption in normal mitochondrial Hsp60 expression. It also suggests that the balance between mitochondrial and cytosolic Hsp60 may be altered by the translocation of more Hsp60 into the cytosol.

Other researchers have found that stress can disrupt the expression of Hsp60. A study of Hsp60 cell surface expression was performed on human umbilical vein endothelial cells (HUVECs). When cells were heat-shocked (42^{o}C) they showed increased surface expression of Hsp60. The heat-shocked cells showed a 10% increase in surface expression when compared to non-heat-shocked controls (Pfister *et al*. 2005). Tsuei & Martinus (2012) found that metformin, an anti-hyperglycaemic agent used for diabetic therapy, could increase levels of Hsp60 mRNA in human acute monocytic leukaemia (THP-1) cells. At higher levels (500 µM) it could induce an upregulation of the Hsp60 protein within the cells by 26-fold. Not all cells have been found to upregulate Hsp60 during stress. In a study by Barutta *et al.* (2008) it was found that human podocytes (involved in kidney filtration) and mesangial cells (support capillaries in the kidney) exposed to high-glucose (25mM; 4-fold lower than our treatment) and mechanical stress did not increase Hsp60 expression. (Shan *et al.* 2010) found that hyperglycaemia can inhibit the synthesis of Hsp60 in murine cardiomyocytes by upregulating the microRNAs miR-1 and miR-206. The researchers found that hyperglycaemia was

responsible for increasing the expression of miR-1 and miR-206 which downregulated Hsp60 allowing apoptosis to take place. Hyperglycaemic stress has been linked to the modification of cytosolic Hsp60. Kim *et al*. (2006) found that O-N-acetylglucosamine (O-GlcNAc), a glucose-derived product formed by the hexosamine pathway, bound to cytosolic Hsp60 in rat β-cells during hyperglycaemia. They also found a two-fold increase in Bax expression in mitochondria. As cytosolic Hsp60 is normally bound to the pro-apoptotic protein Bax, hyperglycaemia was found to disrupt this binding.

Hsp60 has been described as a potential biomarker for stress (Quintana & Cohen 2011). It has been found expressed in exosomes (nm-sized vesicles) secreted by human cancer cells (Meredino *et al.* 2010). These exosomes are considered to be an important path used to translocate Hsp60 to nearby cells and into the circulation (Campanella *et al*. 2012). Type 1 diabetic patients (prone to hyperglycaemia) have shown increased levels of Hsp60 in the circulation accompanied by its increased liganding with TLR4 receptors (Devaraj *et al*. 2009). It was also found that type 2 diabetic patients had elevated levels of Hsp60 in saliva and serum samples (Yuan *et al*. 2011). Studies outside of diabetes and metabolic stress have also shown elevated Hsp60 in blood samples. Wheeler *et al*. (2007) found that levels of Hsp60 in the blood-serum samples of children suffering septic shock were significantly higher.

Our approach to better understand the relationship between Hsp60 and mitochondria during stress employed fluorescent-confocal microscopy. We found this method very effective in determining colocalisation in living cells. As Hsp60 can be used as a biomarker for many different stress conditions, we suggest future studies use our methods to investigate other cellular stressors and their relative therapies. An advantage in these methods is that specific living cells can be

accurately monitored over short periods of time while stressors and therapeutic agents are administered. This may help calculate the rates at which stressors and therapies act within cells.

By adding fluorescent tags to cytosolic transportation vesicles these methods may be used to further determine the pathways used to translocate other Hsps. Chen *et al.* (2005) used western blotting to quantify the amounts of different heat shock proteins (Hsps 90, 70, 60 and 40) found in lipid rafts extracted from rat brain. They found that the Hsps were expressed in the lipid rafts of non-stressed neurons and upon hyperthermic treatment Hsp70 was increased. Use of an Hsp70-GFP with our methods could help quantify the degree of colocalisation between Hsp70 and fluorescently-labelled lipid rafts before and after hyperthermic treatment in live neurons. Hsp60 has been found in the lipid rafts of cancer cell lines (Merendino *et al.* 2010) and the lipid rafts and exosomes secreted by cardiac myocytes (Gupta & Knowlton 2006). Gupta & Knowlton (2006) performed hypoxia on cardiac myocytes and found evidence suggesting the Hsp60 expressed in secreted exosomes originated from lipid rafts within the stressed cells. The use of Brefeldin A (inhibits transport of proteins from the endoplasmic reticulum to the Golgi apparatus) showed that Hsp60 was translocated to exosomes by a pathway other than the common protein secretion pathway (using the Golgi apparatus). Hsps using lipid raft based secretion have been found in other cell types. Heat shocked peripheral blood mononuclear cells have shown that Hsp70 can be secreted in the presence of Brefeldin A (Lancaster & Febbraio 2005). Our methods may help to determine the path cells use to secrete heat shock proteins by using colocalisation techniques. This may be a novel way to test therapies designed to reduce the Hsp60 secretion observed in diabetic patients, potentially reducing inflammation.

6 References

Aich P, Patra M, Chatterjee AK, Roy SS, Basu T 2012. Calcium Chloride Made *E. coli* Competent for Extraneous DNA Through Overproduction of OmpC Protein. The Protein Journal 31(5): 366-373.

Akiyama T, Matsuno S, Okamoto H, Takasawa S, Nata K, Kobayashi S, Abe M, Shervani NJ, Ikeda T, Nakagawa K, Unno M 2001. Activation of Reg Gene, a Gene for Insulin-Producing β-Cell Regeneration: Poly(ADP-Ribose) Polymerase Binds Reg Promoter and Regulates the Transcription by Autopoly(ADP-Ribosyl)ation. Proceedings of the National Academy of the United States of America 98(1): 48-53.

Allt G & Lawrenson JG 2001. Pericytes: Cell Biology and Pathology. Cells, Tissues, Organs 169(1): 1-11.

Aokage T, Oshsawa I, Ohta S 2004. Green Fluorescent Protein Causes Mitochondria to Aggregate in the Presence of the Bcl-2 Family Proteins. Biochemical and Biophysical Research Communications 314(3): 711-716.

Ariff AB, Mohamad R, Mohamed MS, Puspaningsih NNTP, Rusli FM 2009. Kinetics of Xylanase Fermentation by Recombinant *Escherichia coli* DH5α in Shake Flask Culture. American Journal of Biochemistry and Biotechnology 5(3): 109-117.

Assert R, Scherk G, Bumbure A, Pirags V, Schatz H, Pfeiffer AFH 2001. Regulation of Protein Kinase C by Short Term Hyperglycaemia in Human Platelets *in Vivo* and *in Vitro*. Diabetologia 44(2): 188-195.

Barcia RN, Valle NSD, McLeod JD 2003. Caspase Involvement in RIP-Associated CD95-Induced T Cell Apoptosis. Cellular Immunology 226(2): 78-85.

Bar-Nur O, Russ HA, Efrat S, Benvenisty N 2011. Epigenetic Memory and Preferential Lineage-Specific Differentiation in Induced Pluripotent Stem Cells Derived from Human Pancreatic Islet Beta Cells. Cell Stem Cell 9: 17-23.

Barutta F, Cooper ME, Gruden G, Pinach S, Giunti S, Vittone F, Forbes JM, Chiarle R, Arnstein M, Perin PC Camussi G 2008. Heat Shock Protein Expression in Diabetic Nephropathy. American Journal of Physiology – Renal Physiology 295(6): 1817-1824.

Bedard K & Krause K 2007. The NOX Family of ROS-Generating NADPH Oxidases: Physiology and Pathophysiology. Physiological Reviews 87(1): 245-313.

Beilin L, Singh R, Mori T, Barden A 2001. Advanced Glycation End-Products: A Review. Diabetologia 44 (2): 129-146.

Birk OS, Douek DC, Elias D, Takacs K, Dewchand H, Gur SL, Walker MD, van der Zee R, Cohen IR, Altmann DM 1996. A Role of Hsp60 in Autoimmune Diabetes: Analysis in a Transgenic Model. Proceedings of the National Academy of Science of the United States of America 93(3): 1032-1037.

Blasi C, Kim E, Knowlton AA 2012. Improved Metabolic Control in Diabetes, HSP60, and Proinflammatory Mediators. Autoimmune Diseases 2012(346501): 1-8.

Bolzan A & Bianchi MS 2002. Genotoxicity of Streptozotocin. Mutation Research-Reveiws in Mutation Research 512(2): 121-134.

Bonner-Weir S, Baxter LA, Schuppin GT, Smith FE 1993. A Second Pathway for Regeneration of Adult Exocrine and Endocrine Pancreas. A Possible Recapitulation of Embryonic Development. Diabetes 42(12):1715-1720.

Bouvard S, Faure P, Roucard C, Favier A, Halimi S 2002. Characterization of Free Radical Defense System in High Glucose Cultured HeLa-tat Cells: Consequences for Glucose-Induced Cytotoxicity. Free Radical Research 36(9): 1017-1022.

Brocchieri L & Karlin S 2000. Conservation Among HSP60 Sequences in Relation to Structure, Function, and Evolution. Protein Science 9(3): 476-486.

Browlee M 2001. Biochemistry and Molecular Cell Biology of Diabetic Complications. Nature 414 (6865): 813-820.

Brownlee M 2005. The Pathology of Diabetic Complications: A Unifying Mechanism. Diabetes 54 (6): 1615-1625.

Calderwood SK, Mambula SS, Gray PJ Jr. 2007. Extracellular Heat Shock Proteins in Cell Signalling and Immunity. Annals of the New York Academy of Sciences 1113: 28-39.

Callan JF, de Silva AP, Magri DC 2005. Luminescent Sensors and Switches in the Early 21st Century. Tetrahedron 61 (36): 8551-8588.

Campanella C, Zummo G, de Macario EV, Macario AJL, Cappello F, Bucchieri F, Meredino AM, Fucarino A, Burgio G, Corona DFV, Barbieri G, David S, Farina F 2012. The Odyssey of Hsp60 from Tumor Cells to Other Destinations Includes Plasma Membrane-Associated Stages and Golgi and Exosomal Protein-Trafficking. Plos One 7(7): e42008 1-8.

Carlsson C, Jonsson M, Akerman B 1995. Double Bands in DNA Gel Electrophoresis Caused by Bis-Intercalating Dyes. Nucleic Acids Research 23(13): 2413-2420.

Chan EM, Ratanasirintrawoot S, Park I, Manos PD, Loh Y, Huo H, Miller J, Hartung O, Rho J, Ince TA, Daley GQ, Schlaegar TM 2009. Live Cell Imaging Distinguishes Bona Fide Human iPScells form Partially Reprogrammed Cells. Nature Biotechnology 27(11): 1033-1037.

Chandra D, Choy G, Tang DG 2007. Cytosolic Accumulation of HSP60 During Apoptosis With or Without Apparent Mitochondrial Release: Evidence that its Pro-Apoptotic or Pro-Survival Functions Involve Differential Interactions with Caspase-3. The Journal of Biological Chemistry 282(43): 31289-31301.

Chen S, Bawa D, Besshoh S, Gurd JW, Brown IR 2005. Association of Heat Shock Proteins and Neuronal Membrane Components with Lipid Rafts from the Rat Brain. Journal of Neuroscience Research 81(4): 522-529.

Cheng MY, Hartl FU, Horwich AL 1990. The Mitochondrial Chaperonin Hsp60 is Required for its Own Assembly. Nature 348(6300): 455-458.

Cheung CY, Murthy N, Stayton PS, Hoffman AS 2001. A pH-Sensitive Polymer that Enhances Cationic Lipid-Mediated Gene Transfer. Bioconjugate Chemistry 12(6): 906-910.

Christian P, Scherer F, Schillinger U, Bergemann C, Anton M 2003. Magnetofection: Enhancing and Targeting Gene Delivery with Superparamagnetic Nanoparticles and Magnetic Fields. Journal of Liposome Research 13(1): 29-32.

Chung SSM, Ho ECM, Lam KSL, Chung SK 2003. Journal of the American Society of Nephrology 14(8): S233-S236.

Cnop M, Igoillo-Esteve M, Hughes SJ, Walker JN, Cnop I, Clark A 2011. Longevity of Human Islet α and β- Cells. Diabetes, Obesity and Metabolism 13(1): 39-46.

Cohen-Sfady M, Nussbaum G, Pevsner-Fischer M, Mor F, Carmi P, Zanin-Zhorov A, Lider O, Cohen IR 2005. Heat Shock Protein 60 Activates B Cells Via the TLR4-MyD88 Pathway. Journal of Immunology 175(6): 3594-3602.

Collombat P, Hecksher-Sorensen J, Krull J, Berger J, Riedel D, Herrera PL, Serup P, Mansouri A 2007. Embryonic Endocrine Pancreas and Mature Beta Cells Acquire Alpha and PP Cell Phenotypes upon Arx Misexpression. The Journal of Clinical Investigation 117(4): 961-970.

Collombat P, Xu X, Ravassard P, Sosa-Pineda B, Dussaud S, Billestrup N, Madsen OD, Serup P, Heimberg H, Mansouri A 2009. The Ectopic Expression of Pax4 in the Mouse Pancreas Converts Progenitor Cells into Alpha and Subsequently Beta Cells. Cell 138(3): 449-462.

Dalby B, Cates S, Harris A, Ohki EC, Tilkins, MaryL, Price PJ, Ciccarone VC 2004. Advanced Transfection with Lipofectamine 2000 Reagent: Primary

Neurons, siRNA, and High-Throughput Applications. Methods 33(2): 95-103.

Davies EL Bacelar MMFVG, Marshal MJ, Johnson E, Wardle TD, Andrews SM, Williams JHH 2006. Heat Shock Proteins Form Part of a Danger Signal Cascade in Response to Lipopolysaccharide and GroEL. Clinical & Experimental Immunology 145(1): 183-189.

de Ruijter AJM, van Gennip AH, Caron HN, Kemp S van Kuilenburg ABP 2003. Histone Deacetylases (HDACs): Characterization of the Classical HDAC Family. The Biochemical Journal 370(3): 737-749.

Devaraj S, Dasu MR, Park SH, Jailal I 2009. Increased Levels of Ligands of Toll-Like Receptors 2 and 4 in Type 1 Diabetes. Diabetologia 52(8): 1665-1668.

Dohi T, Beltrami E, Wall NR, Plescia J, Altieri DC 2004. Mitochondrial Survivin Inhibits Apoptosis and Promotes Tumorigenesis. Journal of Clinical Investigation 114(8): 1117- 1127.

Du X, Takeshi M, Edelstein D, Rossetti L, Zsengeller Z, Szabo C, Browlee M 2003. Inhibition of GAPDH Activity by Poly(ADP-ribose) Polymerase Activates Three Major Pathways of Hyperglycemic Damage in Endothelial Cells. Journal of Clinical Investigation 112 (7): 1049-1057.

Elmore S 2007. Apoptosis: a Review of Programmed Cell Death. Toxicology Pathology 35(4): 495-516.

Evdokimov AG, Pokross ME, Egrov NS, Zaraisky AG, Yamplosky IV, Merzlyak EM, Shkoporov AN, Sander I, Konstantin AL, Chudakov D 2006. Structural Basis for the Fast Maturation of Arthropoda Green Fluorescent Protein. EMBO Reports 7(10): 1006-1012.

Fan Z, Beresford PJ, Oh DY, Zhang D, Lieberman J 2003. Tumor Suppressor NM23-H1 is a Granzyme A-Activated Dnase During CTL-Mediated Apoptosis, and the Nucleosome Assembly Protein SET is its Inhibitor. Cell 112(5): 659-672.

Feltham JL & Gierasch LM 2000. GroEL-Substrate Interactions. Cell 100(2): 193-196.

Fenton WA, Kashi Y, Furtak K, Horwich AL 1994. Residues in Chaperonin GroEL Required for Polypeptide Binding and Release. Nature 371(6498): 614-619.

Foradada M, Manzano A, Roig T, Estelrich J, Bermudez J 1997. Serum-Liposome Interaction is an Oxygen-Dependant Process. Biochemica et Biophysica Acta 1345(1): 43-55.

Fowler MJ 2010. Diabetes: Magnitude and Mechanisms. (Diabetes Foundation)(Report). Clinical Diabetes 28(1): 42-46.

Gecz J, Cloosterman D, Partington M 2006. ARX: a Gene for All Seasons. Current Opinion in Genetics & Development 16(3): 308-316.

Ghosh JC, Dohi T, Kang BH, Altieri DC 2008. Hsp60 Regulation of Tumor Cell Apoptosis. The Journal of Biological Chemistry 283(8): 5188-5194.

Golzhauser A, Nattkemper T, Niehaus K, Puhler A, Sauer M 2010. Bioimaging: Contributions from Biology, Physics and Informatics. Journal of Biotechnology 149(4): 227-228.

Grynkiewicz G, Poenie M, Tsien RY 1985. A New Generation of Ca^{2+} Indicators with Greatly Improved Fluorescence Properties. The Journal of Biological Chemistry 260 (6): 3440-3450.

Gupta S & Knowlton AA 2005. Hsp60, Bax, Apoptosis and the Heart. Journal of Cellular and Molecular Medicine 9(1): 51-58.

Gupta S & Knowlton AA 2006. Exosome Dependant HSP60 Secretion in Rat Cardiac Myocytes. Journal of Molecular and Cellular Cardiology 40(6): 875-876.

Hanley S, Rosenburg L 2009. Islet-Derived Progenitors as a Source of Islet Regeneration. Stem Cells in Regenerative Medicine: Methods and Protocols. Chapter 23 482: 371-385.

Hanover JA, Krause MW, Love DC 2010. The Hexosamine Signalling Pathway: O-GlcNAc Cycling in Feast or Famine. Biochimica et Biophysica Acta 1800(2): 80-95.

Hashimoto N, Kido Y, Uchida T, Asahara S, Shigeyama Y, Matsuda T, Takeda A, Tsuchihashi D, Nishizawa A, Ogawa W, Fujimoto Y, Okamura H, Arden KC, Herrera PL, Noda T 2006. Ablation of PDK1 in Pancreatic β Cells Induces Diabetes as a Result of Loss of β Cell Mass. Nature Genetics 38(5): 589-593.

Henderson B, Calderwood SK, Coates ARM, Cohen I, van Eden W, Lehner T, Pockley AG 1010. Caught with Their PAMPs Down? The Extracellular Signalling Actions of Molecular Chaperones are Not Due to Microbial Contaminants. Cell Stress and Chaperones 15(2): 123-141.

Henze K, Martin W, Martin W 2003. Evolutionary Biology: Essence of Mitochondria. Nature 426(6963): 127-128.

Horvitz HR 1999. Genetic Control of Programmed Cell Death in the Nematode *Caenorhabditis elegans*. Cancer Research 59(7): 1701S-1706S.

Horwich AL, Fenton WA, Chapman e, Farr GW 2007. Two Families of Cheperonin: Physiology and Mechanism. Annual Review of Cell and Developmental Biology 23(1): 115-145.

Horwich AL, Low KB, Fenton WA, Hirshfield IN, Furtak K 1993. Folding in-Vivo of Bacterial Cytoplasmic Proteins – Role of GroEL. Cell 74(5): 909-917.

Ihnat M, Ceriello A, Thorpe JE 2007. Hypothesis: The 'Metabolic Memory', the New Challenge of Diabetes. Diabetic Medicine 24 (6): 582-586.

Ishikawa T, Zhu B, Maeda H 2006. Effect of Sodium Azide on the Metabolic Activity of Cultured Fetal Cells. Toxicology and Industrial Health 22(8): 337-341.

Isobe K, Kishino S, Inoue K, Takai D, Hirawake H, Kita K, Miyabayashi S, Hayashi JI 1997. Identification of Inheritance Modes of Mitochondrial

Diseases by Introduction of Pure Nucei from mtDNA-less HeLa Cells to Patient-Derived Fibroblasts. The Journal of Biological Chemistry 272(19): 12606-12610.

Jackson G, Orr Walker B, Smith J, Papa D, Field A 2009. Hospital Admissions for People with Diagnosed Diabetes: Challenges for Diabetes Prevention and Management Programmes. The New Zealand Medical Journal 122(1288): 13-21.

Jax TW 2010. Metabolic Memory: a Vascular Perpective. Cardiovascular Diabetology 9(51): 1-8.

Jayakumar J, Yacoub MH, Suzuki K, Sammut IA, Smolenski RT, Khan M, Latif N, Abunarsa H, Murtuza B, Amrani M 2001. Heat Shock Protein 70 Gene Transfection Protects Mitochondrial and Ventricular Function Against Ishemia-Reperfusion Injury. 104(12): I-303-I-307.

Jordan M, Schallhorn A, Wurm FM 1996. Transfecting Mammalian Cells: Optimization of Critical Parameters Affecting Calcium-Phosphate Precipitate Formation. Nucleic Acids Research 24(4): 596-601.

Karthikeyan R, Surianarayanan M, Sudharshan S, Gunasekaran P, Asit Baran M 2011. Biocalorimetric and Respirometric Studies on Production of Penicillin G Acylase from Bacillus *badius pac* in *E. coli* DH5α. Biochemical Engineering Journal 55(3): 223-229.

Kerr JF, Wyllie AH, Currie AR 1972. Apoptosis: a Basic Biological Phenomenon with Wide-Ranging Implications in Tissue Kinetics. British Journal of Cancer 26(4): 239-257.

Kim TK & Eberwine JH 2010. Mammalian Cell Transfection: the Present and the Future. Analytical and Bioanalytical Chemistry 397(8): 3173-3178.

Kim YM, Kim HS, Kim EM, Lee J, Yang WH, Park TY, Cho JW 2006. Heat Shock Protein 60 Modified with O-Linked N-Acetylglucosamine is Involved in Pancreatic β-Cell Death Under Hyperglycaemic Conditions. FEBS Letters 580(9): 2311-2316.

Kischkel FC, Hellbardt S, Behrmann I, Germer M, Pawlita M, Krammer PH, Peter ME 1995. Cytotoxicity-Dependant APO-1 (Fas/CD95)-Associated Proteins Form a Death-Inducing Signalling Complex (DISC) with the Receptor. The EMBO Journal 14(22): 5579-5588.

Knowlton AA & Srivatsa U 2008. Heat-Shock Protein 60 and Cardiovascular Disease: a Paradoxical Role. Future Cardiology 4(2): 151-161.

Knowlton AA & Uma S 2008. Heat-Shock Protein 60 and Cardiovascular Disease: a Paradoxical Role. Future Cardiology 4(2): 151-161.

Komatsuda A, Wakui H, Oyama Y, Imai H, Miura AB, Itoh H, Tashima Y 1999. Overexpression of the Human 72 kDa Heat Shock Protein in Renal Tubular Cells Confers Ressistance Against Oxidative Injury and Cisplatin Toxicity. Nephrology, Dialysis, Transplantation 14(6): 1385-1390.

Kowluru RA, Kanwar M, Zhong Q 2010. Metabolic Memory and Diabetic Retinopathy: Role of Inflammatory Mediators in Retinal Pericytes. Experimental Eye Research 90 (5): 617-623.

Koya D, Haneda M, Nakagawa H, Isshiki K, Sato H, Maeda S, Sugimoto T, Yasuda H, Kashiwagi A, Ways DK, King GL, Kikkawa R 2000. Amelioration of Accelerated Diabetic Measangial Expansion by Treatment with a PKC beta Inhibitor in Diabetic db/db Mice, a Rodent Model for Type 2 Diabetes. The Journal of the Federation for American Societies for Experimental Biology 14 (3): 439-447.

Lancaster GI & Febbraio 2005. Exosome-dependant Trafficking of HSP70. Journal of Biological Chemistry 280(24): 23349-23355.

Latif N, Taylor PM, Khan MA, Yacoub MH, Dunn MJ 1999. The Expression of Heat Shock Protein 60 in Patients with Dilated Cardialmyopathy. Basic Research in Cardiology 94(2): 112-119.

Law HP, Lukoyanova N, Voskoboinik I, Caradoc-Davies TT, Baran K, Dunstone MA, D'Angelo ME, Orlova EV, Coulibaly F, Verschoor S, Browne KA, Ciccone A, Kuiper MJ, Bird MJ, Trapani JA, Saibil HR, Whisstock JC 2010.

The Structural Basis for Membrane Binding and Pore Formation by Lymphocyte Perforin. Nature 468(7322): 447-451.

Laybutt DR, Sharma A, Sgroi DC, Gaudet J, Bonner-Weir S, Weir GC 2002. Genetic Regulation of Metabolic Pathways in Beta-Cells Disrupted by Hyperglycemia. The Journal of Biological Chemistry 277(13): 10912-10921.

Le C, Scholey JW, James LR 2010. Influence of Glucosamine on Glomerular Mesangial Cell Turnover: Implications for Hyperglycaemia and Hexosamine Pathway Flux. American Journal of Physiology-Endocrinology and Metabolism 298 (2): E210-E221

Leary SC, Hill BC, Lyons CN, Carlson CG, Michaud D, Kraft CS, Ko K, Glerum DM, Moyes CD 2002. Chronic Treatment with Azide in Situ Leads to an Irreversible Loss of Cytochrome c Oxidase Activity via Holoenzyme Dissociation. Journal of Biological Chemistry 277(13): 11321-11328.

Lee AY & Chung SS 1999. Contributions of Polyol Pathway to Oxidative Stress in Diabetic Cataract. Federation of American Societies for Experimental Biology 13 (1): 23-30.

Lemasters JJ, Ramshesh VK 2007. Imaging of Mitochondrial Polarization with Cationic Fluorophores. In: Pon LA, Schon EA. Mitochondria 2nd Edition. San Diego, Academic Press. Pp. 293-296.

Levine F & Ilkin-Ansari P 2008. B-Cell Regeration: Neogenesis, Replication or Both? Journal of Molecular Medicine 86(3): 247-258.

Li W, Zhao X, Zou S, Ma Y, Zhang K, Zhang M 2012. Scanning Assay of [Beta]-Galactosidase Activity. Applied Biochemistry and Microbiology 48(6): 668-672.

Li XX & Stark GR 2002. NF Kappa B-Dependant Signaling Pathways. Experimental Hematology 30(4): 285-296.

Li Y, Ochs S, Gao Z, Malo A, Chen C, Lv S, Gallmeier E, Goke B, Schafer C 2009. Regulation of Hsp60 and the Role of MK2 in a New Model of Severe

Experimental Pancreatitis. American Journal of Physiology – Gastrointestinal and Liver Physiology 297(5): 981-989.

Lin KM, Lin B, Lian IY, Mestril R, Schffler IE, Dillman WH 2001. Combined and Individual Mitochondrail HSP60 and HSP10 Expression in Cardiac Myocytes Protects Mitochondrial Function and Prevents Apoptotic Cell Deaths Induced by Simulated Ischemai-Reoxygenation. Circulation 103(13): 1787-1792.

Lin L, Kim SC, Wang Y, Gupta S, Davis B, Simon SI, Torre-Amione G, Knowlton AA 2007. HSP60 in Heart Failure: Abnormal Distribution and Role in Cardiac Myocyte Apoptosis. American Journal of Physiology - Heart and Circulatory Physiology 293(4): H2238-H2247.

Lipsett M, Hanley S, Castellarin M, Austin E, Suarez-Pinzon WL, Rabinovitch A, Rosenburg L 2007. The Role of Islet Neogenesis-Associated Protein (INGAP) in Islet Neogenesis. Cell Biochemistry and Biophysics 48(2): 127-137.

Livingstone C, Lyall H, Gould GW 1995. Hypothalamic GLUT 4 Expression: a Glucose and Insulin Sensing Mechanism? Molecular and Cellular Endocrinology 107(1): 67-70.

Lori E, Marescotti MC, Vedovato M, Ceolotto G, Avogaro A, Tiengo A, Del Prato S, Trevisan R 2003. In Situ Protein Kinase C Activity is Increased in Cultured Fibroblasts from Type 1 Diabetic Patients with Nephropathy. Diabetologia 46(4): 524-530.

Losev E, Reinke CA, Jellan J, Strongin DE, Bevis BJ, Glick BS 2006. Golgi Maturation Visualized in Living Yeast. Nature 441(7096): 1002-1006.

Lv H, Liu J, Zhao J, Zhao B, Miao J 2013. Highly Selective and Sensitive pH-Responsive Fluorecsent Probe in Living HeLa and HUVEC Cells. Sensors & Acuators: B. Chemical 177: 956-963.

Maedler K, Schumann DM, Sculthess F, Oberholzer J, Bosco D, Berney T, Donath MY 2006. Aging Correlates with Decreased Beta-Cell Proliferative

Capacity and Enhanced Sensitivity to Apoptosis: A Potential Role for Fas and Pancreatic Duodenal Homeobox-1. Diabetes 55(9): 2455-2463.

Magen D, Georgopoulos C, Bross P, Ang D, Segev Y, Goldsher D, Nemirovski A, Shahar E, Ravid S, Luder A, Heno B 2008. Mitochondrial Hsp60 Chaperonopathy Causes an Autosomal-Recessive Neurodegenerative Disorder Linked to Brain Hypomyelination and Leukodystrophy. The American Journal of Human Genetics 83(1): 30-42.

Markovitsi D, Gustavsson T, Banyasz A 2010. Absorption of UV Radiation by DNA: Spatial and Temporal Features. Mutation Research/Reviews in Mutation Research 704(1): 21-28.

Martin J, Horwaich AL, Hartl FU 1992. Prevention of Protein Denaturation Under Heat Stress by the Chaperonin Hsp60. Science 258(5084): 995-998.

Mehier-Humbert S & Guy RH 2005. Physical Methods for Gene Transfer: Improving the Kinetics of Gene Delivery into Cells. Advanced Drug Delivery Reviews 57(5): 733-753.

Meredino AM, Conway de Macario E, Macario AJL Capello F, Bucchieri F, Campanella C, Marciano V, Ribbene A, David S, Zummo G, Burgio G, Corona DFV 2010. Hsp60 is Actively Secreted by Human Tumor Cells. Plos One 5(2): e9247 1-7.

Millan-Mendoza B, Hakimi H, Eley A 2007. Apoptotic Effect on HeLa Cells Produced by *Chlamydia trachomatis*-LPS. Kasmera 35(1): 7-14.

Mineshiba J, Myokai F, Mineshiba F, Matsuura K, Nishimura F, Takashiba S 2005. Transcriptional Regulation of Beta-Defensin-2 by Lipopolysaccharide in Cultured Human Cervical Carcinoma (HeLa) Cells. FEMS Immunology and Medical Microbiology 45(1): 37-44.

Molina PE 2006. Endocrine Pancreas. In: Molina PE ed. Endocrine Physiology. Ohio, McGraw-Hill Medical Publishing Division. Pp. 157-179.

Moore MP & Lunt H 2000. Diabetes in New Zealand. Diabetes Research and Clinical Practice 50: S65-S71.

Mora A, Komander D, van Aalten, Daan MF, Alessi DR 2004. PDK1, the Master Regulator of AGC Kinase Signal Transduction. Seminars in Cell & Developmental Biology 15(2): 161-170.

Morales MC & Zahn JD 2010. Droplet Enhanced Microfluidic-Based DNA Purification from Bacterial Lysates via Phenol Extraction. Microfluidics and Nanofluidics 9(6): 1041-1049.

Mussig K, Staiger H, Machcao F, Stancokova A, Kuusisto J, Laakso M, Thamer C, Machann J, Schick F, Clauseen, Stefan N, Fritsche A, Haring H 2009. Association of Common Genetic Variation in the Foxo1 Gene with Beta-Cell Dysfunction, Impaired Glocose Tolerance, and Type 2 Diabetes. The Journal of Clinical Endocrinology and Metabolism 94(4): 1353-1360.

Muto Y, Satoh J, Muto G, Masuda T, Sagara M, Fukuzawa M, Miyaguchi S, Qiang XL, Sakata Y, Nakazawa T, Ikehata F, Toyota T 1997. Effect of Long-Term Treatment with Complete Freund's Adjuvant on KK-Ay Mouse, a Model of Non-Insulin Dependent Diabetes Mellitus. Clinical Immunology and Immunopathology 83(1): 53-59.

Nata K, Shervani NJ, Onogawa T, Takasawa S, Okamoto H, Liu Y, Xu L, Ikeda T, Akiyama T, Noguchi N, Kawaguchi S, Yamauchi A, Takahashi I 2004. Molecular Cloning, Expression ans Chromosomal Localization of Novel Human REG Family Gene, REG III. Gene 340(1): 161-170.

Nathan DM, Cleary PA, Backlund JC, Genuth SM, Lachin JM, Orchard TJ, Raskin P, Zinman B 2005. Intensive Diabetes Treatment and Cardiovascular Disease in Patients with Type 1 Diabetes. New England Journal of Medicine 353 (25): 2643-2653.

Nicholls C, Li H, Liu J 2012. GAPDH: a Common Enzyme with Uncommon Functions. Clinical and Experimental Pharmacology & Physiology 39(8): 674-679.

Nilsson BO 1999. Biological Effects of Aminoguanidine: an Update. Inflammation Research 48(10): 509-515.

Park L, Raman KG, Lee KJ, Lu Y, Ferran LJ Jr, Chow WS, Stern D, Schmidt AM 1998. Suppression of Accelerated Diabetic Atherosclerosis by the Soluble Receptor for Advanced Glycation Endproducts. Nature Medicine 4 (9): 1025-1031.

Pearce JMS 2008. Apoptosis. European Neurology 60(2): 112.

Pfister G, Stroh CM, Perschinka H, Kind M, Knoflach M, Hinterdorfer P, Wick G 2005. Detection of HSP60 on the Membrane Surface of Stressed Human Endothelial Cells by Atomic Force and Confocal Microscopy. Journal of Cell Science 118(8) 1587-1594.

Pockley AG 2002. Heat Shock Proteins, Inflammation, and Cardiovascular Disease. Circulation 105(8): 1012-1017.

Quintana FJ & Cohen IR 2011. The HSP60 Immune System Network. Trends in Immunology 32(2): 89-95.

Raetz CRH & Whitfield C 2002. Annual Review of Biochemistry 71(1): 635-700.

Ranford JC, Coates AR, Henderson B 2000. Chaperonins are Cell-Signalling Proteins: the Unfolding Biology of Molecular Chaperones. Expert Reviews in Molecular Medicine 2(8): 1-17.

Recillas-Targa F 2006. Multiple Strategies for Gene Transfer, Expression, Knockdown, and Chromatin Influence in Mammalian Cell Lines and Transgenic Animals. Molecular Biotechnology 34(3): 337-354.

Reddy VP & Beyaz A 2006. Inhibitors of the Maillard Reaction and AGE Breakers as Therapeutics for Multiple Diseases. Drug Discovery Today 11(13): 646-654.

Rosca MG, Mustata TG, Kinter MT, Ozdemir AM, Kern TS, Saweda LI, Brownlee M, Monnier VM, Weiss MF 2005. Glycation of Mitochondrial Proteins from Diabetic Rat Kidney is Associated with Excess Superoxide Formation. American Journal of Physiology: Renal Physiology 289 (2): F420-F430.

Salozhin SV & Bolshakov AP 2009. Transfection of Nerve Cells. Neuroscience and Behavioral Physiology 40(3): 269-277.

Sarri S, Shaw SM, Gieschen-Krische MA, Archer L, Yonan N, Fildes JE 2009. Myocardial Heat Shock Protein 60 Expression is Upregulaed Following Acute Cardiac Rejection. Transplant Immunology 21(3): 140-142.

Schafler AE, Kirmanoglou AE, Balback J, Pecher P, Hannekum A, Schumacher B 2002. The Expression of Heat Shock Protein 60 in Myocardium of Patients with Chronic Atrial Fibrillation. Basic Research in Cardiology 97(3): 258-261.

Schubert W 2010. On the Origin of Cell Functions Encoded in the Toponome. Journal of Biotechnology 149(4): 252-259.

Shan Z, Zhang Y, Yu X, Lin Q, Lin S, Deng C, Zhu J, Mai L, Liu X, Liu J, Fu Y, Li Y 2010. miR-1/miR-20 Regulate Hsp60 Expression Contributing to Glucose-Mediated Apoptosis in Cardiomyocytes. FEBS Letters 584(16): 3592-3600.

Sjakste N, Bagdoniene L, Gutcaits A, Labeikyte D, Bielskiene K, Trapina I, Muiznieks I, Vassetzy Y, Sjakste T 2010. Proteins Tightly Bound to DNA: New Data and Old Problems. Biochemistry 75(10): 1240-1251.

Slack JM 1995. Developmental Biology of the Pancreas. Development 121(6): 1569-1580.

Sosa-Pineda B, Chowdhury K, Torres M, Oliver G, Gruss P 1997. The Pax4 Gene is Essential for Differentiation of Insulin-Producing Beta Cells in the Mammalian Pancreas. Nature 386(6623): 399-402.

Stolarczyk E, Le Gall M, Even P, Houllier A, Serradas P, Brot-Laroche E, Leturque A 2007. Loss of Sugar Detection by GLUT2 Affects Glucose Homeostasis in Mice. PloS One 2(12): e1288 1-12.

Suri A, Calderon B, Esparza TJ Frederick K, Bittner P, Unanue ER 2006. Immunological Reversal of Autoimmune Diabetes Without Hematopoietic Replacement of Beta Cells. Science 311(5768): 1778-1780.

Susa T, Kato T, Kato Y 2008. Reproducible Transfection in the Presence of Carrier DNA Using FuGENE6 and Lipofectamine2000. Molecular Biology Reports 35(3): 313-319.

Suzuki K, Hamaoka R, Koh YH, Mizuno H, Taniguchi N 1998. Overexpression of Aldehyde Reductase Protects PC12 Cells from the Cytotoxicity of Methylglyoxal or 3-deoxlglucosone. Journal of Biochemistry 123 (2): 353-357.

Szkudelski T 2001. The Mechanism of Alloxan and Streptozotocin Action in B Cells of the Rat Pancreas. Physiological Research 50(6): 537-546.

Tani C, Inoue K, Tani Y, Harun-ur-Rashid M, Azuma N, Ueda S, Yoshida K, Maeda I 2009. Sensitive Fluorescent Microplate Bioassay using Recombinant *Escherichia coli* with Multiple Promoter-Reporter Units in Tandem for Detection of Arsenic. Journal of Bioscience and Bioengineering 108(5): 414-420.

Terai T & Nagano T 2008. Fluorescent Probes for Bioimaging Applications. Current Opinion in Chemical Biology 12 (5): 515-521.

Teuscher A 2007. Insulin: A Voice for Choice. Basel, Karger Publishers. Pp. 10-13.

Thorel F, Ne'pote V, Avril I, Kohno K, Desgraz R, Chera S, Herrera PL 2010. Conversion of Adult Pancreatic Alpha-Cells to Beta-Cells After Extreme Beta-Cell Loss. Nature 464(7292): 1149-1154.

Thornalley PJ, Langborg A, Minhas HS 1999. Formation of Glyoxal, Methylglyoxal and 3-Deoxyglucosone in the Glycation of Proteins by Glucose. The Biochemical Journal 344(1): 109-116.

Tirlapur UK & Konig K 2002. Targeted Transfection by Femtosecond Laser. Nature 418(6895): 290-291.

Tostado CP, Xu JH, Du AW, Luo GS 2012. Experimental Study on Dynamic Interfacial Tension with Mixture of SDS-PEG as Surfactants in a Coflowing Microfluidic Device. Langmuir 28(6): 3120-3128.

Tsuei A & Martinus RD 2012. Metformin Induced Expression of Hsp60 in Human THP-1 Monocyte Cells. Cell Stress & Chaperones 17(1): 23-28.

Tu Z, Shi J, Wu X, He G, Li KX, Chen MJ, Chang J, Chen L, Yao Q, Liu DP, Ye H 2005. An Improved System for Competant Cell Preparation and High Efficiency Plasmid Transformation Using Different *Escherichia coli* Strains. Electronic Journal of Biotechnology 8(1): 113-120.

Tuch BE& Kannangara K 2008. B Cell Regeration. Drug Discovery Today: Therapeutic Stratergies 5(4): 215-221.

Uchida M, Xiong W, Mertens P, Alpar HO 2009. Transfection by Particle Bombardment: Delivery of Plasmid DNA into Mammalian Cells Using Gene Gun. Biochemica et Biophysica Acta – General Subjects 1790(8): 754-764.

Ursano RJ 2012. Science Calls Her HeLa. Psychiatry 75(2): 101-102.

Urushibara M, Kageyama Y, Akashi T, Otsuka Y, Takizawa T, Koike M, Kihara K 2007. HSP60 May Predict Good Pathological Response to Neoadjuvant Chemoradiotherapy in Bladder Cancer. Japanese Journal of Oncology 37(1): 56-61.

Wang S, Xie W, Rylander MM, Tucker PW, Aggarwal S, Diller KR 2008. HSP70 Kinetics Study by Continuous Observation of HSP-GFP fusion Protein Expression on a Perfusion Heating Stage. Biotechnology and Bioengineering 99(1): 146-154.

Wang ZL & Rossman TG 1994. Large-Scale Supercoiled Plasmid Preparation by Acidic Phenol Extraction. Biotechniques 16(3): 460-463.

Wheeler DS, Lahni P, Odoms K, Jacobs BR, Carcillo JA, Doughty LA, Wong HR 2007. Extracellular Heat Shock Protein 60 (Hsp60) Levels in Children with Septic Shock. Inflammation Research 56(5): 216-219.

Winzell MS & Ahren B 2007. G-Protein-Coupled Receptors and Islet Function – Implications for Treatment of Type 2 Diabetes. Pharmacology and Therapuics 116(3): 437-448.

Wojtowicz JM, Kee N 2006. Brdu Assay for Neurogenesis in Rodents. Nature Protocols 1(3): 1399-1405.

World Health Organization. (2006). Definition and Diagnosis of Diabetes Mellitus and Intermediate Hyperglycemia: Report of a WHO/IDF Consultation.

Xia B, Zhan X, Yi R, Yang B 2009. Can Pancreatic Duct-Derived Progenitors be a Source of Islet Regeneration? Biochemical and Biophysical Research Communications 383(4): 383-385.

Xue M, Rabbani N, Thornalley PJ 2011. Glyoxalase in Aging. Seminars in Cell and Developmental Biology 22(3): 293-301.

Yamano S, Dai J, Moursi AM 2010. Comparison of Transfection Efficiency of Non-viral Gene Transfer Reagents. Molecular Biotechnology 46(3): 287-300.

Yu J & Thomson JA 2008. Pluripotent Stem Cell Lines. Genes & Development 22(15): 1987-1997.

Yuan J, Dunn P, Martinus RD 2011. Detection of Hsp60 in Saliva and Serum from Type 2 Diabetic and Non-Diabetic Control Subjects. Cell Stress & Chaperones 16(6): 689-693.

Zeilstra-Ryalls J, Fayet O, Georgopoulos C 1991. The Universally Coserved GroE (Hsp60) Chaperonins. Annual Review of Mirobiology 45(1): 301-325.

Zhang Y & Yu L 2008. Microinjection as a Tool of Mechanical Delivery. Current Opinion in Biotechnology 18(5): 506-510.

Zhong Q & Kowluru RA 2010. Role of Histone Acetylation in the Development of Diabetic Retinopathy and the Metabolic Phenomenon. Journal of Cellular Biochemistry 10 (6): 1306-1313.

Zhou Q, Brown J, Kanarek A, Rajagopal J, Melton DA 2008. In Vivo Reprogramming of Adult Pancreatic Exocrine Cells to β-cells. Nature 455(7213): 627-632.